PNNL-28480

Avista Turner Energy Storage System

Assessment of Battery Technical Performance

July 2019

A Crawford
V Viswanathan
C Vartanian
J Alam
P Balducci
D Wu
T Hardy
K Mongird

U.S. DEPARTMENT OF ENERGY

DISCLAIMER

This report was prepared as an account of work sponsored by an agency of the United States Government. Neither the United States Government nor any agency thereof, nor Battelle Memorial Institute, nor any of their employees, makes **any warranty, express or implied, or assumes any legal liability or responsibility for the accuracy, completeness, or usefulness of any information, apparatus, product, or process disclosed, or represents that its use would not infringe privately owned rights**. Reference herein to any specific commercial product, process, or service by trade name, trademark, manufacturer, or otherwise does not necessarily constitute or imply its endorsement, recommendation, or favoring by the United States Government or any agency thereof, or Battelle Memorial Institute. The views and opinions of authors expressed herein do not necessarily state or reflect those of the United States Government or any agency thereof.

PACIFIC NORTHWEST NATIONAL LABORATORY
operated by
BATTELLE
for the
UNITED STATES DEPARTMENT OF ENERGY
under Contract DE-AC05-76RL01830

Printed in the United States of America

Available to DOE and DOE contractors from the
Office of Scientific and Technical Information,
P.O. Box 62, Oak Ridge, TN 37831-0062;
ph: (865) 576-8401
fax: (865) 576-5728
email: reports@adonis.osti.gov

Available to the public from the National Technical Information Service
5301 Shawnee Rd., Alexandria, VA 22312
ph: (800) 553-NTIS (6847)
email: orders@ntis.gov <http://www.ntis.gov/about/form.aspx>
Online ordering: http://www.ntis.gov

This document was printed on recycled paper.
(8/2010)

PNNL-28480

Avista Turner Energy Storage System

Assessment of Flow Battery Energy Storage System Technical Performance

A Crawford
V Viswanathan
C Vartanian
J Alam
P Balducci
D Wu
T Hardy
K Mongird

July 2019

Prepared for
the U.S. Department of Energy
under Contract DE-AC05-76RL01830

Pacific Northwest National Laboratory
Richland, Washington 99352

Executive Summary

Integration of energy storage into the U.S. electrical grid has been growing, especially as penetration of power generated by renewable resources increases and energy storage technologies become more cost effective. To support continued advances in the integration of energy storage systems (ESSs), this report provides findings on the technical attributes of actual energy storage projects and their ability to provide benefits to stakeholders comprised of a utility (Avista) and the customers it serves. This project, which focuses on ESS performance, was funded jointly by Avista, the Washington Clean Energy Fund (CEF), and the U.S. Department of Energy Office of Electricity Delivery and Energy Reliability (DOE-OE). In addition to advancing Avista's and the State of Washington's understanding of energy storage for facilitating renewables penetration and other intended energy storage applications, there is also a national-level benefit from this project's insights into energy storage technical performance. For example, several states (e.g., California, Oregon, and New York) have storage procurement targets to deal with a variety of issues such as afternoon ramping requirements, frequency regulation/control, and time shifting of energy provided by renewable resources. This report will aid in meeting those targets.

Motivation for This Work

A $3.2 million grid modernization grant was awarded to Avista under the Washington CEF 1 program, which funds projects focused on different batteries and ESSs. Using $3.8M in matching funds, Avista procured a 1 megawatt (MW)/3.2 megawatt-hour (MWh) vanadium-flow battery system from UniEnergy Technologies (UET) and deployed the system between the Turner Station Substation in Snohomish County, Washington, and the Schweitzer Engineering Laboratory (SEL) manufacturing facility in Pullman, Washington. The grant supported exploration of energy storage applications and associated benefits for the following use cases:

- Energy Shifting
- Provide Grid Flexibility
- Improve Distribution Systems Efficiency
- Enhanced Voltage Control
- Grid-Connected and Islanded Microgrid Operations.

These use cases or services were identified as being applicable for Avista and were defined based on utility- and site-specific characteristics. Because flow battery energy storage systems (FBESS) are quite diverse in their characteristics, it was important to first characterize FBESS performance over time using the DOE-OE Energy System Storage Performance Protocol. The DOE-OE protocol includes representative generic duty cycle profiles, test procedure guidance, and calculation guidance for determining key FBESS characteristics, including energy capacity, response time, internal resistance, and round-trip efficiency (RTE).[1] After conducting baseline tests to evaluate the general characteristics of the FBESS, its performance was measured under various energy storage use cases to evaluate key performance metrics relevant to real-world economic operation. Outcomes of these analyses will be beneficial for Avista in understanding the performance of the Turner FBESS in its current state, and when designing appropriate long-term operational strategies for this and future Avista battery energy storage projects.

[1] The RTE is the ratio of discharge energy to charge energy, ensuring the FBESS SOC is brought back to the initial SOC.

Summary of Work Performed

This report describes the technical performance of the 1 MW, 3.2 MWh advanced vanadium FBESS, which consists of two 0.5 MW, 1.6 MWh strings, based on a number of reference performance and use case tests. Reference performance tests (RPT) were undertaken to assess the general technical capability of the FBESS (e.g., stored energy capacity, ramp rate performance, ability to track varying charge/discharge commands, direct current [DC] battery internal resistance). Use case tests were used to examine the performance of the FBESS while engaged in specific grid services (e.g., arbitrage, frequency regulation, balancing, volt ampere reactive support, dynamic peak shaving). The project identified performance metrics that are important for understanding FBESS performance when subjected to field operation for achieving economic benefits from measurements and/or calculations. These metrics were:

- RTE with and without rest, with and without auxiliary power consumption
- Auxiliary power consumption
- Reference signal tracking
- Temperature excursions beyond the normal operating range
- Parasitic power loss unaccounted for by auxiliary load during rest
- State-of-charge (SOC) excursions beyond normal operating range.[2]

The RPT and use case performance metrics were analyzed using recorded test results. In addition, because the assessment methodology remains the same, the results and lessons presented are beneficial for any task or effort requiring a technical assessment of ESSs more broadly.

Key Questions Addressed

A thorough analysis of FBESS performance was carried out using performance metrics developed in the DOE-OE protocol and additional metrics identified in this project. Execution of the project answered the questions listed below that are key for ultimately determining the cost effectiveness of FBESSs used for grid energy storage applications.

1. How does the FBESS perform during baseline and use case testing for various duty cycles? For example, what is the RTE of the FBESS?
2. How does the FBESS perform for high ramp rate duty cycles? For example, what is the FBESS response time and ramp rate?
3. What was the percent of time the FBESS was not available?
4. What are some of the issues identified in this project that are not very obvious?

Key Outcomes

The Turner FBESS was subjected to RPTs that included tracking volatile signals and measuring energy capacity at various rates of charge and discharge, internal resistance, and response time/ramp rate. The RPTs conducted before use case testing are referred to as baseline tests in this report.

[2] The battery management system kept SOC within normal operating range.

In addition, duty cycles were developed for various use cases to be performed for this project, and the FBESS use case performance was tested and analyzed accordingly. Summaries of key outcomes for baseline and use case performance testing follow.

Outcome 1

Outcome 1 revealed findings related to discharge energy capacity and RTE.

A thorough analysis of FBESS performance was performed using metrics developed in the DOE-OE protocol and additional metrics identified in this project. FBESS performance during baseline and use case testing was analyzed. The FBESS SOC was allowed to go as high as the battery management system would allow, while the discharge time was estimated to ensure the entire constant power region was included. Note that the energy provided was normalized for two strings because both strings were not always available during the test period.

Discharge Energy Capacity

RPTs were done at various discharge rates at a fixed charge rate of 600 kW. The discharge energy varied non-linearly with the SOC because of the sloping nature of open circuit voltage as a function of SOC and coupled mass transport-kinetics related losses at low SOCs. The range of discharge energy capacity for all tested cycles, and C-rates ranged from 2,020 to 3,600 kWh. The energy delivered at rated power of 1,000 kW was about two-thirds the rated energy of 3,200 kWh, with 520 kW discharge delivering 94% of the rated energy. Warmer ambient conditions for baseline tests consumed more cooling load than was balanced by improved performance at higher temperatures. Energy delivered at 400 kW was 4% higher than the rated energy, with the increase in RTE resulting from higher electrochemical efficiency. At the power conversion system (PCS) level, excluding auxiliary load, the FBESS provided the rated energy at 520 kW and provided 11% higher than rated energy at 400 kW.

RTE

The range of RTEs for all RPTs performed was 57 to 75%, depending on which losses were included. RTEs at the grid ranged from 57 to 65% and increased to 63 to 75% at the PCS when auxiliary consumption losses were excluded. The RTE for the baseline peak shaving and energy intensive use case tests were similar. For tests such as dynamic peak shaving, the RTE was less than 8% for several runs because the FBESS was called on to discharge for very brief durations. RTE as a metric is not indicative of FBESS effectiveness in situations in which the FBESS is either not called upon to discharge where RTE is not applicable or when the discharge duration is a very small fraction of the test duration. For grid services with volatile signals such as frequency regulation, the RTE is lower because average power levels are a percentage of rated power. In such services, the ability of the FBESS to track the reference signal is the key metric, not RTE. The increase in RTE when excluding auxiliary consumption was highest for low power levels and high rest periods, as would be expected.

Figure ES.1 shows charge/discharge energies and RTEs for energy capacity RPTs, while Figure ES.2 shows the frequency regulation RPT results.

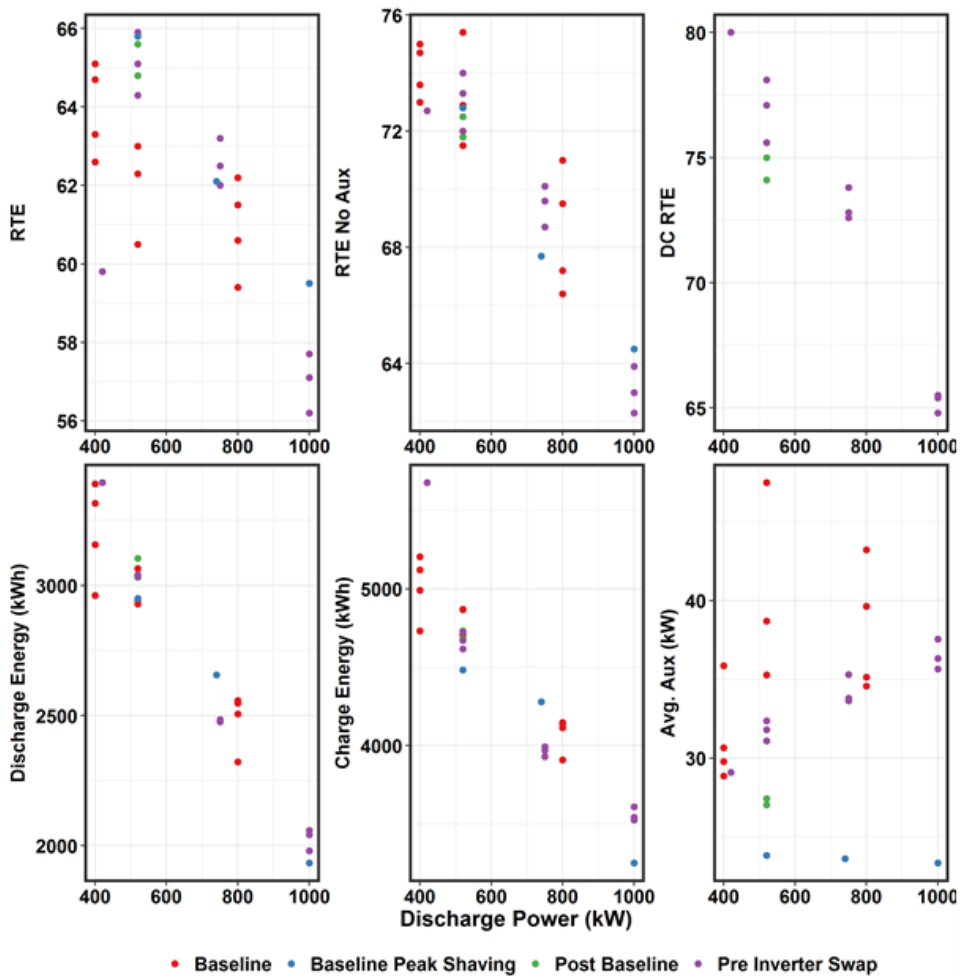

Figure ES.1. Reference Performance Test Results for Energy Capacity – Charge, Discharge Energy, Auxiliary Consumption, and RTE at Various Discharge Power Levels. Charging done at 600 kW

Outcome 2

Outcome 2 reports findings related to response time and internal resistance.

Response Time

The response time of the FBESS ranged from 3 to 10 seconds for the range of test cycles performed. For charge, the response time increased from 4 to 10 seconds as SOC increased from 20 to 60%, reaching a maximum power of 800 kW. At >60% SOC, the maximum power attained dropped linearly to 400 kW at 100% SOC. Hence, it is important for the battery owner to bid the power that can be supported at the SOC operating range or for the manufacturer to provide charge and discharge achievable power ratings across the SOC range of operation. This also stresses the importance of redefining the response time as the time taken to reach the maximum achievable power at that SOC.

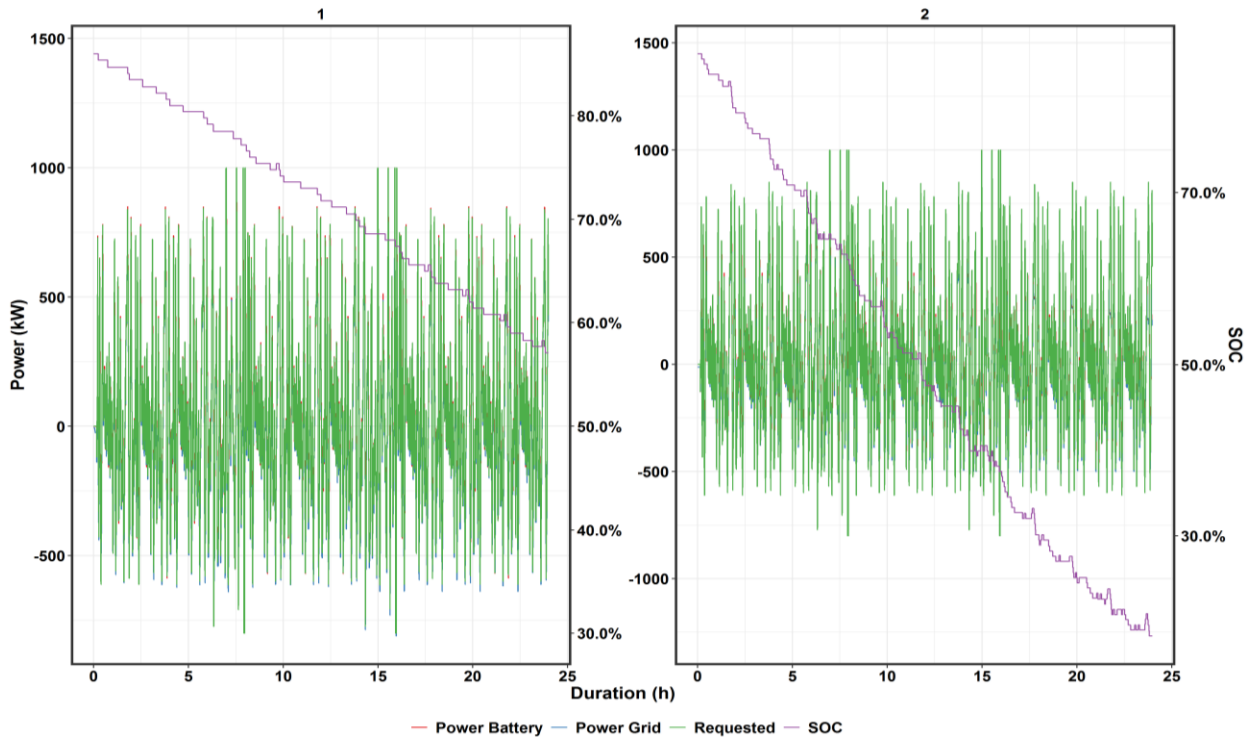

Figure ES.2. Reference Performance Test Signal, Response, and SOC for Frequency Regulation

At high SOC, while the response time for charge pulses to attain the maximum power was lower, the ramp rate decreased from a maximum of 200 kW/s at 30% SOC to 50 kW/s at 90 to 100% SOC. The results are consistent with UET limiting charge ramp rates to 200 kW/s.

The response time for discharge was 3 seconds. The ramp rate and maximum achieved power were flat across the SOC range investigated. The response time ranged from 340 kW/s at 90% SOC to 315 kW/s at 30% SOC, while the maximum achieved power was ~1,000 kW in the 90 to 40% SOC range, dropping slightly to 950 kW at 30% SOC. The results are consistent with UET limiting discharge ramp rates to 300 kW/s. The rated discharge power could not be reached at SOC ≤30% SOC. Hence, it is important for the battery owner to bid the power that can be supported at the SOC operating range.

Note that only one string was active during this test, and that the battery suffered throughout the tests with strings coming on and off line.

FBESS Internal Resistance

The FBESS charge and discharge resistance, corrected for two strings, was in a tight range for discharge, increasing from 0.100 ohms to 0.110 ohms as SOC decreased from 90 to 40%. There was a spike in internal resistance at 30% SOC to 0.125 ohms. On a four-string normalized basis, the resistance ranged from 0.05 to 0.055 ohms, which is in line with Snohomish Public Utility District Modular Energy Storage Architecture (MESA) 2 findings. MESA 2 was also a FBESS provided by UET.

The internal resistance during charge was slightly lower than discharge pulse resistance across the SOC range investigated. It decreased from 0.11 ohms at 20% SOC to 0.095 ohms at 100% SOC.

Outcome 3

Outcome 3 reports findings on system availability.

The aggregate availability of the FBESS over the test period was 56%. The total test duration was 365 days, out of which 162 days, or 44%, were lost for various reasons. The distribution of lost days for various categories is shown in Figure ES.3. Note that the FBESS ultimately could not continue operation and the field tests were not entirely completed.

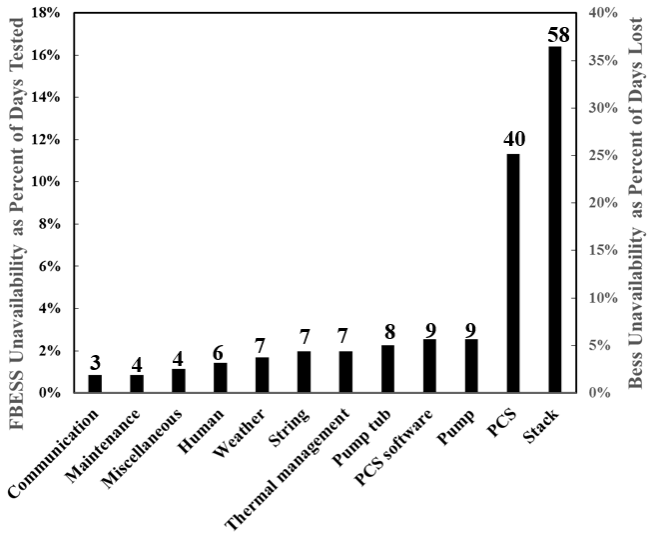

Figure ES.3. Distribution of Lost Time from Various Categories

Fifty-eight days or 16% of the test duration were lost due to stack-related issues, which include stack SOC mismatch and a stack leak. Forty days or 11% of test duration were lost due to PCS-related issues, which included prolonged use of the PCS during charge at high SOCs and corrosion of electronic components from exposure to leaked electrolyte. PCS software related issues resulted in 9 lost days.

Pump-related issues and a pump tub housing leak contributed to 9 and 8 lost days, respectively. Failure of thermal management contributed to 7 lost days, and AC breaker trips that could not be reset remotely contributed to 7 lost days. Human errors and weather contributed to 6 and 7 lost days, respectively. Maintenance, communication failure, and miscellaneous contributed to a total of 11 missed days.

The break for inverter changes and tank/stack replacement from November 2016 to April 2018 was not counted as part of the test duration. Accounting for this period and assuming 20 additional days of testing in April and May 2018, the availability was 24%.

Outcome 4

Outcome 4 captures findings for issues that surfaced in testing that were outside of specific, structured objectives (e.g., testing to measure and report RTE).

There were multiple issues identified during testing that were neither obvious nor anticipated before testing commenced. These issues are briefly described below and in detail in Appendix A.

- Not all data was available in 1-second increments. Hence, for response time and ramp rate analysis, the FBESS response to signals sent every 20 seconds was used.

- Auxiliary power consumption was not monitored because this tag was not part of the MESA tag list for the FBESS.
- Auxiliary consumption was calculated from the difference between power flow at the 735 meter and the inverters at SEL. Hence, auxiliary consumption for each string could be determined individually.
- UET defined a "Connection Point," which was a virtual meter that added the power flow through each PCS.
- The requested power commands were met by the PCS without accounting for auxiliary consumption. Hence, the power exchange with the grid differed from requested power by the auxiliary consumption, in addition to any tracking error for power at the PCS. Because the grid operator cares only about the power that is exchanged between the FBESS and the grid, it is prudent to have the battery management system adjust the PCS input or output such that the requested power is exchanged with the grid. Otherwise, there would be significant tracking error for volatile signals. For use cases such as peak shaving, if auxiliary consumption is too high, the power delivered to the grid during peak periods may not be sufficient to meet the demand. This error between the power requested by the grid operator and the actual power absorbed or (charge or discharge) delivered by the FBESS, would also negatively impact revenue for frequency regulation service for markets that included accuracy related compensation components (e.g., PJM, ISO-NE).
- The string at a low SOC absorbed more charge power and provided lower discharge power.
- Charging for this chemistry is thermodynamically endothermic, with temperature decreasing during charge at 600 kW continuous power; that is, the thermodynamics overwhelm the exothermicity of the resistive heating during charge.
- The normal operating temperature was 40 to 45°C per UET, with cooling kicking in any time when temperature is > 40°C and at > 35°C for continuous power operation.
- Auxiliary consumption at fixed power for charge is higher compared to discharge. Charge may require greater flow rate per kilowatt to prevent gas evolution by facilitating faster mass transport and lowering over-potential. Charge resistance is lower than discharge resistance across the SOC range, thus lending support to this hypothesis.
- The minimum power factor (PF) was assumed to be 0.5, based on UET's software settings. Tests indicated the actual minimum PF was 0.01.
- On one occasion, when the FBESS needed to provide volt ampere reactive (var) power, the real power increased such that PF was 0.85, resulting in an inability of the FBESS to provide the required vars. The inverter was being operated in vars limiting mode. Subsequently, the appropriate mode that gave vars priority was selected.
- To overcome limitations associated with 1 kW resolution at the SEL 735 meter, at times the real power had to be set higher than that required by the minimum PF for use cases such as volt ampere reactive (var) support and conservation voltage reduction (CVR).
- For var support, the FBESS was able to provide vars with both capacitor banks in the feeder circuit opened.
- For CVR reduction, only one string was available. Hence, the capacitor banks had to be left closed in. The FBESS was treated as two virtual capacitors at 150 kvar and 300 kvar and had to be manually engaged to be under the control of integrated voltage var control (IVVC). Because of var adjustments being done asynchronously, the total vars requested was over- or under-adjusted, resulting in requests for 900 kvar to 1,500 kvar at times, which are much greater than the 450 kvar capacity for a single string.

- The FBESS received only occasional commands to provide vars in the virtual capacitor setting, sometimes going hours without receiving commands. To facilitate keeping the contactor closed, the setting was changed to PF regulation where var requests were sent every 15 seconds. However, the system faulted as soon as this change was made.
- To automate the CVR under IVVC control, the voltage control feature of IVVC was enabled rather than capacitor bank control. The FBESS was set to "var-following" and thus got closer to 1.0 PF compared with the virtual capacitor's coarse settings.
- The FBESS provided the requested vars for the relevant use case. However, the effectiveness of the Avista algorithm to keep the PF at 1 or the feeder voltage at 118 VAC at the specific location in the feeder was verifiable only by the Avista engineer, since this data was not available to Pacific Northwest National Laboratory.
- For dynamic peak shaving, there were occasions when the FBESS was not sent any commands to shave the peak due to feeder peak load overestimation, while on other occasions the FBESS was called upon to deliver power for 12 hours continuously because the feeder load was underestimated. This shows the importance of a reliable tool to accurately predict peak load levels and duration.
- Pump operation is necessary even during rest at high SOC and high temperature to remove heat generated from short circuit current. A way to drain the stacks when not operating would probably mitigate thermal excursions beyond the normal operating range.
- The communication lag between the time the signal was sent from Avista headquarters and the time it was received by the FBESS was estimated to be 10 seconds. Surprisingly, for some pulse tests, the BESS started to respond before the signal was received. Since this is not possible from a physical point of view, this appears to be due to an error in the reporting of either the requested power tag or in the system response data.
- The cumulative charge and discharge ampere hours, along with coulombic efficiency for String 2 is shown in Figure ES.4. The coulombic efficiency was close to 100% initially, and decreases with time, ending up at 95%, indicative of electrolyte crossover.

Key Conclusions

Following are major conclusions, selected from the full set of conclusions reported in the body of the report below:

- The FBESS provided the energy specified at various power levels as expected, with the largest energy at 3,395 kWh at 420 kW at an 81% depth of discharge.
- The FBESS performed as expected for both energy intensive duty cycles and volatile duty cycles, where the requested power changed magnitude and direction frequently.
- The energy available for discharge was highly dependent on the power (kilowatt) levels during the tested cycle. For example, the energy available at full rated 1 MW power was approximately two-thirds of the energy that can be discharged at approximately 50% of full rated power.
- The response time was dependent on power level, mode, and SOC.[3]
- The FBESS availability factor was lower than expected.

[3] UniEnergy Technologies' specifications simply state response time < 100 ms, without defining response time

- This report's detailed findings on FBESS technical performance will be beneficial for Avista to understand the performance of the Turner FBESS at its current state, and to apply the results in designing appropriate operational strategies.

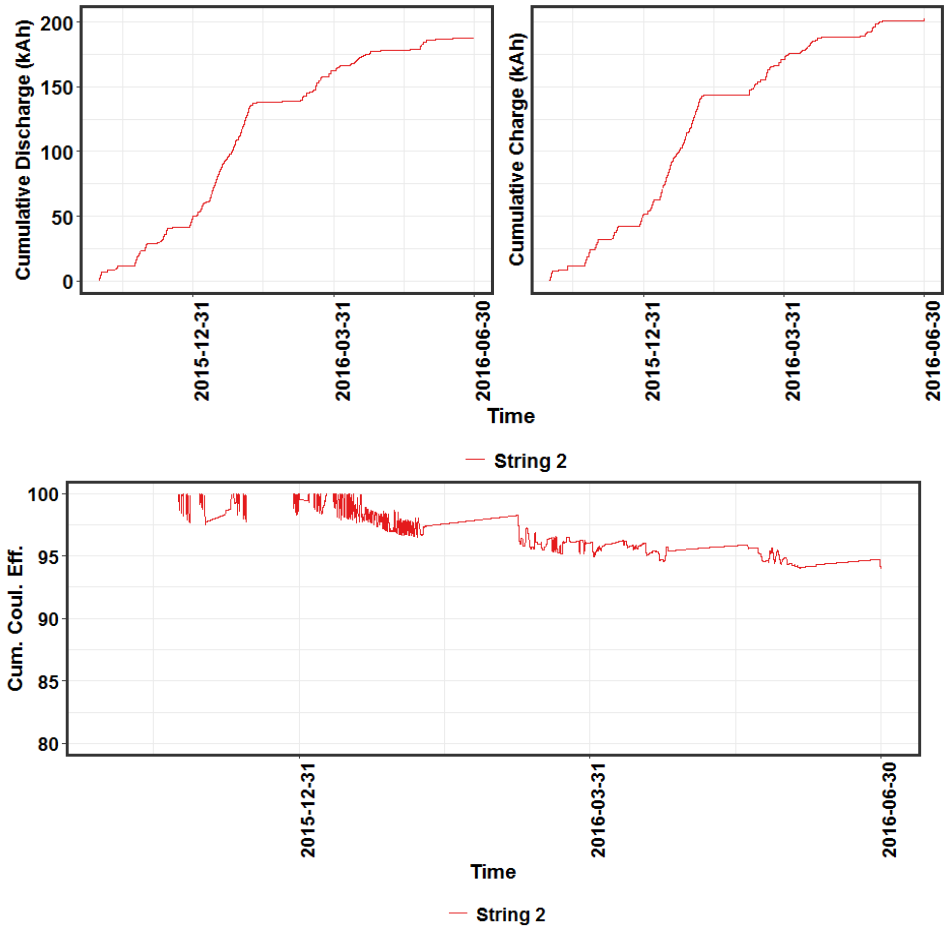

Figure ES.4. Cumulative Charge and Discharge Ampere Hours and Coulombic Efficiencies for String 2

- The results and lessons presented herein would also be beneficial in general for any task or effort that needs technical assessment on similar types of FBESS based on technical specifications or field deployment results.

Acknowledgments

We are grateful to Mr. Bob Kirchmeier, Senior Energy Policy Specialist at the Washington Department of Commerce, for providing technical guidance to Pacific Northwest National Laboratory (PNNL) during the execution of this project. We are also grateful to Dr. Imre Gyuk, who is the Energy Storage Program Manager in the Office of Electricity Delivery and Energy Reliability at the U.S. Department of Energy, for providing financial support and leadership on this and other related work at PNNL. We wish to acknowledge Philip Craig from BlackByte Cyber Security. We also wish to recognize team members from Avista Utilities, including Matt Michael, Robert Cloward, James Gall, Reuben Arts, John Gibson, Curt Kirkeby, and Kenny Dillon. Finally, we wish to acknowledge Chauncey Sun, Brad Kell, and David Ridley of UniEnergy Technologies for their technical support during this project.

Acronyms and Abbreviations

A	amperes
AC	alternating current
ACE	area control error
AEG	AEG Power Solutions
AGC	automatic generation control (
BMS	battery management system
BSET	Battery Storage Evaluation Tool
CBC	Capacitor Bank Control
CEF	Clean Energy Fund
CTL	Crestchic Test Load
CVR	conservation voltage reduction
DC	direct current
DMS	distribution-management system
DNP3	Distributed Network Protocol
DOE	U.S. Department of Energy
ESS	energy storage system
FBESS	flow battery energy storage system
IVVC	integrated volt/VAR control
kV	kilovolts
kVA	kilovolt-ampere
kvar	kilovolt-ampere reactive
kW	kilowatts
kWh	kilowatt-hours
MAE	mean absolute error
MESA	Modular Energy Storage Architecture
MW	megawatt(s)
MWh	megawatt-hour(s)
NPS	Northern Power Systems
OE	Office of Electricity Delivery and Energy Reliability
PCS	power conversion system
PF	power factor
PFREG	power factor regulation
PJM	Pennsylvania New Jersey Maryland LLC
PNNL	Pacific Northwest National Laboratory
RMS	root mean square

RMSE	root mean square error
RPT	Reference Performance Test
RTE	round-trip efficiency
SCADA	supervisory control and data acquisition
SEL	Schweitzer Engineering Laboratory
SOC	state of charge
TES	Turner Energy System
TESS	Turner Energy Storage System
TTD	time to derate
UET	UniEnergy Technologies
VAC	voltage alternating current
var	volt ampere reactive
VDC	voltage direct current
V	volts
W	watt
Wh	watt hour(s)

Contents

Executive Summary iii
Acknowledgments xiii
Acronyms and Abbreviations xv
1.0 Introduction 1.1
2.0 Avista Battery 2.1
2.1 Battery Energy Storage System Layout 2.1
2.2 Battery Technical Specifications 2.2
2.3 Battery Management System 2.4
2.4 Energy Throughput 2.4
2.4.1 Power Conversion System One-Way and Round-Trip Efficiency 2.6
2.4.2 Thermal Management 2.7
2.4.3 DC Round-Trip Efficiency 2.9
2.4.4 SOC Decrease during Rest 2.9
2.4.5 VAR Consumption or Delivery during Real Power Requests 2.10
2.4.6 Site Control System 2.11
3.0 Battery Performance Test Results 3.1
3.1 Baseline Test Results 3.2
3.2 Response Time/Ramp Rate Test 3.9
3.3 Frequency Regulation Test 3.16
3.4 Baseline Peak Shaving 3.20
3.5 Use Case 1: Energy Arbitrage 3.21
3.5.1 Duty Cycle Summary 3.21
3.5.2 Test Results 3.22
3.6 Use Case 1: System Capacity 3.23
3.6.1 Duty Cycle Summary 3.23
3.6.2 Test Results 3.23
3.7 Use Case 2: Regulation 3.25
3.7.1 Duty Cycle Summary 3.25
3.7.2 Test Results 3.25
3.8 Use Case 2: Frequency Regulation Auto 3.27
3.8.1 Duty Cycle Summary 3.27
3.8.2 Test Results 3.27
3.9 Load Following 3.29
3.9.1 Duty Cycle Summary 3.29
3.9.2 Test Results 3.29
3.10 Use Case 3: Load Shaping dpdt 3.31

3.10.1 Duty Cycle Summary 3.31
3.10.2 Test Results 3.31
3.11 Use Case 3: VAR Support – Power Factor Regulation 3.33
3.11.1 Duty Cycle Summary 3.33
3.11.2 Test Results 3.33
3.12 Use Case 3: Deferment of Distribution Upgrade – Peak Shaving Dynamic 3.36
3.12.1 Duty Cycle Summary 3.36
3.12.2 Test Results 3.36
3.13 Use Case 5: Enhanced Voltage Control 3.39
3.13.1 Duty Cycle Summary 3.39
3.13.2 Test Results 3.39
3.14 Use Case 6: Microgrid Operations 3.41
3.14.1 Duty Cycle Summary 3.41
3.14.2 Test Results 3.42
3.15 Use Case 7: Optimal Utilization of Energy Storage 3.42
4.0 Lessons Learned 4.1
4.1 Lessons Learned from Test Results 4.1
4.2 Lessons Learned in Design of Data Transfer 4.2
4.3 Lessons Learned in Design of Test Setup 4.2
4.4 Lessons Learned from Site Related Issues 4.3
5.0 Novel Findings 5.1
5.1 State-of-Charge Model 5.1
5.2 Temperature Change Analysis 5.2
6.0 Conclusions 6.1
7.0 References 7.1
Appendix A – Supplemental Information A.1

Figures

1.1 Main Components of the Use Case Analysis Project 1.1
2.1 1 MW, 3.2 MWh FBESS at Schweitzer Engineering Laboratory 2.1
2.2 One-Line Diagram of 1 MW, 3.2 MWh FBESS at SEL 2.2
2.3 FBESS Cumulative Performance at the Grid 2.5
2.4 Cumulative RTE for Both Strings 2.5
2.5 Cumulative Charge and Discharge Ampere Hours and Coulombic Efficiencies for String 2 ..... 2.6
2.6 PCS Conversion Power Losses (left) and One-Way Efficiency (right) 2.7
2.7 Single-String Auxiliary Power Consumption during Charge, Discharge, and Rest as a Function of Deviation from Various Temperatures 2.8
2.8 Auxiliary Consumption at Various Charge and Discharge Power Levels 2.8
2.9 DC RTE for Baseline Capacity Tests 2.9
2.10 Effect of PCS State and Reactive Power on DC Power Consumption during Rest 2.10
2.11 Reactive Power as a Function of Requested Power for Post-Baseline and Post-Cycle Tests 2.10
2.12 Control Architecture for UET FBESS 2.11
2.13 FBESS Modes of Operation 2.12
3.1 MESA 2 Power Flow Schematic 3.1
3.2 Reference Performance Test Profiles 3.5
3.3 Reference Performance Test DC Voltage and Current Profiles 3.5
3.4 FBESS Performance Curves from Baseline Tests 3.7
3.5 Energy Charged or Discharged at the Grid and PCS Levels as a Function of FBESS SOC 3.8
3.6 Battery Temperature Profile during RPT Capacity Tests 3.9
3.7 Requested Power from Data and From Schedule File during the Pulse Test 3.10
3.8 Difference between Time Stamp for Requested Power Data and Schedule File Time Stamp during the Pulse Test 3.10
3.9 RMS Error between Requested and Scheduled Power as a Function of Lag during the Frequency Regulation Test 3.11
3.10 FBESS Response with Signal Request 3.12
3.11 Reference Performance Test for Response Time, Ramp Rate, and Internal Resistance 3.13
3.12 Voltage and Current during Pulse Tests 3.14
3.13 In Situ Charge and Discharge Resistance for Each String 3.16
3.14 Frequency Regulation US DOE-OE ESS Performance Protocol Tests 3.17
3.15 Error and Absolute Error as a Function of Power during the Baseline Frequency Regulation Test 3.18
3.16 Frequency Regulation Profile for Run 2 with Requested Power Removed for Clarity 3.18
3.17 Error Distribution for Frequency Regulation Test 3.20
3.18 Baseline Peak Shaving Test Profiles 3.21
3.19 Energy Arbitrage Test Profiles 3.22

3.20 System Capacity Test Profiles 3.24
3.21 Frequency Regulation Test Profiles – Duty Cycle and Response 3.26
3.22 Frequency Regulation Test Error Distribution 3.27
3.23 Frequency Regulation Auto Test Error Distribution 3.28
3.24 Frequency Regulation Auto Test Error Distribution 3.29
3.25 Load Following Test Error Distribution 3.30
3.26 Load Following Test Profiles 3.30
3.27 Load Shaping Test Profiles 3.32
3.28 Load Shaping Test Error Distribution 3.33
3.29 VAR Support Power Factor Regulation Test Error Distribution 3.35
3.30 VAR Support Power Factor Regulation Test Profile 3.35
3.31 Dynamic Peak Shaving Error Distribution for Reactive Power 3.37
3.32 Dynamic Peak Shaving Test Profiles 3.38
3.33 Error Distribution for IVVC 3.40
3.34 CVR/IVVC Grid Service 3.41
5.1 Example of dSOC/dt vs SOC for an Example Half-Cycle 5.1
5.2 Example of Applying Non-Linear Model 5.2
5.3 Temperature Change for the Various Baseline Capacity Tests for Charge, Rest, and Discharge 5.3

Tables

1.1 CEF Project Use Cases 1.2
2.1 Technical Specifications for the UET Battery String 2.3
2.2 Technical Specifications for the 600 kW, 2,200 kWh UET FBESS String 2.3
2.3 Regression Parameters for Inverter Losses vs. Inverter Power 2.7
2.4 Auxiliary Power Regression 2.8
3.1 Baseline Reference Performance Capacity Test Results 3.4
3.2 Overview of RPT Results 3.6
3.3 Performance Comparison with Technical Specifications for the Avista Turner FBESS 3.15
3.4 Frequency Regulation Test Results 3.19
3.5 Baseline Peak Shaving Results 3.21
3.6 Energy Arbitrage Test Results 3.22
3.7 System Capacity Test Results 3.24
3.8 Frequency Regulation Test Results 3.26
3.9 Frequency Regulation Auto Test Results 3.28
3.10 Load Following Test Results 3.31
3.11 Load Shaping Test Results 3.32
3.12 VAR Support Power Factor Regulation Test Results 3.36
3.13 Dynamic Peak Shaving Test Results 3.38
3.14 CVR-IVVC Test Results 3.41
5.1 Regression Constants for Non-Linear Model 5.2
5.2 Regression Results for Rate of Temperature Change as Function of Power, Power Squared, and Difference between FBESS and Ambient Temperature 5.3

1.0 Introduction

Pacific Northwest National Laboratory (PNNL) was chosen to provide analytical support under the Use Case Analysis Project. This project is designed to assist flow battery energy storage system (FBESS) grid integration efforts by providing a framework for evaluating the technical and financial benefits of the energy storage system (ESS) and exploring the role of energy storage in delivering value to utilities and the citizens they serve. This framework, and the tools used to implement it, will evaluate a number of use cases as applied to energy storage projects deployed by the participating utilities under the Clean Energy Fund (CEF) program. The methodologies that emerge from this project for evaluating multiple storage benefits, and the detailed operational results from utility use of energy storage, will have broad national relevance and applicability. As depicted in Figure 1.1, Use Case Test Support, Technical Performance Analysis, and Economic Evaluation are the three main components in the Use Case Analysis Project.

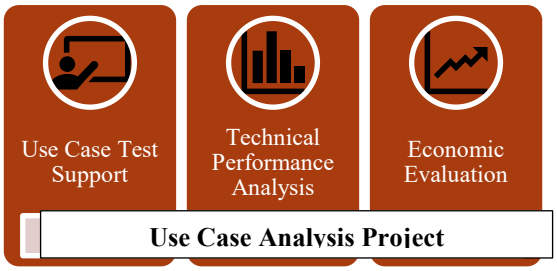

Figure 1.1. Main Components of the Use Case Analysis Project

This report documents baseline and use case technical performance of the Avista Turner FBESS based on the framework and approaches defined by PNNL in the test plan report, and the lessons learned on the technical aspects of the Avista Turner FBESS. The technical support provided by PNNL included:

1. Development of protocols and duty cycles to test the ability of the FBESS to safely and effectively be used for the tested use cases.
2. Determination of performance metrics (e.g., ramp rate, round-trip efficiency [RTE], internal resistance, etc.) to be evaluated.
3. Analysis of test results against a predefined set of performance metrics to determine the effectiveness of storage for each use case.
4. The baseline testing used cycles intended to quantify basic FBESS characteristics including power and energy capacities, ramp rate/response time and internal resistance. Reference performance for this project's FBESS used several duty cycles defined and described in the U.S. Department of Energy (DOE) Energy Storage Protocol and were performed at the beginning of the project (baseline tests). Because of string failure, reference performance tests (RPT) could not be repeated after use case testing.
5. This project designed and tested six use cases. These use cases combined several energy storage applications as follows:
    a. Use Case 1 consisted of energy arbitrage and system capacity.
    b. Use Case 2 consisted of regulation, load following, and real-world flexibility.
    c. Use Case 3 consisted of volt/volt ampere reactive (var) control with local and/or remote information and load shaping.

d. Use Case 5 consisted of enhanced voltage control during conservation voltage reduction events.

e. Use Case 6 consisted of grid-connected and islanded microgrid operations including black start, microgrid operation when grid connected, and microgrid operation in islanded mode. Test results were not shared with PNNL.

f. Use Case 7 involved optimal utilization of the FBESS across Use Cases 1-3. This use case could not be conducted as testing was stopped due to string failure.

These use cases were selected from the full set of use cases being evaluated across several CEF FBESS projects. Table 1.1 illustrates the full range of use cases under investigation and those are relevant to this specific project.

Table 1.1. CEF Project Use Cases

Use Case and application as described in PNNL Catalog	Avista	PSE	Sno – MESA1	Sno – MESA2	Sno - Controls Integration
UC1: Energy Shifting					
Energy shifting from peak to off-peak on a daily basis	Y	Y	Y	Y	
System capacity to meet adequacy requirements	Y	Y	Y	Y	
UC2: Provide Grid Flexibility					
Regulation services	Y	Y		Y*	
Load following services	Y	Y		Y*	
Real-world flexibility operation	Y	Y		Y*	
UC3: Improving Distribution Systems Efficiency					
Volt/Var control with local and/or remote information	Y		Y	Y	
Load-shaping service	Y	Y	Y	Y	
Deferment of distribution system upgrade	Y	Y			
UC4: Outage Management of Critical Loads		Y			
UC5: Enhanced Voltage Control					
Volt/Var control with local and/or remote information and during enhanced CVR events	Y				
UC6: Grid-connected and islanded micro-grid operations					
Black Start operation	Y				
Micro-grid operation while grid-connected	Y				
Micro-grid operation in islanded mode	Y				

This project developed the composite cycle profiles and used these for testing the project FBESS for these use cases scenarios. The duty cycles and associated test results are described and discussed in the body of the report.

As the baseline and use case tests were conducted, PNNL analyzed test results against a predefined set of performance metrics such as ramp rate, RTE, and internal resistance to determine the effectiveness of storage for each use case.

Understanding of the technical features and limitations is essential and provides much of the input data used to perform the economic evaluation of the use cases to which a FBESS is subjected. Therefore, technical information on the Modular Energy Storage Architecture (MESA 2) (MESA 2016) FBESS is provided in the following section.

2.0 Avista Battery

2.1 Battery Energy Storage System Layout

The 1 MW, 3.2 MWh vanadium redox FBESS evaluated in this project consists of four strings, each rated at 0.5 MW and 1.6 MWh. The system is shown in Figure 2.1. The stack contains only a small amount of the total electrolyte volume needed for the system. Hence, short circuit conditions are not expected to result in thermal runaway.[1] Pumps are operated to remove heat at high states of charge (SOC), and temperature mitigates thermal runaway conditions. The hydrochloric and sulfuric acid content is less than 10%, which is a factor of three lower than that for lead-acid batteries. Each battery container has three 50 kW stacks connected in series.

Figure 2.1. 1 MW, 3.2 MWh FBESS at Schweitzer Engineering Laboratory (SEL). Two strings each containing four battery modules and a Power Conversion System (PCS) container with Battery Management System (BMS) are shown.

Each string consists of five containers, with four battery containers housing the stacks and electrolyte, with the fifth container housing the PCS and associated controls. The strings are connected in parallel at the PCS level to the grid. The arrangement of the two strings is also shown in Figure 2.2.

Within each string during charge, auxiliary power flows via 45 kVA 283 VAC – 480V AC transformers to the auxiliary load for cooling and pumping needs, with the remaining power directed to the AC side of the 600 kVA bi-directional AEG inverter with a DC range of 450 to 1,000 voltage direct current (VDC), and a maximum efficiency of 98.4%. During discharge, the DC battery powers the auxiliary load by sending power through a bi-directional inverter to the 45 kVA transformer.

There are no meters to measure auxiliary power flow. Additionally, there are no meters to measure power exchange with the grid at the 283 V side of transformer T1-X. Power exchange with the grid is measured only at the 15-kV level. Hence, estimation of auxiliary load includes losses related to transformer T1-X one-way efficiency.

Additional details on the site layout are provided in Appendix A (Figure A.4 and Figure A.5).

[1] Tests were not performed to verify this.

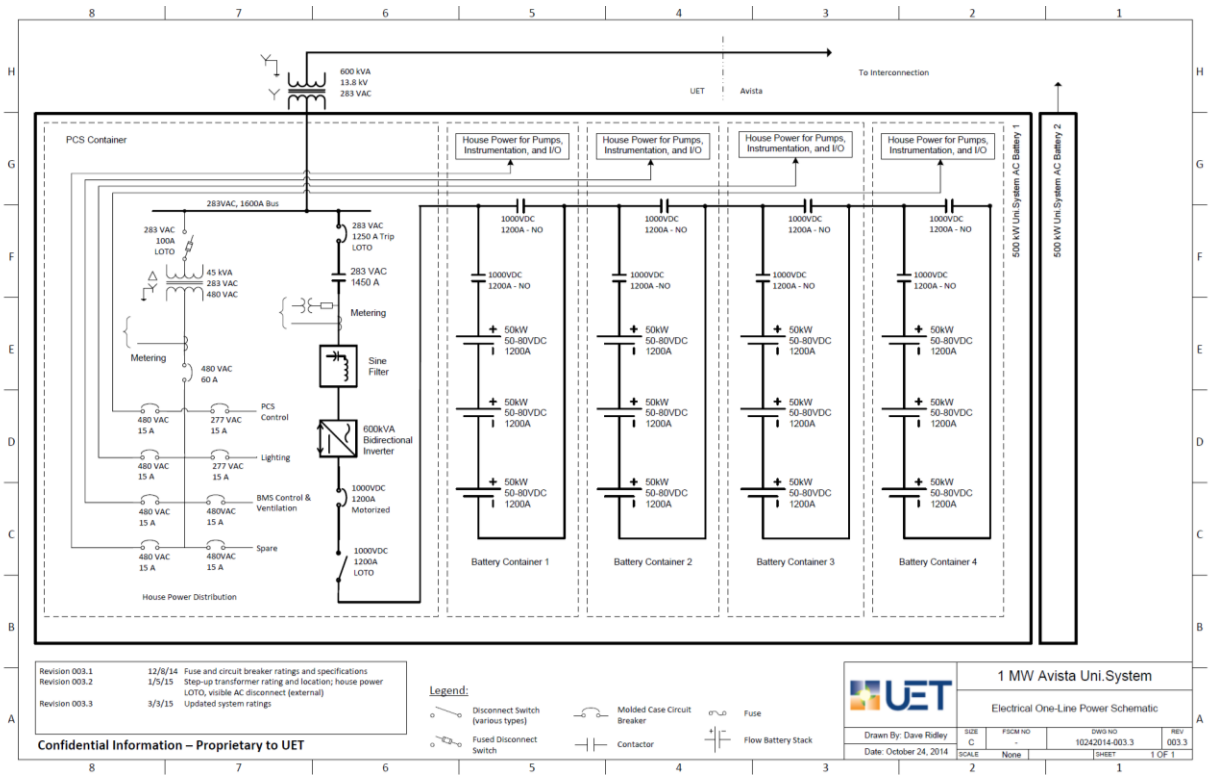

Figure 2.2. One-Line Diagram of 1 MW, 3.2 MWh FBESS at SEL

2.2 Battery Technical Specifications

According to the UniEnergy Technologies (UET) Product Sheet, the DC FBESS consists of two strings, each rated at 600 kW AC and 2.2 MWh AC. Each string has five containers, with four containers containing three 50 kW series-connected stacks and electrolyte tanks within each, and the fifth containing the PCS. The three series-connected stacks within each container are also referred to as 150 kW battery modules. To bypass faulty modules, DC contactors, rated at 1,000 VDC, 1,200A, and connected in parallel with each module but normally in the OPEN state, allow faulty modules to be bypassed. In addition, DC contactors, rated at 1,000 VDC, 1,200A, are connected in series with each module. Per a UET engineer, these contactors are normally in the CLOSED position. When there is a fault in the string, the DC contactor in parallel with the string opens. Immediately afterward, the series-connected contactor is opened.

For the containers housing stacks and tanks, secondary containment is built-in. The electrolyte is reusable, but it is not clear if infrastructure is in place to recycle and/or reuse stack components. The containers are rated to transport and seismic codes.

The technical specifications for this AC battery string is shown in Table 2.1 (Schenkman and Borneo 2015).

The nameplate rated power provides only 2 MWh, while the nameplate energy is obtained at 520 kW. These values are in line with the findings of this work. The maximum DC current was -1,000 amperes (A) (or -2,000 A for two strings) during discharge and 800 A (or 1,600 A for two strings) during charge (UET 2015). As seen later, 1850 A was the maximum discharge DC current observed during this work for a 1,000 kW discharge, while the maximum charge current was 900 A for two strings.

Table 2.1. Technical Specifications for the UET Battery String

Nameplate and Peak Power, AC	1 MW, 1.2 MW
Maximum Energy, AC	3.2 MWh
Rated Power: Discharge Duration, AC	1 MW: continuous cycling, 1 MW at 2 hr, 640 kW at 4 hr, 520 kW at 6.2 hr
Efficiency	65-70% AC round trip at the inverter
Self-Discharge	<2% in standby mode
Cycle Life	Unlimited cycles within system design life
System Design Life	20 years
DC Voltage Range	465 VDC – 1,000 VDC
AC Voltage Output	Medium Voltage (4,160 VAC – 34.5 kVAC)
Power Factor (PF) Range	Available Option
Power Control Modes	Dispatch and Autonomous, 50 ms response time
Communications and Data Protocols	DNP 3.0 or IEC 61850
Ambient Temperature	-40°C to 50°C, active cooling for extended operation

Additional technical specifications for each string were provided by UET as part of the MESA 2 work for the Snohomish County Public Utility District (see Table 2.2) (UET Undated).[2] The energy and power ratings have been removed, while the parameters that are common to the Avista tests have been retained.

Table 2.2. Technical Specifications for the 600 kW, 2,200 kWh UET FBESS String

Parameter	Value
AC RTE	70%
AC Voltage, kV	12.47
Response Time (ms)[(a)]	<100
Reactive Power (kvar)	±450
Humidity	95% noncondensing
Footprint, m^2	76
Envelop (m)	12.5 W × 6.1 D × 2.9 H
Volume (m^3)	221.125
Weight (kg)	170,000
Wh/L	9.9
W/L	2.7
Wh/kg	12.9
W/kg	3.5
Cycle life	Unlimited over the 20-year design life
Ambient Temperature (°C)	-40 to 50
Self-discharge rate[(b)]	Maximum of 2% of stored energy

(a) The definition of response time was not given in the technical specifications.
(b) Self-discharge rate has not been defined adequately.

[2] This specification was for the next generation product installed at MESA 2.

2.3 Battery Management System

The control architecture is described in this section.

The battery management system (BMS) distributes power between the two strings according to a proprietary algorithm. Both the BMS and the site controller, which sends signals to the FBESS using a scheduler named "the Izer," ensure that the maximum power rating of the string of 500 kW during discharge and 400 kW during continuous charge is not exceeded. This provides a dual layer of safety. Note that for short durations, the maximum charge power is 900 kW.

Each string operates independently of the other. If one string fails, the other string continues performing grid services and provides or absorbs the required real and/or reactive power, subject to the per-string power ratings.

Each string has five containers, four containing one battery module each and the fifth consisting of the bi-directional power inverter with the BMS. Each battery module has three 50 kW stacks connected in series, with each stack consisting of 50 series-connected cells with open circuit voltage limits of 1.25 V on the low end to 1.49 V on the high end. The 1.25 V/cell is denoted as 0% SOC, while 1.49 V/cell is denoted as 100% SOC. Open circuit voltage is measured for each battery module separately by placing reference electrodes in the flow path of the catholyte and anolyte and measuring the potential difference.

During operation, the BMS monitors the string SOC and ensures it stays in the 0% SOC to 100% SOC range. The SOC is calculated from the measured open circuit voltage for the four battery modules in each string, with SOC varying linearly from 0 to 100% as the open circuit voltage increases from 1.25 V to 1.50 V. This linear relationship is extrapolated to yield a negative SOC, -100% at 1.00 V. If any module voltage within the four-module string reaches an average voltage of 1.00 V/cell, the string is automatically faulted and disconnected from the grid.

String faults occur for a variety of reasons. One reason is a low performing stack within the string. If all stacks are uniform in terms of design and performance, the modules with each string will remain well balanced after balancing performed during scheduled maintenance. During the execution of this project, stack-related delays contributed to the highest percent of lost time. Most of this time corresponded to time needed to replace stacks, as opposed to time lost due to stack failure.

2.4 Energy Throughput

During testing, all four strings were available for only a fraction of the time. The availability of number of strings as percent of test time is given below:

- One string: 36%
- Two strings: 64%
- The availability of each string follows:
  - String 1: 69% of the time tested
  - String 2: 90% of the time tested.

The cumulative performance of individual strings is captured by Figure 2.3. String 1 was out of commission after March 26, 2016, and had a cumulative energy throughput of 125 MWh, or 78 full discharges. String 2 had 165 MWh cumulative energy throughput, corresponding to 103 full discharges.

The cumulative RTE with and without auxiliary load were nearly the same for both strings, at 52 and 60%, respectively (Figure 2.4). A data hole that made it appear as if the FBESS was charging, resulting in a steep drop in RTE, was removed. The corresponding DC values, along with ampere hours throughput and coulombic efficiency also are shown. DC data was available for only String 2. The battery DC-DC RTE tracked the AC-AC RTE at the PCS level, with cumulative RTE of 64%.

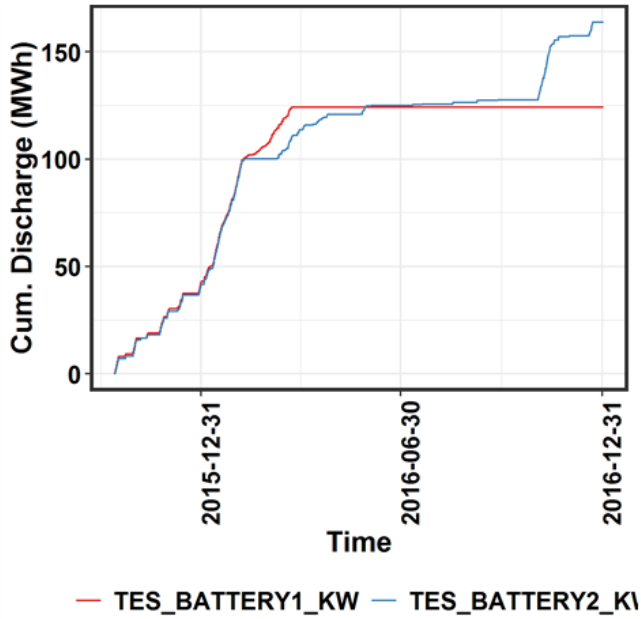

Figure 2.3. FBESS Cumulative Performance at the Grid

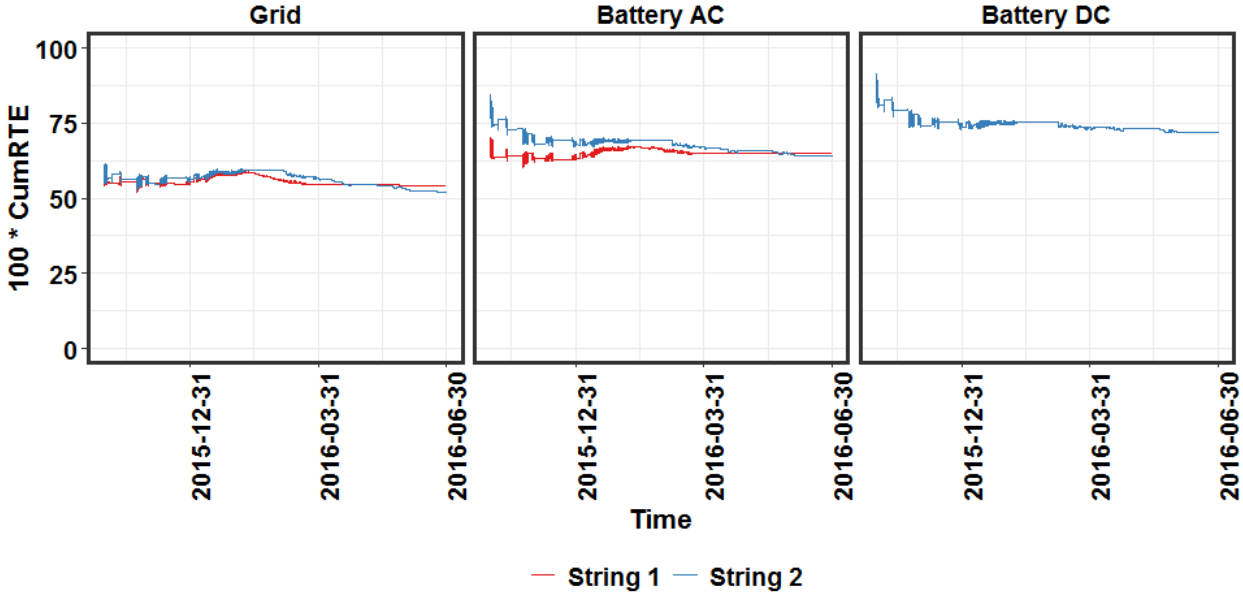

Figure 2.4. Cumulative RTE for Both Strings

The cumulative charge and discharge ampere hours, along with coulombic efficiencies for String 2 is shown in Figure 2.5. The coulombic efficiency was close to 100% initially and decreased with time, ending up at 95%, which is indicative of electrolyte crossover.

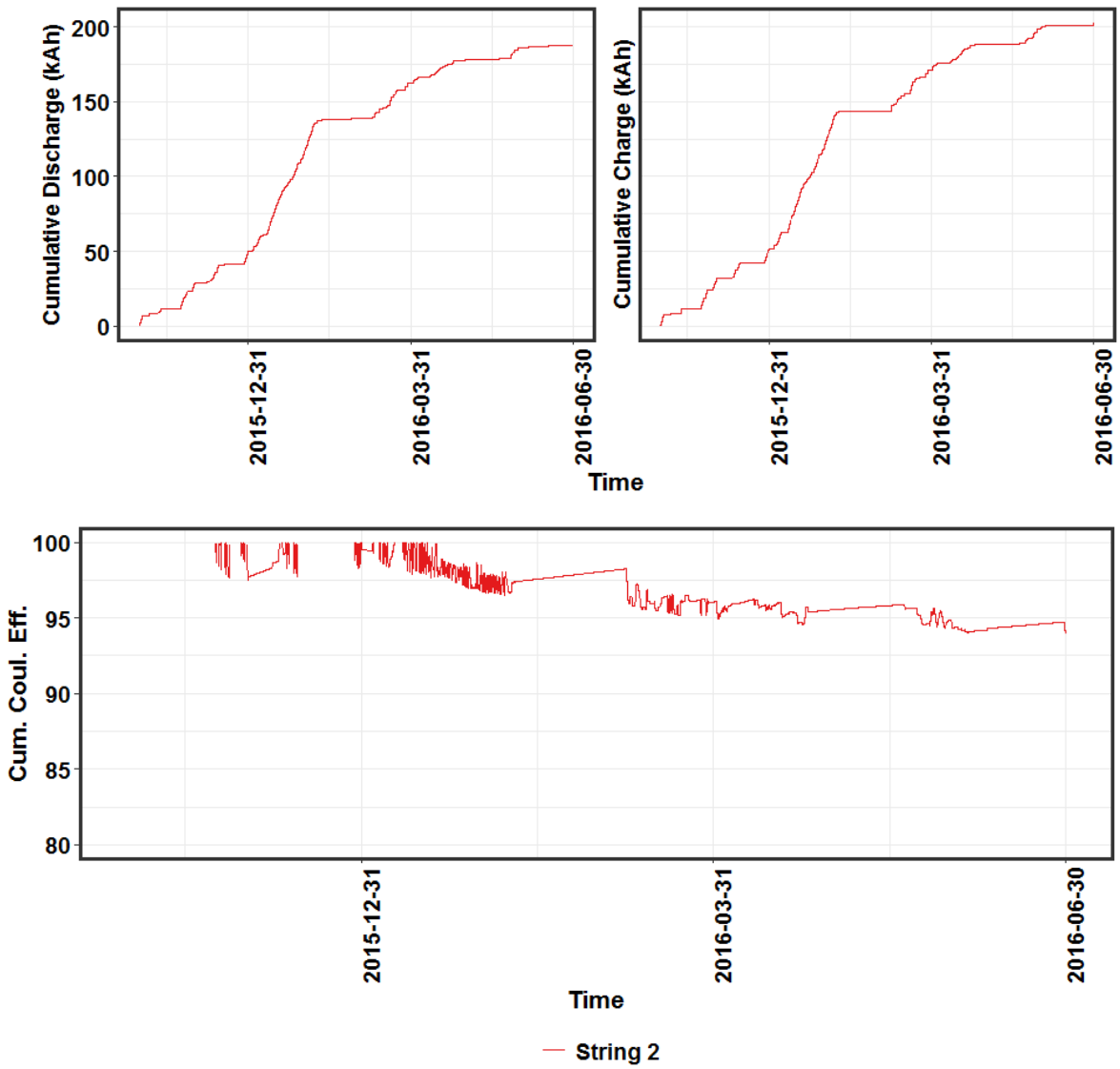

Figure 2.5. Cumulative Charge and Discharge Ampere Hours and Coulombic Efficiencies for String 2

2.4.1 Power Conversion System One-Way and Round-Trip Efficiency

The ratio of PCS power to DC power is inverter one-way efficiency during discharge, while the ratio of DC power to PCS power during charge is one-way efficiency during charge. The difference between DC power and PCS power is plotted below in Figure 2.6. For a fixed power, losses during charge are less than losses during discharge. The DC voltage range for the FBESS is 400 to 1,000 VDC, while the inverter AC side is at 283 VDC. According to UET, inverters are most efficient when the DC side voltage is the AC voltage multiplied by the square root of 2 ($283 \times \sqrt{2} = 400$) (Ridley 2019). The DC voltage during discharge is closer to 400 V than during charge at the same power and SOC.

Regression of the losses with respect to PCS power gives the coefficients in Table 2.3, with an adjusted R^2 of 0.63. The PCS one-way efficiency is >0.95 at power levels less than -1,000 kW and more than 1,000 kW. As expected, the efficiency at a low percent of rated power decreases. At 500 kW discharge, the one-way efficiency is surprisingly low at 0.93.

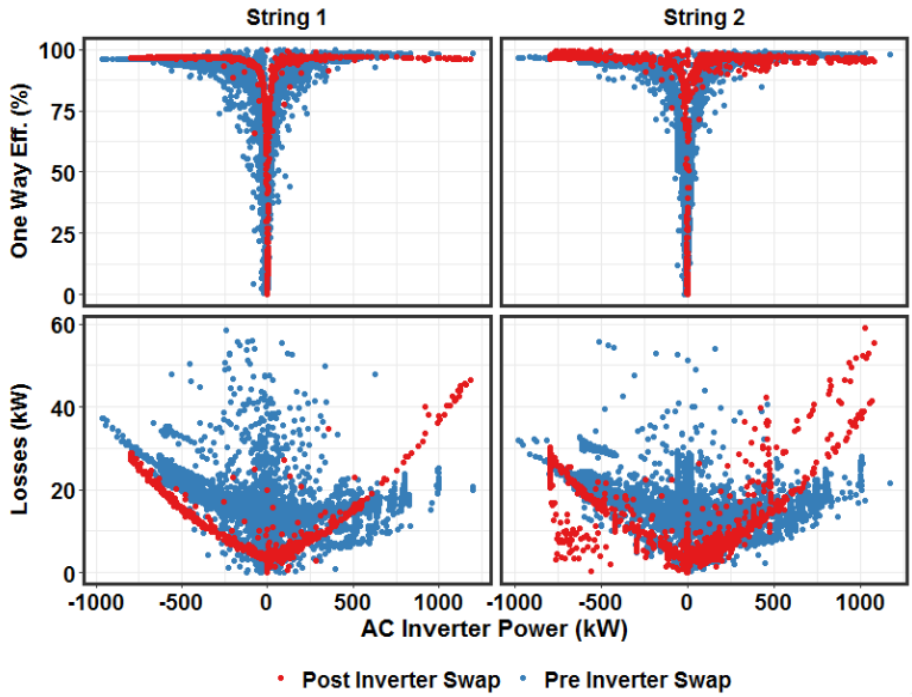

Figure 2.6. PCS Conversion Power Losses (left) and One-Way Efficiency (right)

Table 2.3. Regression Parameters for Inverter Losses vs. Inverter Power

Parameter	Coefficient	Standard. Error	Units
Intercept	13.7	0.0512	kW
Power	-0.00992	0.000147	kW/kW
Power Squared	6.54e-05	7.58e-07	$(kW/kW)^2$

After the inverter swap, the losses at 0 kW inverter power decreased from 14 kW for the AEG inverter to 5 kW for the Northern Power Systems (NPS) inverter. However, the losses increased with increased magnitude of power much faster for the new inverter, resulting in lower inverter efficiency at the highest discharge rates.

2.4.2 Thermal Management

Auxiliary power consumption decreases with decreasing battery temperature and decreasing ambient temperature. This is consistent with the fact that thermal management consists only of cooling. Hence, low temperature corresponds to less auxiliary power consumption. According to UET, the auxiliary power consumption per string is 12 kW without cooling and 18 kW with cooling. Cooling is activated when providing continuous power at >35°C and any time the temperature exceeds 40°C (Sun 2015). For a two-string system, this corresponds to 24 kW and 36 kW, respectively. Based on linear regression, the data show that the auxiliary power consumption is in the 15 to 20 kW range per string for both strings (Figure 2.7), with auxiliary power consumption increasing with ambient or FBESS temperature.

The auxiliary consumption was regressed vs. temperature, power, and power squared with an adjusted R^2 of 0.47 as shown in Figure 2.7 and Table 2.4. Figure 2.7 shows auxiliary consumption at various charge and discharge power levels and during rest. At rest, auxiliary power per string is ~10 to 12 kW, which is in line with information provided by UET (Sun 2015).

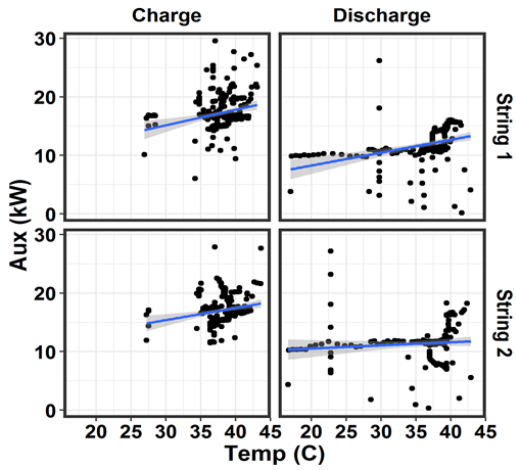

Figure 2.7. Single-String Auxiliary Power Consumption during Charge, Discharge, and Rest as a Function of Deviation from Various Temperatures

Table 2.4. Auxiliary Power Regression

Parameter	Coefficient	Standard Error	Units
Intercept	8.81	0.969	kW
Temperature	0.134	0.025	kW/C
Power	-0.00967	0.000401	kW/kW
Power Squared	7.07e-06	2.64e-06	kW/kW^2

Auxiliary power consumption increased with increasing temperature and was less during discharge at fixed power. The higher auxiliary consumption at fixed power for charge compared to discharge is counter-intuitive because the charge process is thermodynamically endothermic. As seen later in Figure 3.6, the average temperature during charge and discharge is nearly the same. One explanation is that charge requires a greater flow rate per kilowatt to prevent gas evolution by facilitating faster mass transport and lowering over-potential. The charge resistance is lower than discharge resistance across the SOC range as seen from Figure 2.8, thus lending support to this hypothesis.

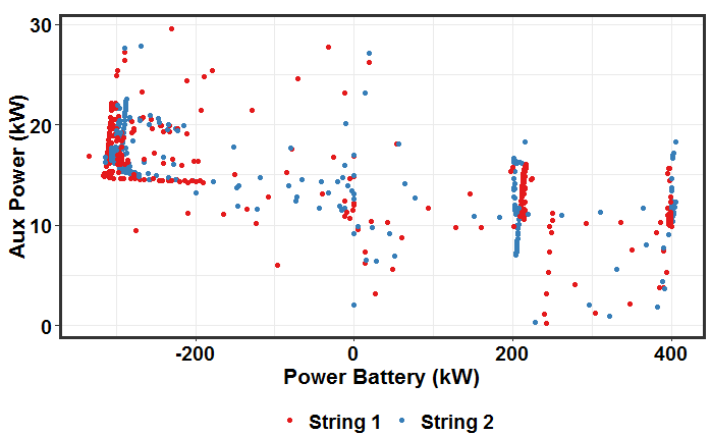

Figure 2.8. Auxiliary Consumption at Various Charge and Discharge Power Levels

Because of the cooling effect during charge and heating effect during discharge, thermal management is simplified. If ambient temperature is too high, a pre-charge brings the battery temperature to levels that prevent temperature excursions on the high side during subsequent discharge. If ambient temperature is too low, cycling at a maximum charge rate of -400 kW and a discharge rate of 500 kW brings the battery temperature to normal operating levels. Because active material precipitation occurs at the cathode side at high temperatures, cooling is done on the cathode loop. The excellent heat transfer within the stack ensures the anolyte temperature closely tracks the catholyte temperature.

2.4.3 DC Round-Trip Efficiency

DC RTE as a function of SOC was determined by taking the ratio of discharge to charge energy in the -5 to +5% SOC range for all baseline capacity tests (Figure 2.9). The taper portions are shown in blue. As expected, during charge, taper occurs at high SOCs, and during discharge, taper occurs at low SOCs. The DC-DC RTE as a function of SOC for String 2 is shown in Figure 2.9. The RTE decreased with decreasing SOC, and was highest at 520 kW. For example, at 90% SOC, the RTE at 520 kW was 84%, while at 32% SOC, it was 76%. The RTE at 90% SOC for 1000 kW discharge was 73%, while it was 61% at 50% SOC.

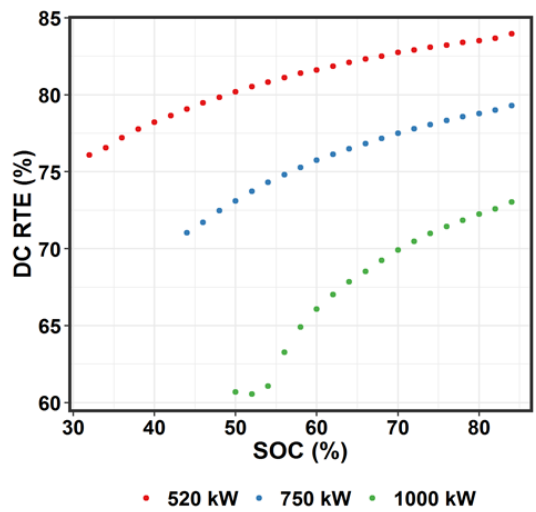

Figure 2.9. DC RTE for Baseline Capacity Tests

2.4.4 SOC Decrease during Rest

The SOC drop rate during rest is ~0.1% per hour under normal operation. Approximately 5% of the time during rest, the PCS is in a switching state. When the PCS switches, the DC current is 7 to 9 A as seen in Figure 2.10. The PCS reactive power when it switches is -0.5 to -2.5 kvar. The average DC power is 2.1 kW when the PCS switches and 1 kW when it does not switch.

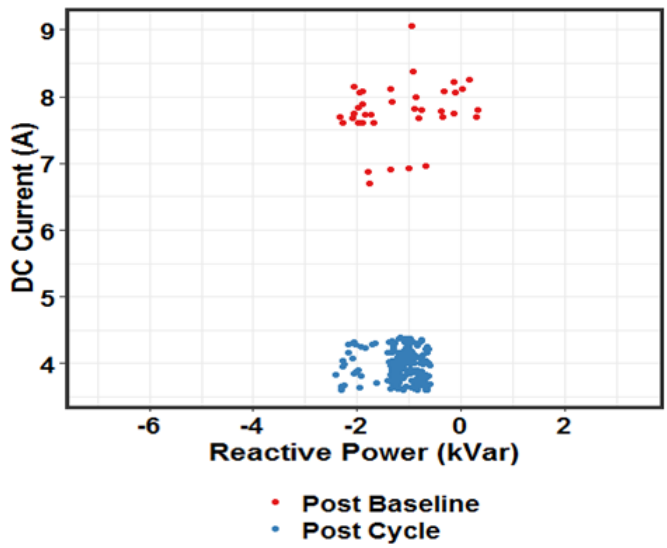

Figure 2.10. Effect of PCS State and Reactive Power on DC Power Consumption during Rest

2.4.5 VAR Consumption or Delivery during Real Power Requests

Var consumption during various real power requests is shown in Figure 2.11. For all charge power levels, the FBESS absorbed inductive vars that increased slightly from 3 kvar at 200 kW charge to 5 kvar at 600 kW charge. Capacitive kvars increased more steeply with increasing discharge power levels from 5 kvar at 170 kW to 12 kvar at 520 kW discharge. This may be because the maximum PF for the inverter may be slightly less than 1.0. At rest, the inverter provided 0 to -2.5 kvar. The inverter switched for 5% of the time during rest. Auxiliary load is always powered from the grid. Hence, during rest, the PCS does not have to provide switching. For cases in which it does switch because it is connected to the grid, the grid can provide the power needed for this switching.

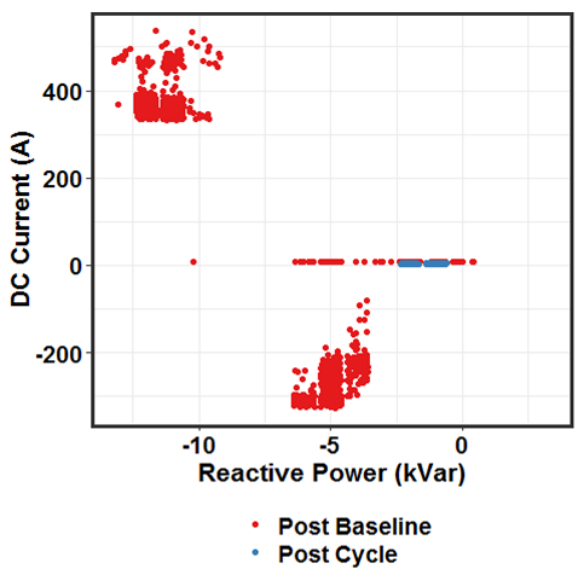

Figure 2.11. Reactive Power as a Function of Requested Power for Post-Baseline and Post-Cycle Tests

2.4.6 Site Control System

The control architecture for the UET FBESS is shown in Figure 2.12 (Siemens Undated). Key components from the Siemens Totally Integrated Architecture portfolio were integrated with software engineering via the Totally Integrated Architecture Portal. A Siemens WinCC supervisory control and data acquisition (SCADA) software and small Siemens variable frequency drives were some of the key Siemens components used.

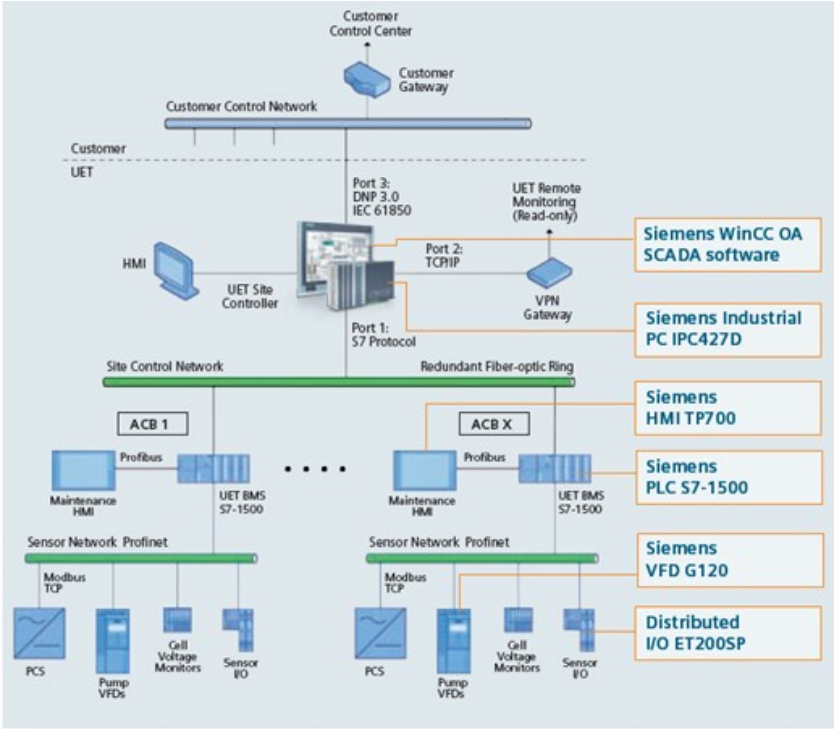

Figure 2.12. Control Architecture for UET FBESS

Each string is controlled by a single Siemens Programmable Logic Controller, which is the master while the PCS in each string is the slave. The Programmable Logic Controller has two isolated ports: one port communicates with the local instrument network such as the various metering devices while the other port communicates with the SCADA network. The SIMATIC WinCC Open Architecture SCADA, using the object-oriented architecture of the WinCC Open Architecture, allows a generic template to be built for battery data, thus enabling incorporation of multiple batteries.

The WinCC software provides an interface for interactions between maintenance staff and the FBESS. Industrial ethernet switches provide communications between containers and avoid the need for multiple analog and digital wires. The SINAMICS Siemens G120 variable frequency drives run the electrolyte pumps in each container. The electrolyte flow rate is optimized for the power needs to minimize pumping and electrochemical losses. This is more conducive to efficient FBESS operation compared to fixed speed drives. The inputs/outputs from each container are made available on the same bus using the SIMATIC ET 200DP distributed input/output. This allows similar 20-ft containers for the flow batteries, thus taking advantage of manufacturing efficiencies.

The Siemens Totally Integrated Architecture Portal provided libraries of validated software code that could be used to implement battery logic unique to the FBESS. The “plug and play” feature of the Siemens control system reduces site-specific engineering costs.

Multiple strings can be managed by the site controller, which is the interface for the FBESS with the external energy-management or distribution-management system. Real-time notifications related to operating states and/or error conditions are provided to the site operators. The Avista FBESS was monitored by UET for error messages, which responded by sending service personnel as required to address system problems (UET 2015).[3]

The various modes of operation—connected, limited watts, constant var, PF—are shown in Figure 2.13 (UET 2015).

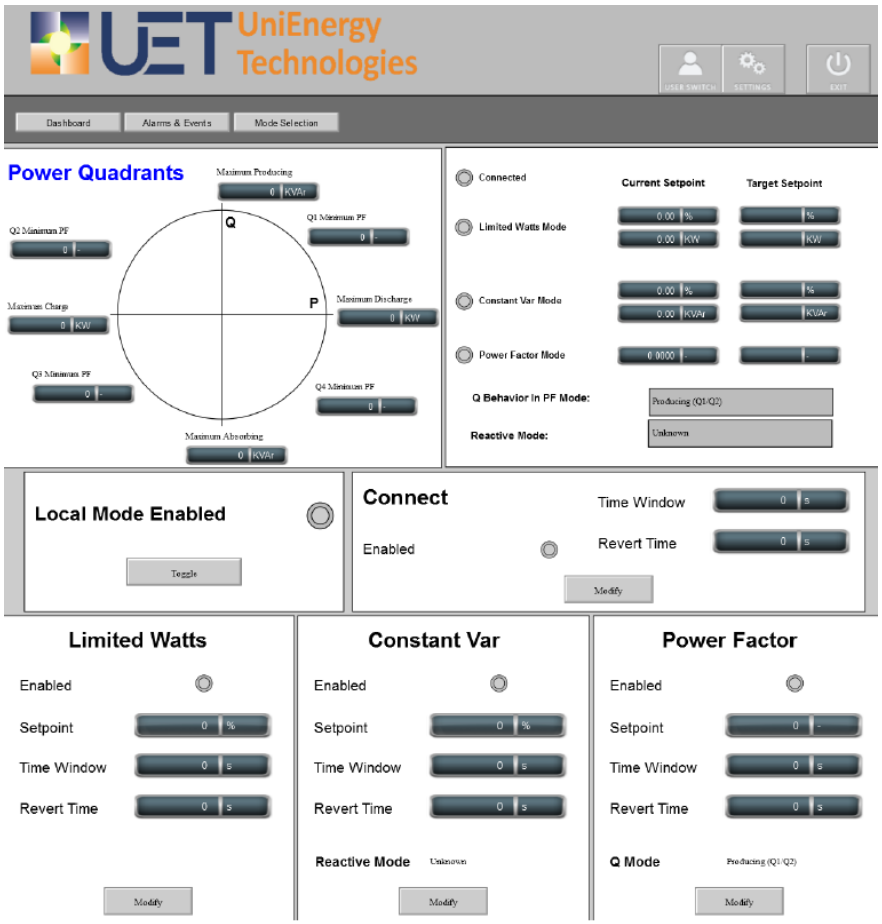

Figure 2.13. FBESS Modes of Operation

A toggle button can be used to switch the FBESS to local or remote mode. When the FBESS is in local mode, commands from the DNP3 interface will not be accepted. DNP3 is a communications protocol used in remote monitoring systems such as SCADA [DPS Telecom 2019]. In terms of command, the minimum PF for the FBESS can be specified such that kvar commands will be accompanied by suitable real power requests in each quadrant. Discharge power and capacitive vars (or producing vars) are assigned a positive sign. The connect mode needs to be enabled for the FBESS to operate in any of the other modes.

Data tags for the energy storage were set based on the SunSpec Alliance Interoperability Specification (Miller 2017).

[3] Paraphrased from document marked confidential and used with permission from UniEnergy Technologies, LLC.

3.0 Battery Performance Test Results

During the first test phase, the FBESS was subjected to baseline testing as described in the U.S. Department of Energy Office of Electricity (DOE-OE) Performance Protocol (Viswanathan et al. 2014), with discharge at various C-rates for a constant C-rate charge and at various charge rates for a constant rate discharge. Response times and ramp rates were measured at various SOCs, along with charge and discharge resistance. The results of these tests are presented in this chapter. The battery was hypothesized to be set up as shown in Figure 3.1, with meters measuring the power at P_{Feeder} and P_{PCS}. Hence P_{Aux} must be estimated based on the values of the other two meters.

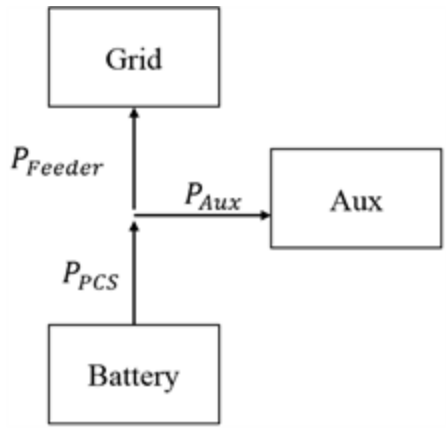

Figure 3.1. MESA 2 Power Flow Schematic

For evaluating battery performance, we used the following definitions:

$$P_{grid} = P_{Feeder}$$

$$P_{batt} = P_{PCS}$$

$$P_{grid} = P_{batt} - P_{aux}$$

$$E_{Chg} = \int \left(P_{grid} < 0\right) P_{grid} dt$$

$$E_{Dis} = \int \left(P_{grid} > 0\right) P_{grid} dt$$

$$E_{Chgnorest} = \int \left(P_{req} < 0\right) P_{grid} dt$$

$$E_{Disnorest} = \int \left(P_{req} > 0\right) P_{grid} dt$$

$$E_{Chgnoaux} = \int \left(P_{req} < 0\right) P_{batt} dt$$

$$E_{Disnoaux} = \int \left(P_{req} > 0\right) P_{batt} dt$$

$$RTE = -\frac{E_{Dis}}{E_{Chg}}$$

$$RTE_{norest} = -\frac{E_{Disnorest}}{E_{Chgnorest}}$$

$$RTE_{noaux} = -\frac{E_{Disnoaux}}{E_{Chgnoaux}}$$

3.1 Baseline Test Results

The RTE ranged from 57 to 65% when rest and auxiliary consumption were included, increasing to 63 to 75% when auxiliary consumption was excluded (Table 2.4). The rest was a small fraction of test duration at 2%, hence, RTE when excluding rest increased by 1 to 2 percentage points. The RTE increase without auxiliary consumption ranged from 6 to 13%, with higher increases when charge or discharge power was lower.

For constant power charge, RTE peaks at 520 kW discharge when auxiliary consumption is included. Excluding auxiliary consumption, the RTE increased with decreasing discharge power, thus reflecting higher DC efficiency at low power levels. Note that PCS efficiency decreases rapidly at <150 kW, hence, at lower power levels, the increasing RTE trend is expected to reverse. The AC-AC RTE peaks at 520 kW, while it plateaus at 400 kW discharge if auxiliary consumption is ignored. The DC-DC RTE, on the other hand, increases with decreasing power levels in the power range investigated.

Post-baseline capacity tests and post-use case capacity test were done in January and November 2016, respectively, while baseline capacity tests were done under warmer ambient conditions in September 2015. The RTE at 520 kW discharge was lowest for baseline tests at 520 kW discharge. This was probably because only the baseline capacity tests needed cooling. If auxiliary consumption was ignored, the RTE for all tests at 520 kW discharge were more tightly packed in the 72 to 76% range. This shows that the RTE without auxiliary consumption is a good proxy for DC side RTE.

At a 400 kW discharge, RTEs for baseline tests were higher than for post-cycle tests, possibly because at this low discharge rate, there is no cooling load for baseline tests done in September 2015. Excluding auxiliary consumption, the same trend prevailed, but the gap had decreased. This appears to indicate auxiliary consumption was greater during post-cycle tests. This is consistent with the RTE at 520 kW being higher for post-cycle tests, possibly due to replacement stacks.

Note that temperature information was not available for baseline tests. The temperature for post-baseline tests were about 35ºC. It can be assumed that the baseline tests, done in September, would have temperatures at least as high as the post-baseline tests done in November 2015. The RTE at 520 kW discharge without auxiliary consumption was higher for post-cycle tests compared to post-baseline tests, possibly due to replacement of stacks.

While the results appear to indicate the FBESS has not degraded in the time frame from September to November 2016, stack replacements were needed to ensure performance met expectations.

The pre-and post-inverter swap results for -600 kW charge and 520 kW discharge show that the inverters perform similarly. The DC-DC RTE values indicate that in the November 2016 to April 2018 time frame, the DC performance of the FBESS was not degraded.

For the baseline tests, temperature was available for only one run on January 13, 2016. The temperature increase at 520 kW was 6ºC for the baseline run, whereas it was only 4ºC for the post-use case run.

The higher RTE at 400 kW for baseline tests indicates there is little or no cooling needed at this low power level. While it may be logical to assume the higher temperature for the baseline test leads to a higher RTE, this also should have led to a lower end SOC for this test. However, the discharge power tapered below 27% SOC, whereas for the post-cycle test, the discharge power remained constant until 18% SOC. Longer durations at 400 kW led to auxiliary consumption being a greater percent of total energy exchange for the post-cycle test. Hence, when auxiliary consumption is excluded, the gap between the baseline and post-cycle tests decreases. One possible reason the post-cycle run reaches a lower end

SOC in spite of the lower temperature could be that some stacks were replaced, thus allowing for deeper depth of discharge before power tapers.

At 520 kW, the energy delivered and RTE is lowest for baseline tests, possibly due to higher temperatures needing active cooling. The energy delivered was highest for baseline tests, once auxiliary consumption was ignored. Once the auxiliary consumption is credited to the FBESS, the highest energy of 3,318 kWh was delivered for the baseline run. The energy delivered at 750 kW is 2,480 kWh, while the RTE is 69.5%. Excluding auxiliary power, the numbers are 2,590 kWh and 69.5%.

At 1,000 kW, 2,025 kWh is obtained at an RTE of 57%. When auxiliary consumption is excluded, the numbers increase to 2,098 kWh and 63.1%. The energy delivered when auxiliary consumption is excluded was quite similar for peak shaving runs at 750 kW and 1,000 kW. Note that rest durations were higher for peak shaving, hence auxiliary consumption was also higher.

Appendix A.1 presents the results for constant power for both charge and discharge. This results in lower charge energy, lower maximum SOC, lower auxiliary losses because there is no taper, and lower discharge energy. Figure A.1 can be used by the systems planner to exercise the FBESS at various power levels to get the desired energy in and out of the FBESS without SOC excursions beyond design limits.The lower maximum SOC and lower auxiliary losses for constant power charge counteract each other. Appendix A.2 provides results that include taper for both charge and discharge. As expected, this results in higher values for discharge energy, while charge energy values remain unchanged from the results presented in Table 3.1.

Results of RPTs for the FBESS are shown in Figure 3.2 and Figure 3.3.

Table 3.1. Baseline Reference Performance Capacity Test Results

Test	Run	Cycle	Date	Duration (h)	Rest Time (min)	Strings Active	Req Discharge Power (kW)	Req Charge Power (kW)	SOC Range	Charge Energy (kWh)	Discharge Energy (kWh)	RTE	Charge Energy No Rest (kWh)	RTE No Rest	Charge Energy No Aux (kWh)	Discharge Energy No Aux (kWh)	RTE No Aux	DC RTE	Coul Eff.	Mean Temp (ºC)
Baseline	1	1	2015-09-08	16	10	2	520	600	37-100	4,704	2,929	62.3	4,691	62.4	4,295	3,070	71.5	NA	NA	NA
Baseline	2	1	2015-09-09	16	10	2	520	600	33-100	4,869	3,066	63.0	4,857	63.1	4,473	3,261	72.9	NA	NA	NA
Baseline	2	2	2015-09-10	17	16	2	520	600	29-100	4,867	2,944	60.5	4,789	61.5	4,476	3,374	75.4	NA	NA	NA
Baseline	2	Cumulative	NA	33	26	2	NA	NA	NA	9,736	6,010	61.7	9,646	62.3	8,949	6,635	74.1	NA	NA	NA
Baseline	2	Mean	NA	17	13	2	520	600	31-100	4,868	3,005	61.8	4,823	62.3	4,474	3,318	74.2	NA	NA	NA
Baseline	3	1	2015-09-15	18	10	2	400	600	38-100	4,732	2,962	62.6	4,728	62.6	4,285	3,152	73.6	NA	NA	NA
Baseline	4	1	2015-09-26	20	10	2	400	600	31-100	4,991	3,158	63.3	4,987	63.3	4,596	3,353	73.0	NA	NA	NA
Baseline	4	2	2015-09-26	20	10	2	400	600	26-100	5,122	3,316	64.7	5,118	64.8	4,740	3,539	74.7	NA	NA	NA
Baseline	4	3	2015-09-27	20	10	2	400	600	24-100	5,206	3,391	65.1	5,180	65.5	4,824	3,618	75.0	NA	NA	NA
Baseline	4	Cumulative	NA	60	30	2	NA	NA	NA	15,319	9,865	64.4	15,285	64.5	14,160	10,510	74.2	NA	NA	NA
Baseline	4	Mean	NA	20	10	2	400	600	27-100	5,106	3,288	64.4	5,095	64.5	4,720	3,503	74.2	NA	NA	NA
Baseline	5	1	2015-10-02	11	5	2	800	600	45-100	4,139	2,507	60.6	4,139	60.6	3,831	2,576	67.2	NA	NA	NA
Baseline	6	1	2015-10-10	11	10	2	800	600	50-100	3,907	2,322	59.4	3,903	59.5	3,602	2,392	66.4	NA	NA	NA
Baseline	6	2	2015-10-10	11	10	2	800	600	46-100	4,146	2,548	61.5	4,087	62.3	3,794	2,636	69.5	NA	NA	NA
Baseline	6	3	2015-10-11	11	10	2	800	600	47-100	4,114	2,558	62.2	4,106	62.3	3,714	2,636	71.0	NA	NA	NA
Baseline	6	Cumulative	NA	33	30	2	NA	NA	NA	12,167	7,428	61.1	12,096	61.4	11,110	7,664	69.0	-	-	NA
Baseline	6	Mean	NA	11	10	2	800	600	48-100	4,056	2,476	61.0	4,032	61.4	3,703	2,555	69.0	NA	NA	NA
Post-Baseline	1	1	2016-01-13	16	3	2	520	600	31-99	4,680	3,031	64.8	4,675	64.8	4,436	3,184	71.8	74.1	94.3	31.7
Post-Baseline	1	2	2016-01-13	16	2	2	520	600	30-99	4,732	3,105	65.6	4,732	65.6	4,496	3,261	72.5	75.0	94.5	34.2
Post-Baseline	1	Cumulative	NA	32	5	2	NA	NA	NA	9,412	6,136	65.2	9,407	65.2	8,932	6,445	72.2	-	-	NA
Post-Baseline	1	Mean	NA	16	3	2	520	600	30-99	4,706	3,068	65.2	4,704	65.2	4,466	3,222	72.2	74.5	94.4	32.9
Pre-Inverter Swap	1	1	2016-11-08	15	3	1	520	600	31-99	4,725	3,037	64.3	4,721	64.3	4,459	3,209	72.0	75.6	93.3	36.3
Pre-Inverter Swap	1	2	2016-11-09	15	3	1	520	600	32-99	4,670	3,041	65.1	4,666	65.2	4,401	3,226	73.3	77.1	94.9	36.9
Pre-Inverter Swap	1	3	2016-11-10	14	2	1	520	600	32-99	4,616	3,040	65.9	4,616	65.9	4,362	3,226	74.0	78.1	96.0	36.6
Pre-Inverter Swap	1	Cumulative	NA	44	8	1	NA	NA	NA	14,011	9,118	65.1	14,003	65.1	13,222	9,661	73.1	-	-	NA
Pre-Inverter Swap	1	Mean	NA	15	3	1	520	600	32-99	4,670	3,039	65.1	4,668	65.1	4,407	3,220	73.1	76.9	94.7	36.6
Pre-Inverter Swap	2	1	2016-11-10	10	2	1	750	600	44-99	3,992	2,476	62.0	3,991	62.0	3,756	2,582	68.7	72.6	94.7	37.1
Pre-Inverter Swap	2	2	2016-11-11	10	3	1	750	600	44-99	3,929	2,485	63.2	3,929	63.2	3,702	2,595	70.1	73.8	96.0	37.2
Pre-Inverter Swap	2	3	2016-11-11	11	1	1	750	600	45-99	3,969	2,479	62.5	3,967	62.5	3,726	2,594	69.6	72.8	94.4	37.7
Pre-Inverter Swap	2	Cumulative	NA	31	6	1	NA	NA	NA	11,890	7,440	62.6	11,887	62.6	11,184	7,771	69.5	-	-	NA
Pre-Inverter Swap	2	Mean	NA	10	2	1	750	600	44-99	3,963	2,480	62.6	3,962	62.6	3,728	2,590	69.5	73.1	95.0	37.3
Pre-Inverter Swap	3	1	2016-11-12	10	3	1	1,000	600	51-99	3,524	1,980	56.2	3,516	56.3	3,291	2,049	62.3	64.8	95.1	38.6
Pre-Inverter Swap	3	2	2016-11-12	10	3	1	1,000	600	50-99	3,541	2,042	57.7	3,541	57.7	3,312	2,115	63.9	65.5	95.5	39.1
Pre-Inverter Swap	3	3	2016-11-13	10	3	1	1,000	600	50-99	3,609	2,059	57.1	3,605	57.1	3,385	2,131	63.0	65.4	95.4	38.6
Pre-Inverter Swap	3	Cumulative	NA	30	9	1	NA	NA	NA	10,674	6,081	57.0	10,662	57.0	9,988	6,295	63.0	-	-	NA
Pre-Inverter Swap	3	Mean	NA	10	3	1	1,000	600	50-99	3,558	2,027	57.0	3,554	57.0	3,329	2,098	63.1	65.2	95.0	38.8
Pre-Inverter Swap	4	1	2016-11-13	33	28	1	420	600	18-99	5,679	3,396	59.8	5,304	64.0	5,005	3,637	72.7	80.0	99.0	36.2

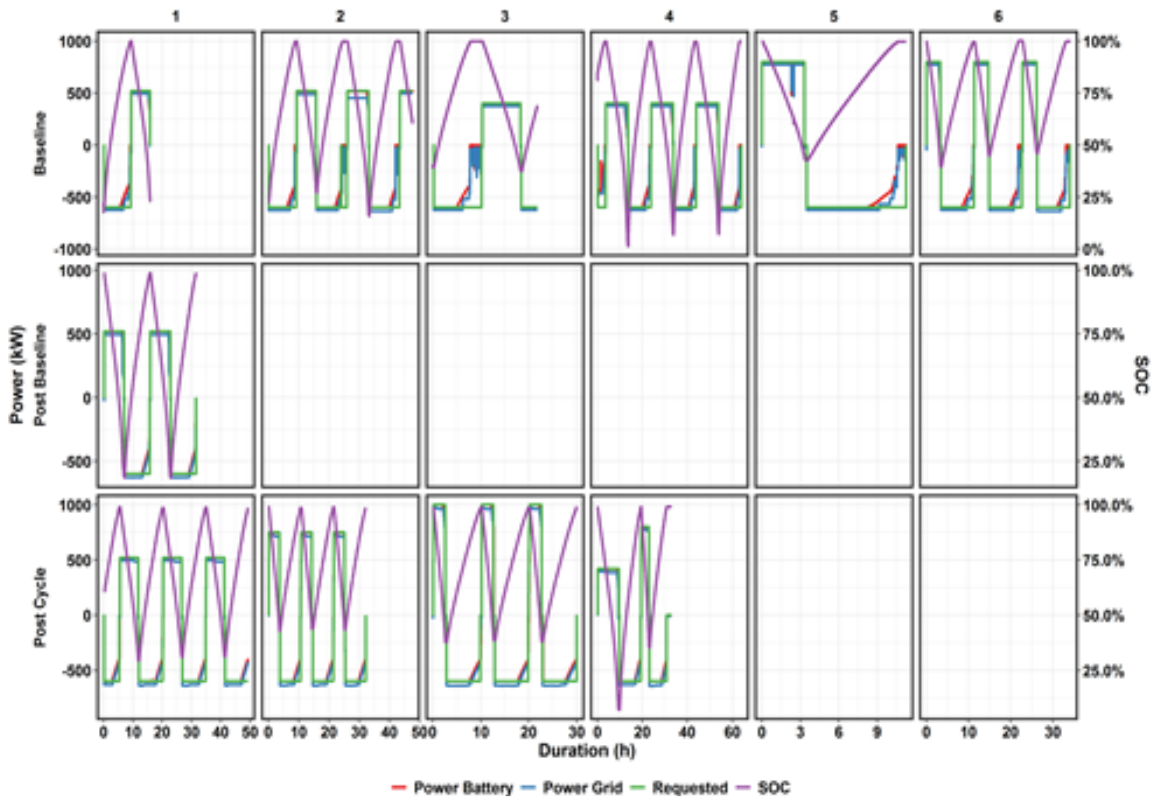

Figure 3.2. Reference Performance Test Profiles

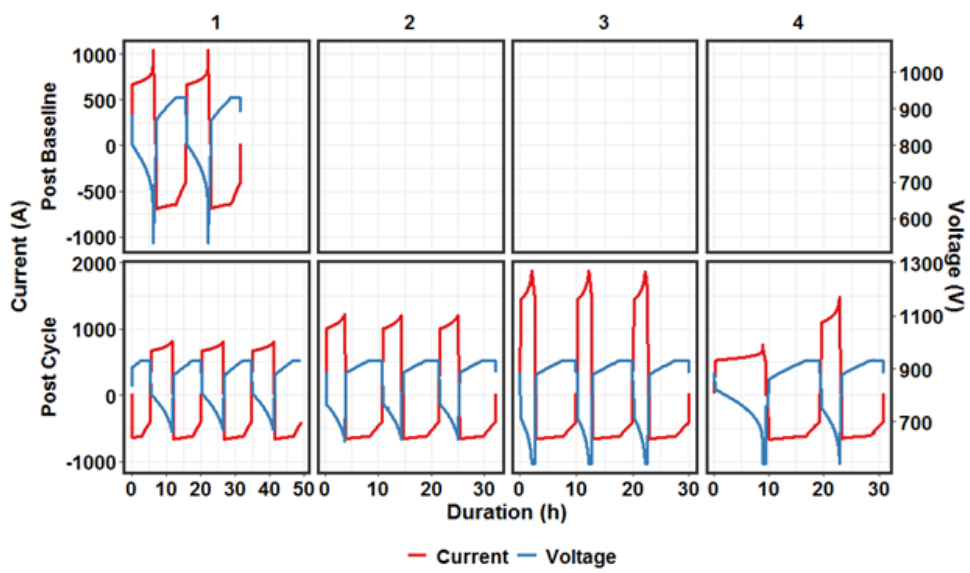

Figure 3.3. Reference Performance Test DC Voltage and Current Profiles

The DC current and voltage profile for the post-baseline and post-cycle runs are shown in Figure 3.3. For 600 kW charge, the maximum current is 700 A. As voltage increases, the current decreases. Once the voltage reaches 920 V, with the current at 650 A, the charge power tapers, as the current starts to taper with the DC battery in constant voltage mode. During discharge, as voltage decreases, the current increases. Comparison of 520 kW discharge profiles for post-baseline and post-cycle runs shows that the

former was discharged down to 18% SOC, while the latter down to 31% SOC. Hence, the end of discharge voltage was 545 V, with an associated current of 1,050 A. This shows that the power requested is delivered until the maximum DC current set point is not exceeded at any SOC, or the FBESS does not have the ability to provide this maximum current at the SOC. For the post-cycle 520 kW discharge, due to the higher-end SOC, the end of discharge voltage is 690 V, accompanied by end of discharge current of 780 A. The current profile as a function of discharge duration or SOC shows that as discharge proceeds, discharge current increases, resulting in a higher rate of decrease of SOC. During charge, as the voltage increases, the rate of SOC change decreases. This leads to lower discharge and charge efficiency respectively.

At 750 kW discharge, the end of discharge voltage is 670 V, with end of discharge current at 1,250 A. These numbers are 550 V and 1,850 A respectively at 1,000 kW discharge. For perspective, the maximum discharge current is more than twice the maximum charge current of 900 A observed at 20% SOC as seen later during pulse tests. While charge power gets capped as SOC increases due to the battery entering constant voltage regime, the discharge power starts to taper when the current needed to meet the power exceeds the maximum current rating of the DC battery and/or the DC side of the PCS.

Table 3.2 provides the RPT results in a concise format, highlighting the trends in energy and RTE with and without auxiliary consumption at various discharge power levels. Maximum discharge energy of 3,395 kWh was obtained at 400 kW discharge. When auxiliary consumption is excluded, 3,635 kWh was obtained. At this power level, the RTE was competitive with the maximum RTE obtained at 520 kW discharge, with 10% higher energy delivered.

Table 3.2. Overview of RPT Results

Discharge kW, Discharge Energy, RTE with or without Auxiliary	Baseline (09/15)	Post-Baseline (01/16)	Peak Shaving (date)	Post-Cycle (11/16)
400 kW, kWh	3,288			3,396 (420 kW)
400 kW, RTE	64.4			59.8
400 kW, kWh (no auxiliary)	3,503			3,637
400 kW, RTE (no auxiliary)	75.0			72.7
520 kW, kWh	3,005	3,068	2,950	3,039
520 kW, RTE	61.8	65.2	65.8	65.1
520 kW, kWh (no auxiliary)	3,318	3,222	3,096	3,220
520 kW, RTE (no auxiliary)	74.2	72.2	72.8	73.1
750 kW, kWh			2,657	2,480
750 kW, RTE			62.1	62.6
750 kW, kWh (no auxiliary)			2,750	2,590
750 kW, RTE (no auxiliary)			67.7	69.5
1,000 kW, kWh			1,933	2,027
1,000 kW, RTE			59.5	57.0
1,000 kW, kWh (no auxiliary)			1,986	2,098
1,000 kW, RTE (no auxiliary)			64.1	63.1

Figure 3.4 shows cumulative discharge and charge energy as a function of SOC. The cumulative energy increases linearly with decreasing SOC until ~50% SOC. At lower SOC levels, the slope decreases, as less energy is obtained per unit change in SOC. The DC current increases at constant power with decrease in SOC, with an estimated 9% increase at 50% SOC and 17% increase at 10% SOC over the initial

discharge current. The total discharge energy in the range investigated is 3,395 kWh, with the most energy available at 420 kW discharge. Results are also plotted for energy discharged excluding auxiliary consumption. For this case, the maximum energy of ~3,635 kWh is obtained at 420 kW. Hence, 420 kW appears to be the optimal power for this FBESS in terms of getting the maximum energy at constant power, with higher DC-DC RTE making up for greater contribution of auxiliary consumption.

The energy obtained during taper is also shown as dotted lines and is marginally higher for each discharge power level.

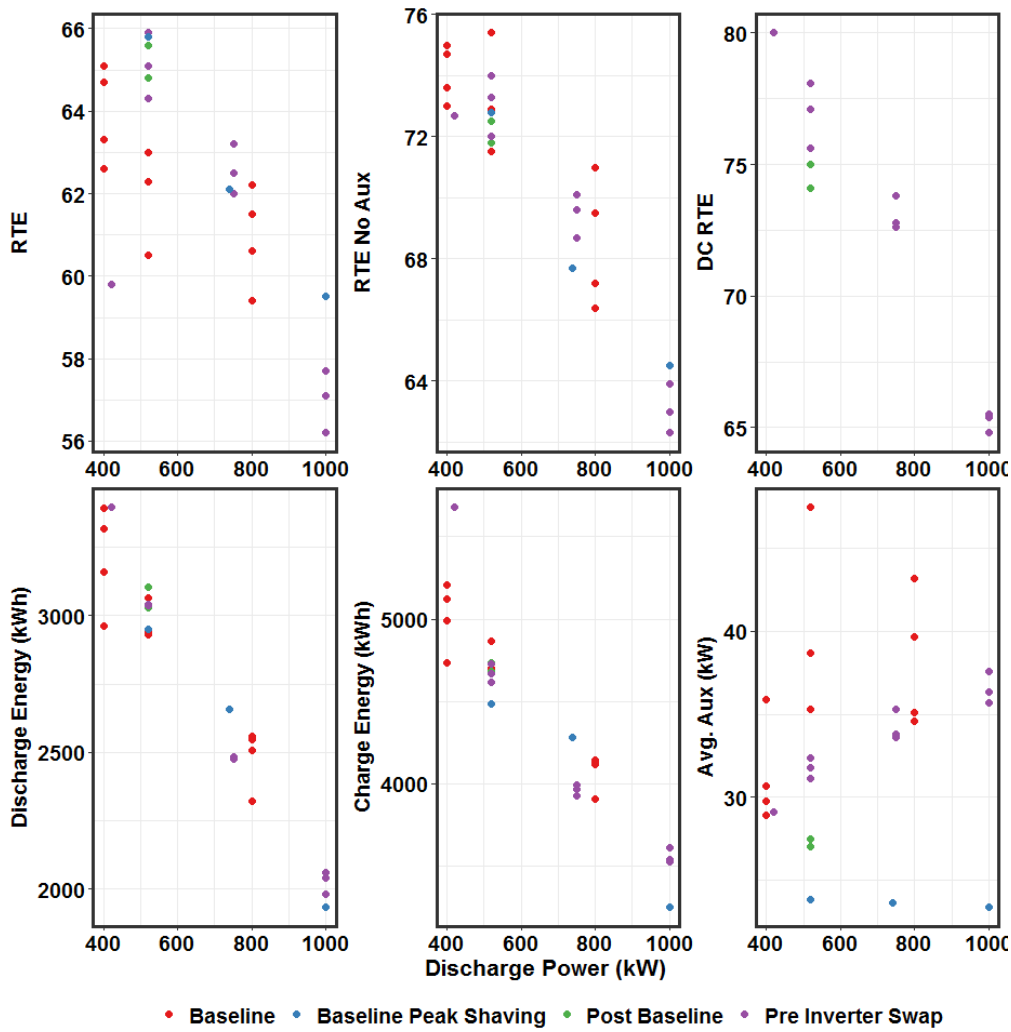

Figure 3.4. FBESS Performance Curves from Baseline Tests. All graphs are AC data, except the top right graph, which is DC-DC RTE.

As shown in Figure 3.5, charge energy increases linearly in the 40 to 90% range. At lower SOCs, because of low operating voltage and associated greater current at fixed power, the charge energy needed for a unit change in SOC is lower. As SOC increases, at 50% SOC, charge current decreases to ~93% of the current at 10% SOC, and further decreases to ~85% at 100% SOC. The maximum charge energy is 5,680 kWh during 600 kW charge after 420 kW discharge. When auxiliary consumption is excluded, the maximum charge energy is 5,005 kWh after 420 kW discharge. The decrease in temperature for 600 kW charge indicates that the endothermic effect coupled with heat loss to the ambient air is greater than resistive heating.

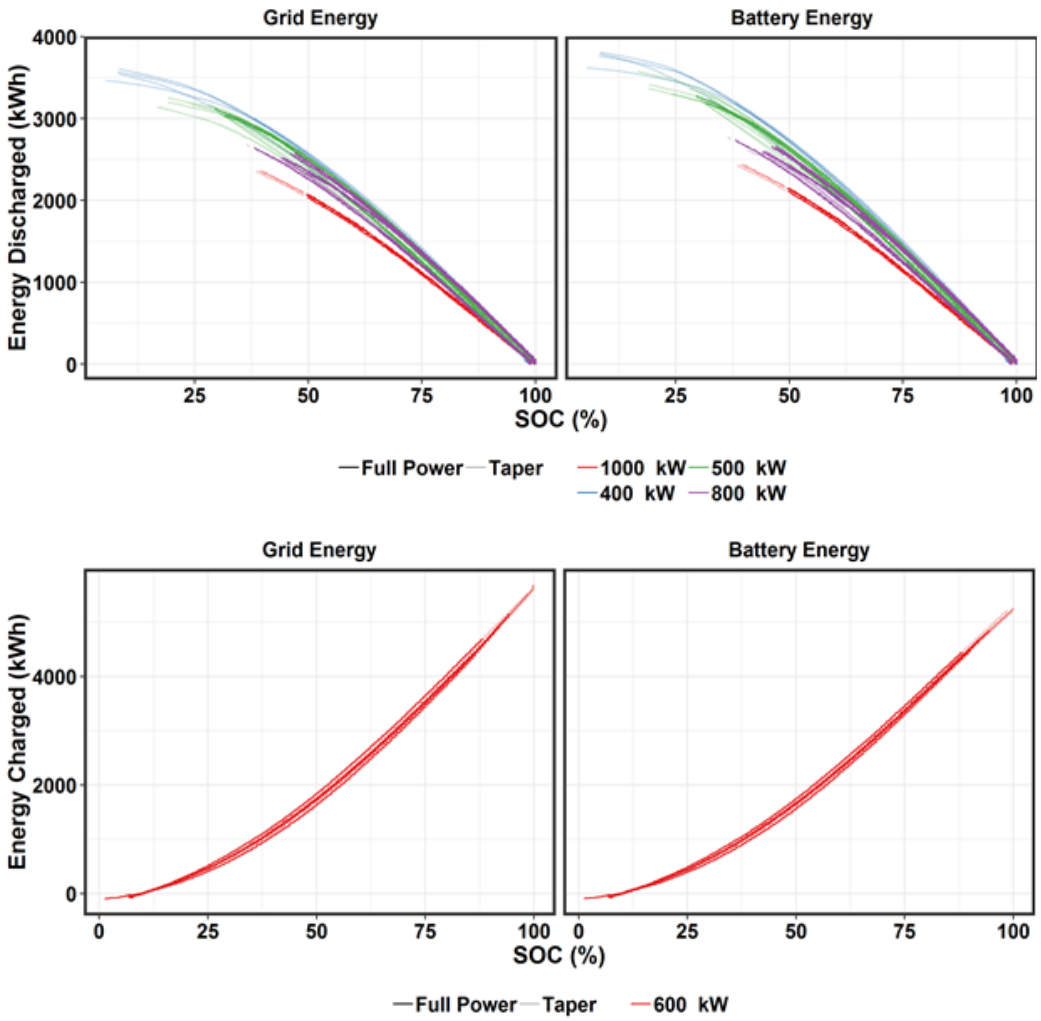

Figure 3.5. Energy Charged or Discharged at the Grid and PCS Levels as a Function of FBESS SOC

Figure 3.6 shows the temperature profile for the FBESS during charge, rest, and discharge. The regime of increasing temperature corresponds to discharge, the stabilization regime is the rest period, and the decreasing regime is the charge. The rate of increase of temperature during discharge increases with discharge power.

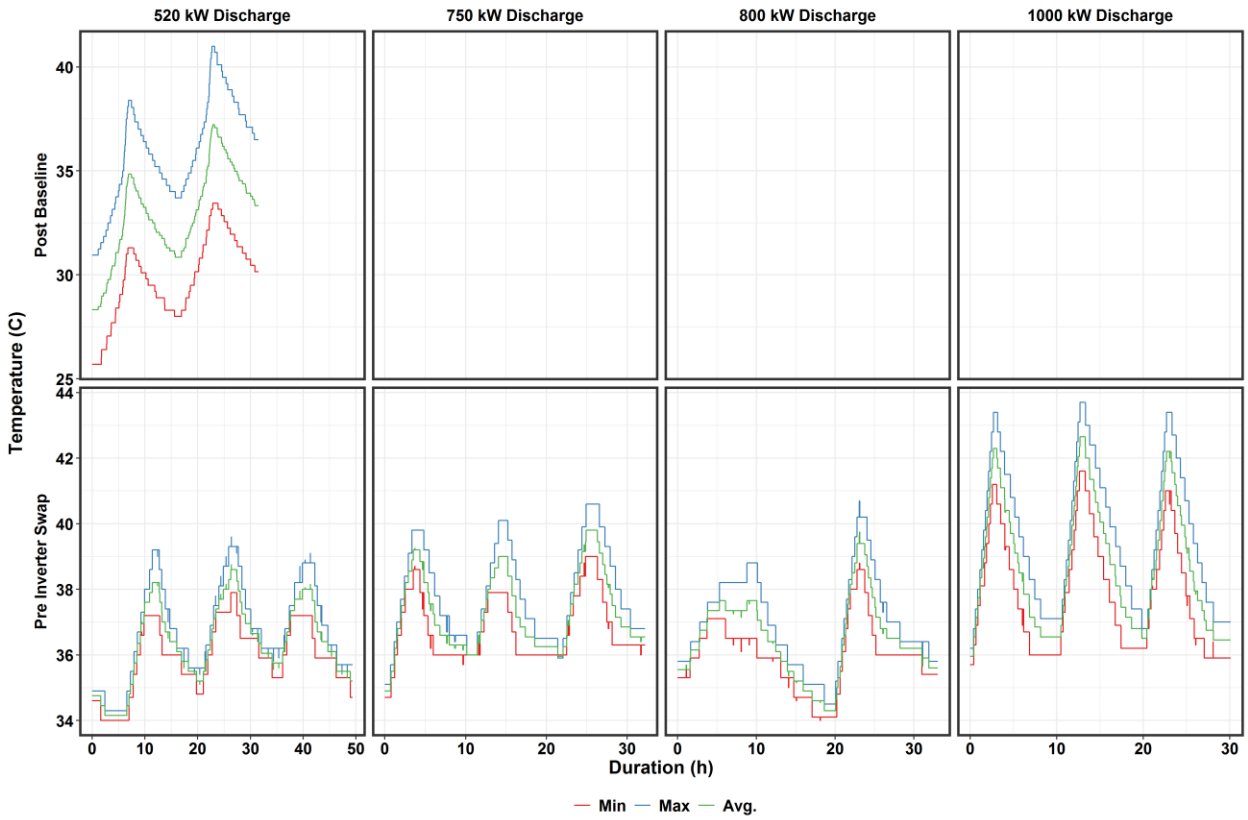

Figure 3.6. Battery Temperature Profile during RPT Capacity Tests

3.2 Response Time/Ramp Rate Test

Most tests included a "WAITSOC" command that triggers moving to the next step once the target SOC is reached. This resulted in a large difference existing between the timestamps in the schedule file vs. the requested power tag timestamp. Figure 3.7 shows the requested power signal sent by the schedule file and the requested power data timestamp as received by the FBESS for the pulse test. As shown in Figure 3.8, there is a wide gap between the two signal timestamps, which is in the 0.25- to 2-hour range. The main reason for this lag is due to the WAITSOC command in the schedule file that goes to the next step once the target SOC is reached. In future work, an analysis of communication lag for fields that do not use WAITSOC commands will be conducted as part of conference proceedings or peer-reviewed journal publications.

To determine communication lag, the root mean square (RMS) of the difference between requested power in the data file and requested power in the schedule file was plotted as a function of lag as shown in Figure 3.9. The communication lag was estimated at 10 seconds, as this minimizes the error.

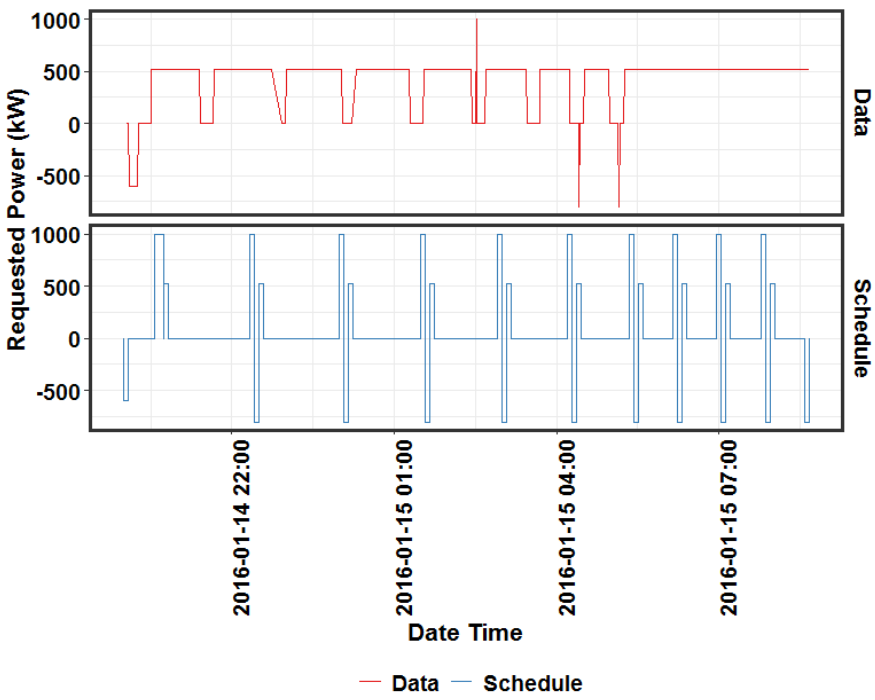

Figure 3.7. Requested Power from Data and From Schedule File during the Pulse Test

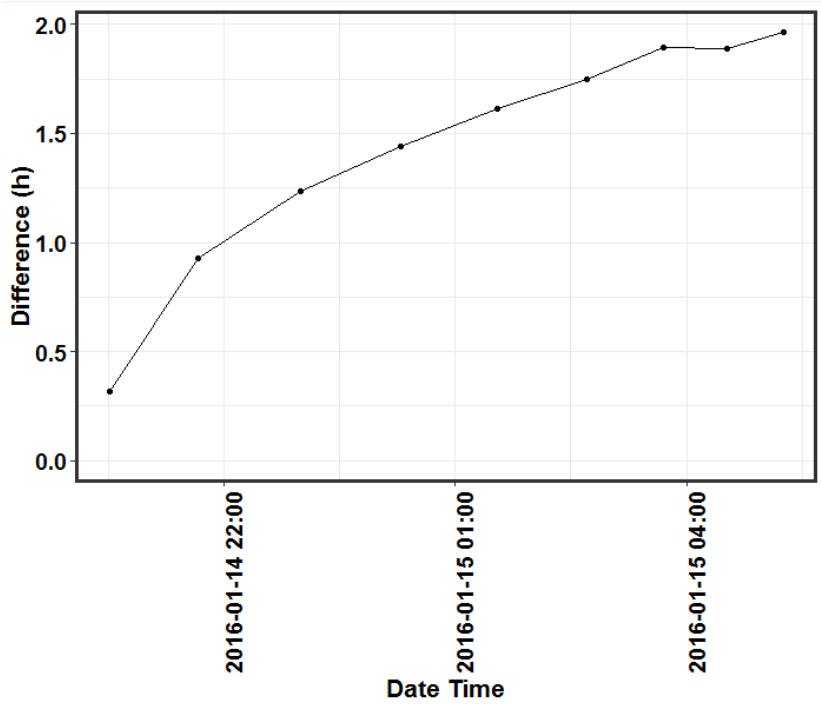

Figure 3.8. Difference between Time Stamp for Requested Power Data and Schedule File Time Stamp during the Pulse Test

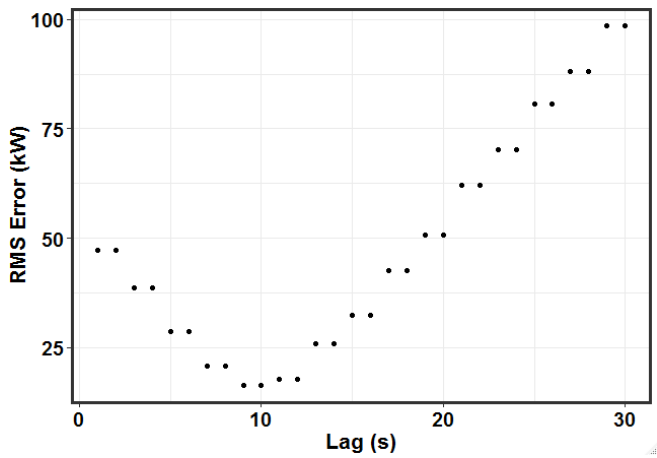

Figure 3.9. RMS Error between Requested and Scheduled Power as a Function of Lag during the Frequency Regulation Test

The pulse test started with discharge at 95% SOC, followed by discharge pulses at ~10% decrements down to 40% SOC. This was followed by discharging down to 12% SOC and charge pulsing at every ~10% SOC increment. The charge pulse was 800 kW while the discharge pulse was 1,000 kW on a two-string basis. Only one string was active for this test.

The FBESS response to the signal is shown in Figure 3.10. The FBESS starts responding within 1 second of receiving the command, with only the charge pulse test at 41% SOC taking 2 to 3 seconds for the hardware to respond. Surprisingly, for 3 pulse tests – discharge at 51% SOC, 61% SOC and 91% SOC, the BESS started to respond *before* the signal was received. Since this is not possible from a physical point of view, this appears to be due to an error in the reporting of either the requested power tag or in the system response. The time to reach maximum power is 5 to 10 seconds.

The response of the FBESS at the PCS is shown in Figure 3.11. UET had set the ramp rate at 200 kW/s for charge and 300 kW/s for discharge. The response time of the FBESS ranged from 3 to 10 seconds for the range of test cycles performed. For charge, the response time increased from 4 to 10 seconds as SOC increased from 20 to 60%, reaching a maximum power of 800 kW. At >60% SOC, the maximum power attained dropped linearly to 400 kW at 100% SOC. Hence, while the response time was lower (to attain this lower maximum power), the ramp rate decreased from a maximum of 200 kW/s at 30% SOC to 50 kW/s at 90 to 100% SOC. The results are consistent with UET limiting charge ramp rates to 200 kW/s.

The maximum charge and discharge power attained at various SOCs is consistent with the frequency regulation RPT results (Run 2) as shown in Figure 3.11.

The response time for discharge was 3 seconds. The ramp rate ranged from 340 kW/s at 90% SOC, with a slight decrease to 315 kW/s at 30% SOC, with maximum attained power at ~1,000 kW in the 90 to 40% range, dropping slightly to 950 kW at 30% SOC. The results are consistent with UET limiting discharge ramp rates to 300 kW/s.

The FBESS charge and discharge resistance, corrected for two strings, was in a tight range for discharge, decreasing from 0.100 ohms to 0.110 ohms as SOC decreased from 90 to 40%. There was a spike in internal resistance at 30% SOC to 0.125 ohms. On a four-string normalized basis, the resistance is 0.05 to 0.055 ohms, which is in line with MESA 2 findings. The charge resistance was slightly lower than discharge resistance across all SOCs, which may be related to higher auxiliary consumption at fixed power for charge as discussed earlier.

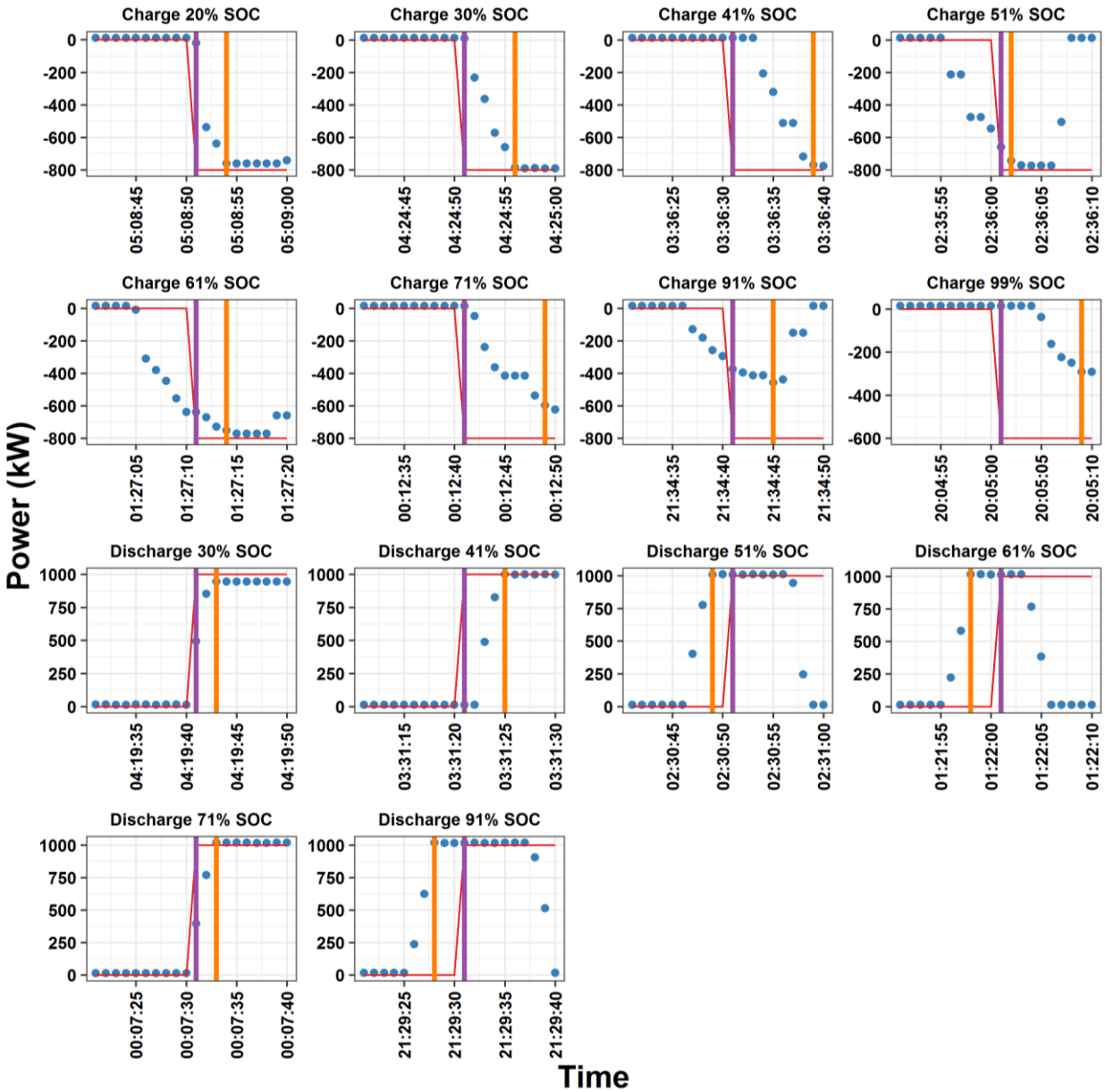

Figure 3.10. FBESS Response with Signal Request

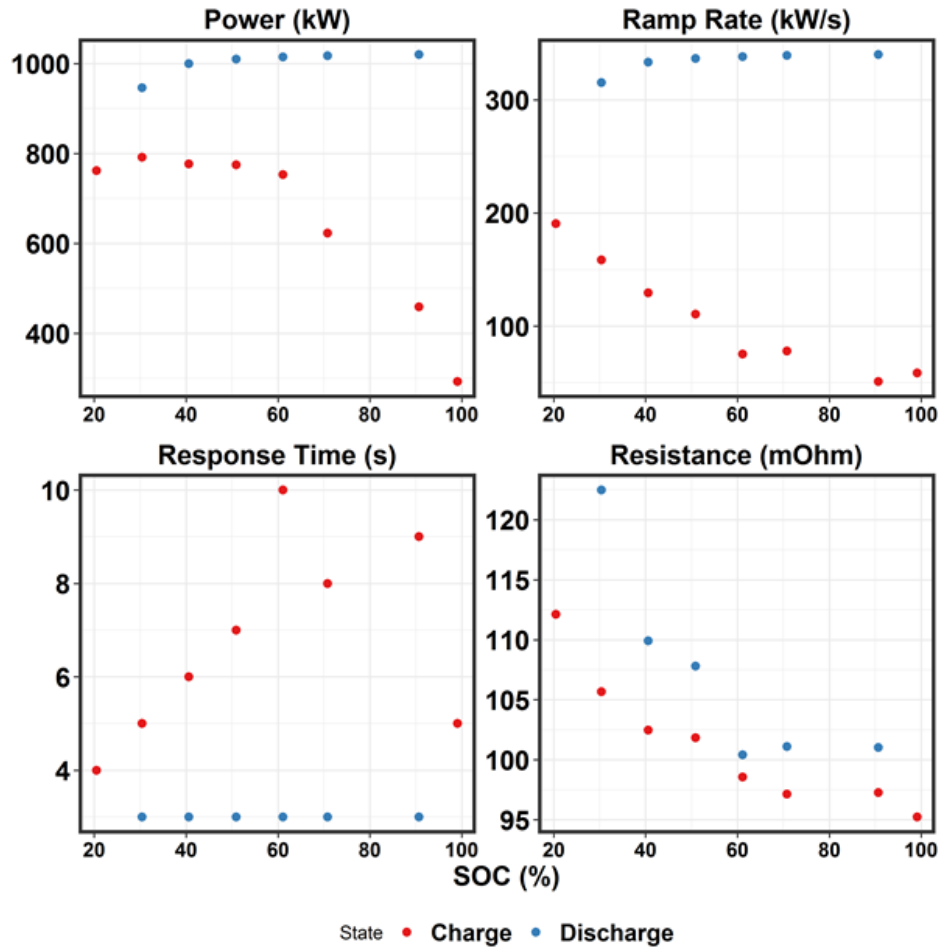

Figure 3.11. Reference Performance Test for Response Time, Ramp Rate, and Internal Resistance

It is counter-intuitive that the internal resistance for charge increases with decreasing SOC, because at lower SOCs, the charge acceptance is higher. In addition, it is not clear if the decrease in charge power to 600 kW at 70% SOC and to 450 kW at 90% SOC is due to setting of charge rates as a function of SOC by the BMS, or simply due to the fact that the FBESS has entered the constant voltage regime of the constant current constant voltage charge. The decreasing internal resistance with increasing SOC is probably due to electrolyte resistance decreasing as SOC increases.

The DC voltage and current profiles are shown in Figure 3.12 for charge and discharge across the SOC range. As SOC increases, the maximum charge current decreases from 900 A at 20% SOC to 500 A at 91% SOC. The corresponding maximum voltage during charge ranged from 875 to 915 V. The pulses did not last long enough to observe any taper.

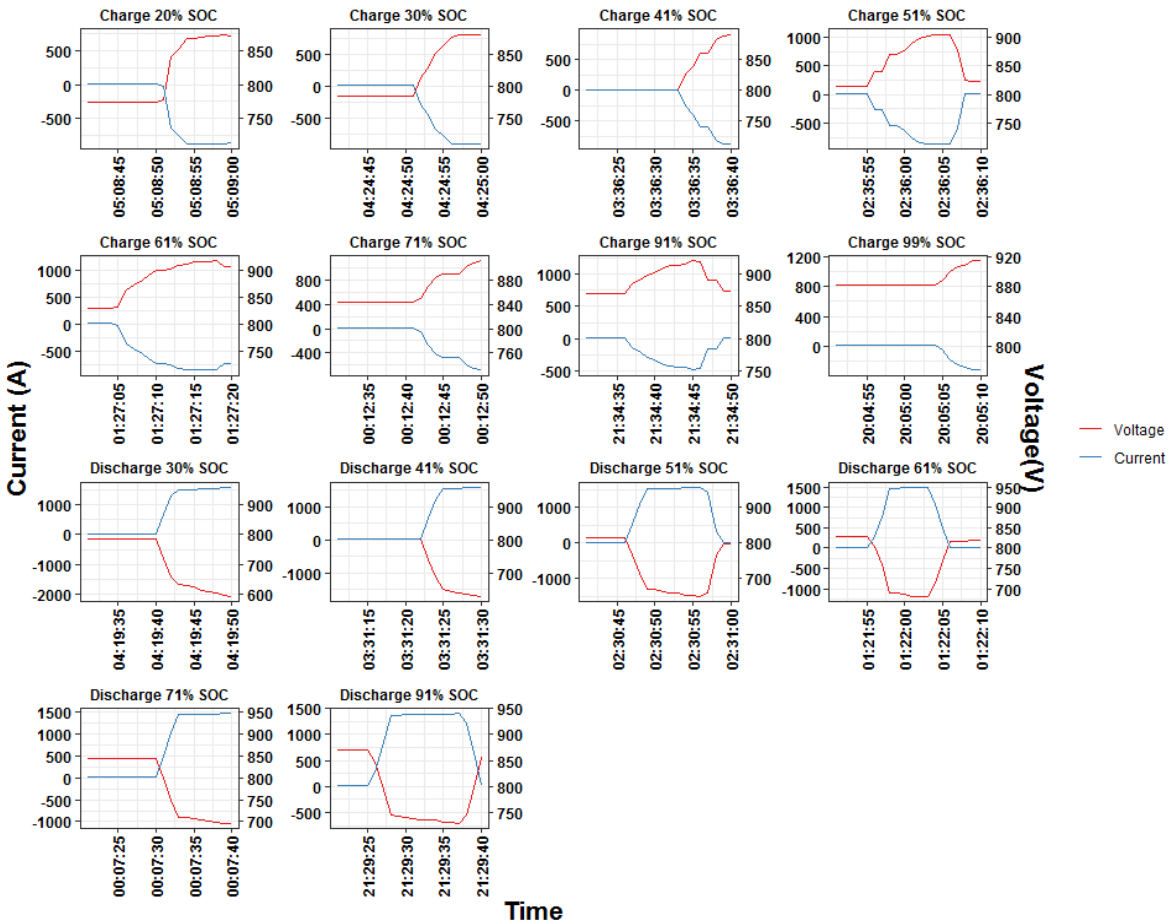

Figure 3.12. Voltage and Current during Pulse Tests

During discharge, as voltage decreased, the current increased at a faster rate than during charge. The rate of increase of current was faster at low SOC. The maximum current was 1,520 A at 30% SOC, while it decreased to 1,375 at 91% SOC. The swing in maximum current was much less for discharge than for charge as SOC changed. This appears to indicate the BMS restricts current flow during charge as SOC increases, with a maximum of 500 A at 91% SOC, thus limiting charge power as SOC increased, with a maximum power of 420 kW at 91% SOC. Whereas, for discharge, in the 30 to 91% SOC range, the maximum discharge power remains constant at close to 1,000 kW. Hence the current increase with decreasing SOC is simply related to voltage decrease, as opposed to additional decreases due to clamping of discharge power as SOC decreases. Note that the maximum discharge current of 1,520 A is three times the maximum charge current at 61% SOC, while the maximum power for discharge is 2.5 times the maximum charge power at 91% SOC. This setting of charge power as SOC increases may further contribute to cooling during the charge half cycle.

The internal resistance during charge was slightly lower than discharge pulse resistance across the SOC range investigated. It decreased from 0.11 ohms at 20% SOC to 0.095 ohms at 100% SOC.

Table 3.3 compares the AC and DC characteristics of the FBESS and compares them with the UET Technical Specifications. The energy obtained at various discharge power levels and the RTE at the inverter are in line with the technical specifications. The maximum DC discharge current observed in this work is 8% lower than the technical specifications, while the maximum DC charge current value observed was only 56% of the value reported in the specifications.

Table 3.3. Performance Comparison with Technical Specifications for the Avista Turner FBESS

Operating Condition Parameter	Operating Condition Parameter Value	FBESS Property	Specifications	Report
Discharge power (kW)	520	Energy (kWh)	3,225	3,070
Discharge power (kW)	640	Energy (kWh)	2,560	
Discharge power (kW)	750	Energy (kWh)		2,480
Discharge power (kW)	1,000	Energy (kWh)	2,000	2,025
Overall		RTE (%)	65-70	63-74
Maximum charge current for capacity tests	600 kW charge at 20% SOC			700
Maximum charge current for pulse tests (UET 2015)[c]	800 kW charge at 20% SOC		1,600[a]	900
Maximum discharge current for capacity tests (UET 2015) [c]	1,000 kW discharge at 30% SOC		2,000[a]	1,850
Maximum discharge current for pulse tests	1,000 kW discharge at 30% SOC			1,520
Maximum discharge current for frequency regulation	Maximum discharge current at 2,400 kW discharge at 48% SOC[b]			2,245
Maximum charge current for frequency regulation	Maximum charge current at 2,000 kW 18-23% SOC			1,050

(a) The specifications maximum current was not related to specific tests such as pulse or capacity.
(b) One string faulted, while the schedule file called for 2,000 kW discharge. The discharge power was capped at 1,200 kW for the one string.
(c) Document marked confidential, used with permission from UniEnergy Technologies, LLC.

Note than when the maximum two-sting charge or discharge power was requested with one string having dropped off, the maximum charge and discharge currents were 1,050 A and 2,245 A respectively. These were 66 and 112% of the values provided in the technical specifications, respectively.

The in situ resistance for all strings (normalized to two-string value) is shown in Figure 3.13. In general, the charge and discharge resistance increase slightly at SOCs <40%.

Overall, there is no trend with increasing test duration.

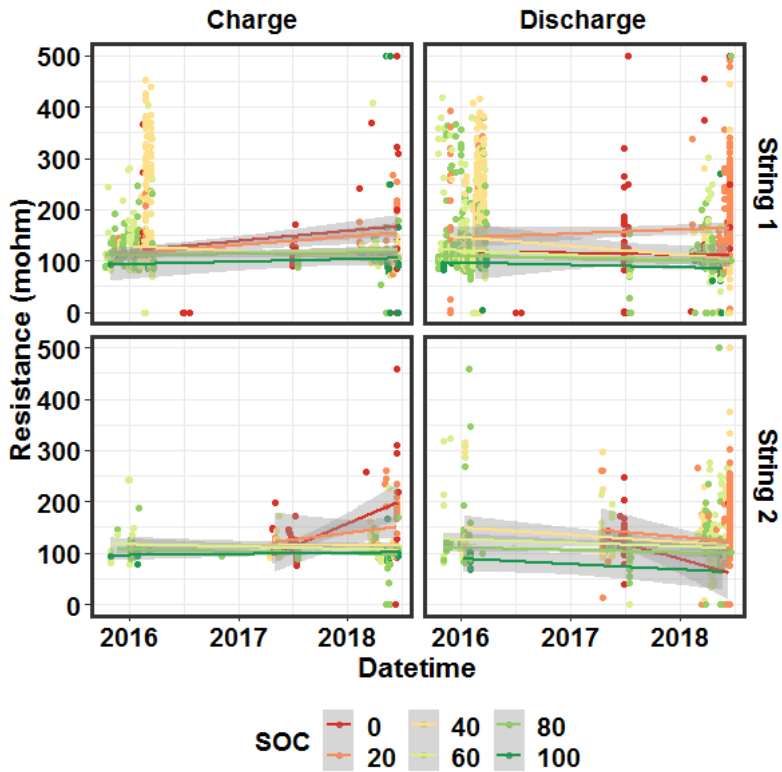

Figure 3.13. In Situ Charge and Discharge Resistance for Each String. Resistance is normalized to a two-string basis.

3.3 Frequency Regulation Test

The FBESS was subjected to the 24-hour US DOE-OE Performance Protocol Frequency Regulation Signal as part of the RPT. The starting SOC was set at 86% to ensure the FBESS could provide the necessary power throughout the test. One power unit was set at -800 kW for charge and 1,000 kW for discharge to comply with charge power levels not exceeding 800 kW for extended durations. As expected, the SOC decreased with test duration, due to RTE <1 and the signal being biased toward discharge. For Run 2, one string dropped out before the test began, resulting in double the power per string with average power levels being nearly two times that of Run 1. Results from frequency regulation tests are shown in Figure 3.14.

The average charge and discharge power levels were 26 and 27% of rated power, respectively. The auxiliary power consumption is about 10% of these power levels. Hence, the RTE when auxiliary consumption is excluded increases from 61 to 72.2%. As expected, for Run 2, the increase in RTE when auxiliary load was excluded was lower, from 55 to 62%. The higher average power levels resulted in a greater depth of discharge for Run 2, with the end SOC at 18% compared to 57% for Run 1. This results in a lower RTE of 62% compared to 72% for Run 1 when auxiliary consumption was excluded. Run 2 demonstrates that the FBESS is robust enough to handle double the DOE Protocol power levels (while capping maximum power levels per string).

Signal tracking within 2% of signal was 60% at the grid and 69% at the PCS. The corresponding numbers within 2% of the rated power are 89 and 70%, respectively. The lower tracking when auxiliary consumption is excluded is a quirk of the meter resolution limiting the accuracy of measurements, which dominates low power levels.

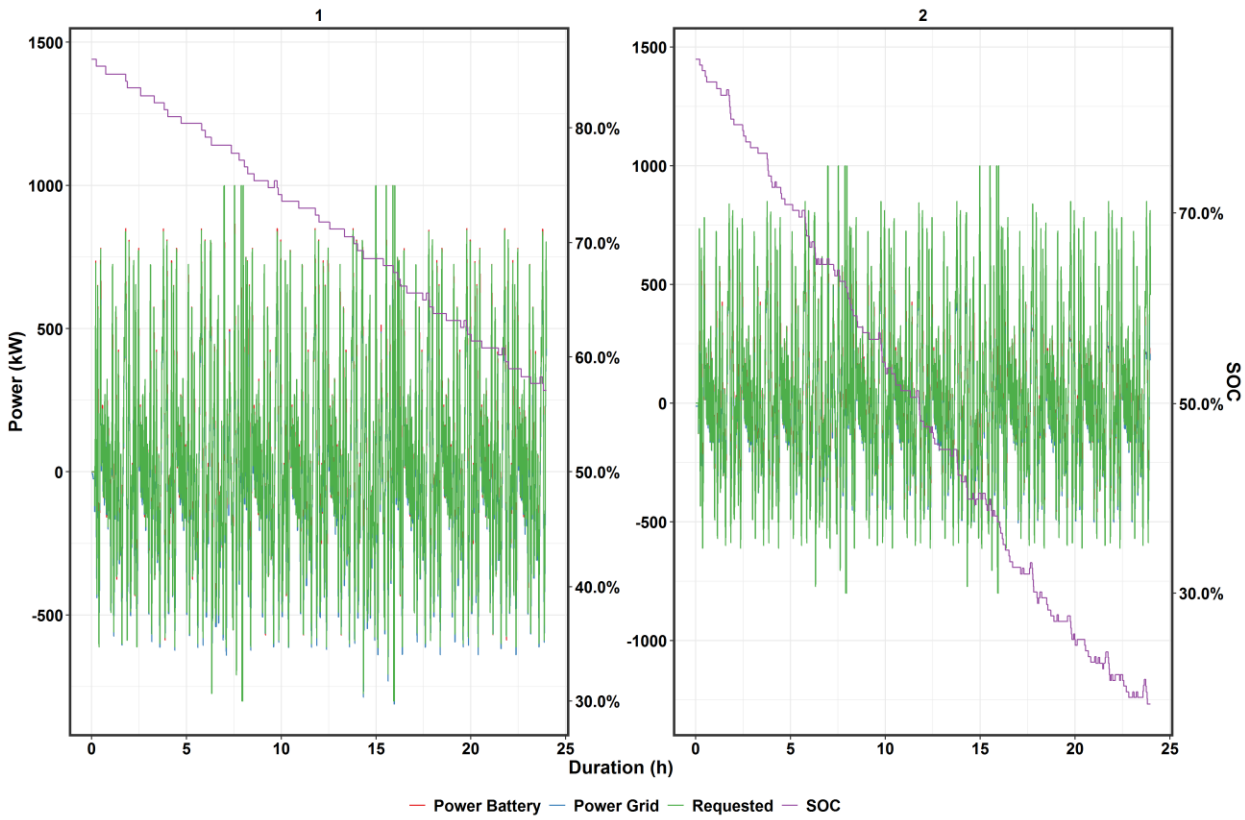

Figure 3.14. Frequency Regulation US DOE-OE ESS Performance Protocol Tests

The root mean square error (RMSE) normalized with respect to rated power is 0.04 and 0.032 with and without auxiliary power for Run 1. As expected, for Run 2, these numbers are higher.

For this 24-hour duty cycle, the starting SOC could be lowered somewhat such that high charge power levels at the start SOC can be sustained without taper. For this particular duty cycle, the highest charge levels are requested about 6 hours into the test, at which stage the SOC had decreased to 78%, and could sustain these charge power levels. For real-world frequency regulation service, it would be prudent to set the SOC range such that the maximum charge and discharge power levels can be sustained for the desired duration.

The error for Run 1 is shown in Figure 3.15 as a function of power. The trend line is flat, indicating the error magnitude does not depend on mode or magnitude of power. The isolated points with error as high as 300 to 400 kW is probably due to communication lag once the requested power signal reaches the FBESS. For those instances, it is possible that the response is for a signal that arrived earlier. An analysis of the two types of lags – communication lag from signal to FBESS and from FBESS computer to hardware, will be conducted for the frequency regulation Run 1 for future publication.

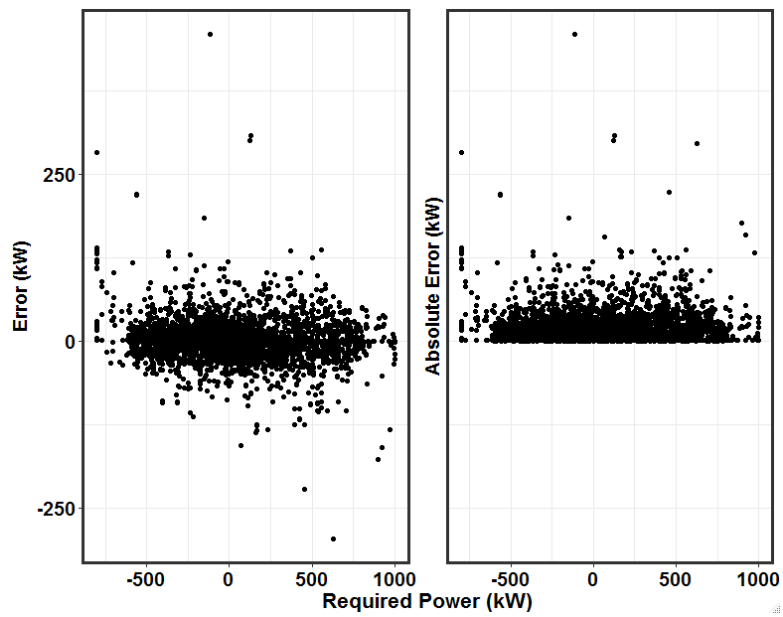

Figure 3.15. Error and Absolute Error as a Function of Power during the Baseline Frequency Regulation Test

As seen from Figure 3.2, the maximum requested charge power was -600 to -800 kW, while the maximum discharge power was 800 to 1,000 kW during the run.

Power levels at the grid and inverter for Run 2 are shown in Figure 3.16.

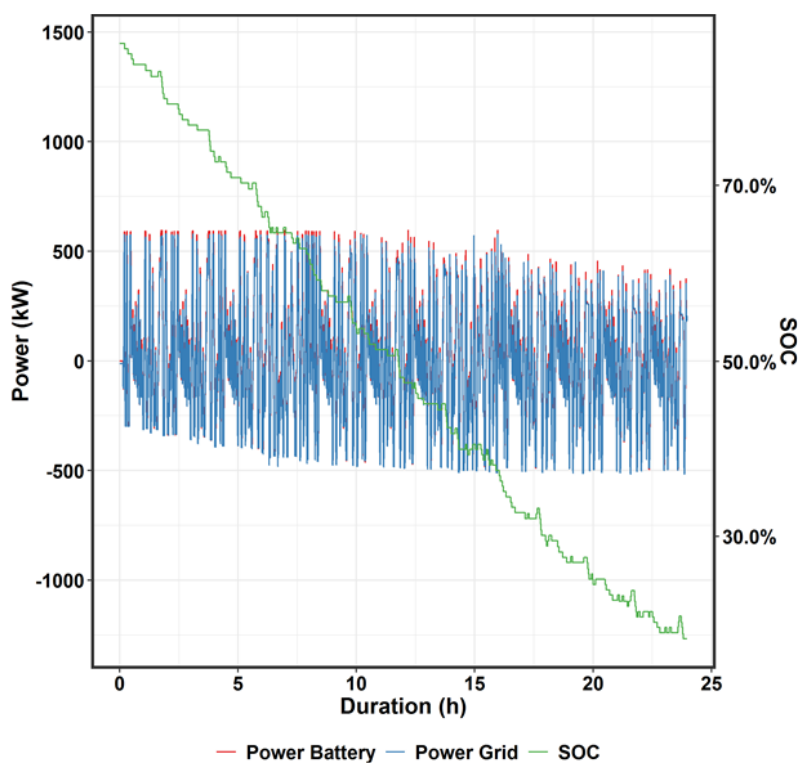

Figure 3.16. Frequency Regulation Profile for Run 2 with Requested Power Removed for Clarity

The requested power has been removed so these values can be seen clearly. As the run proceeds, the SOC decreases from 85 to 27%. The FBESS provided its maximum rating of close to 600 kW during for the first two-thirds of the run, with the SOC decreasing to 37%. At <37% SOC, the maximum discharge power decreased progressively to 375 kW at the end of the run with the SOC at 15%. These maximum power levels are consistent with the discharge power levels obtained during the response time ramp rate test at various SOCs.

The reverse was true for charge. At the beginning of the run, with SOC at 85%, the maximum charge power was -300 kW. This increased progressively until SOC decreased to 50%, after which the maximum charge was -500 kW. This shows that the FBESS can absorb up to -500 kW per string for short durations. More importantly, in the 37 to 50% range, the FBESS met the frequency regulation duty cycle requirement using 1 power unit equal to 1,000 kW for both charge and discharge. Using the criterion of -800 kW maximum charge and 1,000 kW maximum discharge, the SOC range is expanded to 64 to 37%. The maximum charge power of -800 kW at <64% SOC is consistent with the findings of the response time ramp rate test, where the SOC >60%, the maximum power decreased. This shows the value of doing the RPTs described in the US DOE-OE protocol in order to characterize the FBESS performance.

Because Run 2 was done with one string faulted while requested power was for two strings, the normalized RMSE was high as expected. To assess the real performance of the FBESS, the requested power was capped at ±500 kW. The response was deemed to have tracked the requested power when its magitude was greater than 500 kW. Its RMSE, at 0.29, was lower than for the raw data for Run 2 (0.55 nRMSE), but still higher than for Run 1 due to the FBESS not being able to meet the maximum charge and discharge power requirements at high power levels at extreme SOCs. Frequency regulation test results are shown in Table 3.4.

Table 3.4. Frequency Regulation Test Results

Date	2016-01-08	2016-11-15	2016-11-15
Strings Active	2	1	1
Adjust Requested Power and Response	None	None	500 kW/-400 kW
Duration (h)	24	24	24
Start SOC (%)	86.0	86.2	86.2
End SOC (%)	57.1	18.3	18.3
Average Charge Power (kW)	261	470	446
Average Discharge Power (kW)	274	455	446
RTE (%)	61	55	56
RTE No Auxiliary (%)	72.2	62.0	61.8
Normalized RMSE (kW/rated kW)	0.040	0.552	0.291
Normalized RMSE No Auxiliary (kW/rated kW)	0.032	0.569	0.327
Normalized Mean Absolute Error (MAE) (kW/rated kW)	0.035	0.282	0.158
Normalized MAE No Auxiliary (kW/rated kW)	0.019	0.325	0.201
Tracking 2%	0.24	0.09	0.22
Tracking 2% No Auxiliary	0.74	0.10	0.21
Signal Tracking 2%	0.55	0.63	0.67
Signal Tracking 2% No Auxiliary	0.71	0.67	0.68

The error distribution shows that for Run 1, the error is close to the 2% rated power band around 0 kW, while for Run 2, the error bands fall well outside this region (Figure 3.17).

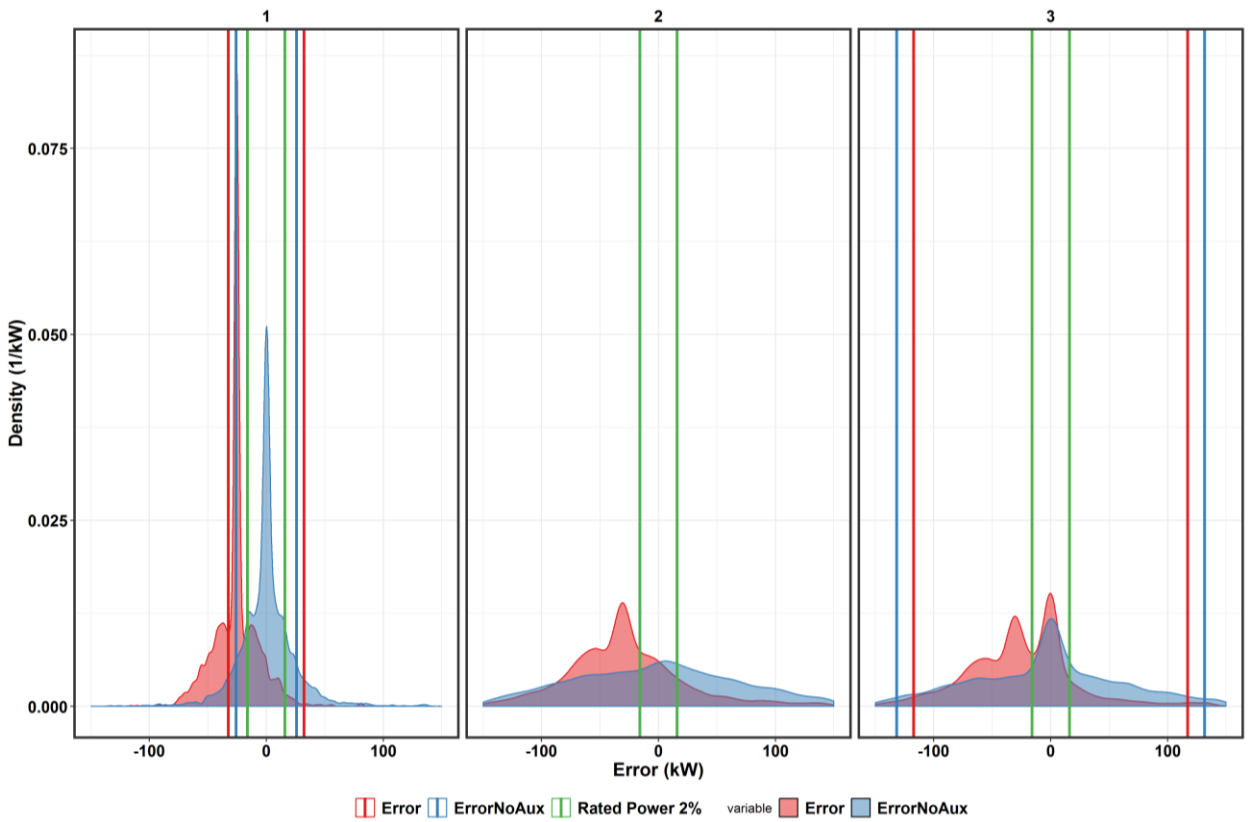

Figure 3.17. Error Distribution for Frequency Regulation Test

3.4 Baseline Peak Shaving

Peak shaving was done at a charge power of 600 kW and discharge power levels of 520, 750, and 1,000 kW. A rest time of 3 hours was set after charge and discharge. The RTE increased with decreasing discharge power levels, and was in the 60 to 66% range. The RTE when auxiliary consumption was excluded was in the 65 to 73% range, again increasing with decreasing discharge power levels. The end of discharge SOC increased with increasing discharge power levels, and was 36% at 520 kW and 55% at 1,000 kW.

Because these tests are similar to the baseline capacity tests, they have been included in the baseline capacity RPTs to quantify degradation of the FBESS over time. Results from the baseline peak shaving tests are shown in Figure 3.18 and Table 3.5.

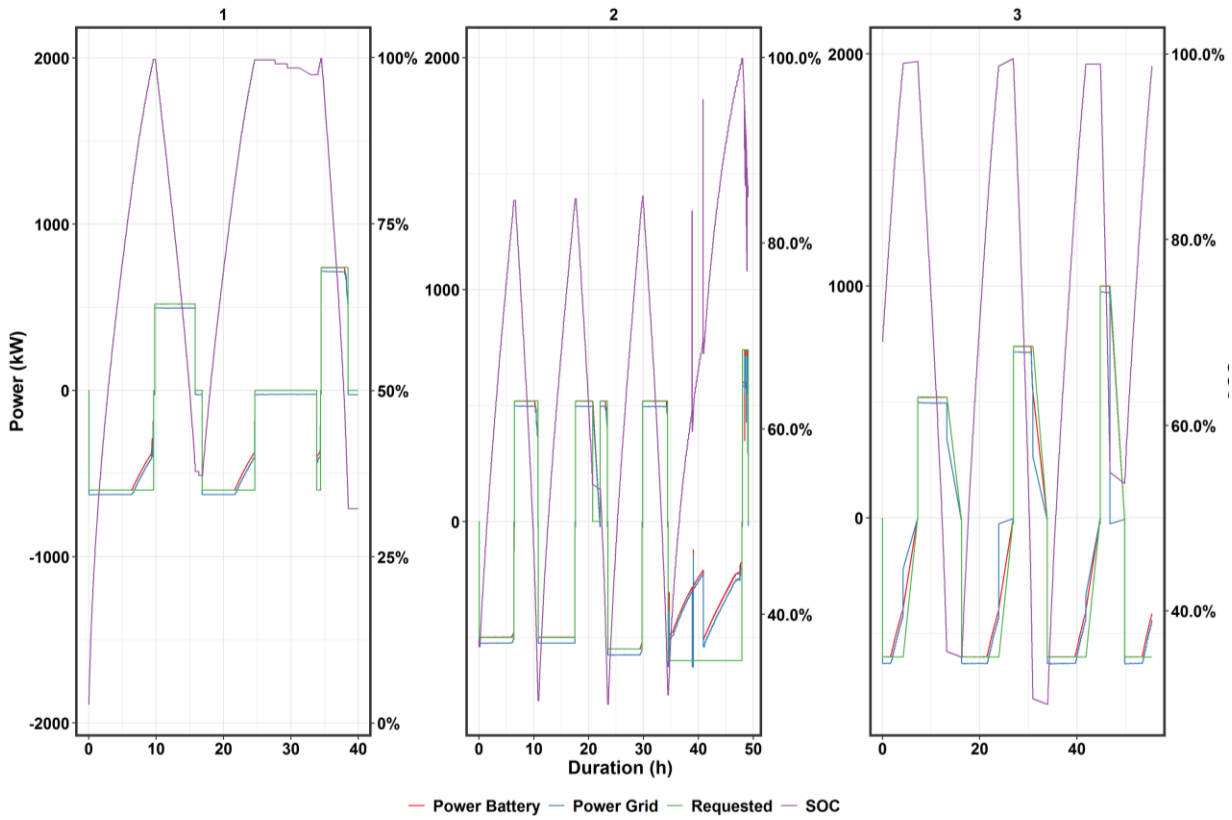

Figure 3.18. Baseline Peak Shaving Test Profiles

Table 3.5. Baseline Peak Shaving Results

Date	Duration (h)	Rest Time (h)	Strings Active	Req. Discharge Power (kW)	Req. Charge Power (kW)	SOC Range	Charge Energy (kWh)	Discharge Energy (kWh)	RTE	Charge Energy No Rest (kWh)	RTE No Rest	Charge Energy No Aux (kWh)	Discharge Energy No Aux (kWh)	RTE No Aux	Mean Temp (ºC)
2016-01-06	17	3	2	520	600	36-99	4,482	2,950	65.8	4,482	65.8	4,253	3,096	72.8	32.2
2016-01-07	15	3	2	740	600	39-99	4,279	2,657	62.1	4,279	62.1	4,061	2,750	67.7	35.1
2016-01-07	11	3	2	1,000	600	55-99	3,249	1,933	59.5	3,249	59.5	3,079	1,986	64.5	36.7

3.5 Use Case 1: Energy Arbitrage

3.5.1 Duty Cycle Summary

The arbitrage duty cycle for Avista is developed using the forecast hourly energy prices obtained by Avista from Pattern Recognition Technologies, Inc. Hourly prices are forecast for the next week and are updated hourly throughout the week. Forecast energy price data for the next day will be provided to PNNL by Avista through a secure site. This data will be used as an input into the Battery Storage Evaluation Tool (BSET). The optimization engine within BSET will then be used to define an hourly schedule for battery charging/discharging over the next day, maximizing "buy low, sell high" transactions. BSET will be used to define the optimal charging and discharging schedule in order to either maximize value to the system or minimize losses. That is, even if the transaction results in financial losses, the test should be carried out for testing/learning reasons.

3.5.2 Test Results

Multiple runs were conducted, with the longest run being 71 hours. The average power levels were 25 to 57% of rated power, resulting in RTEs in the 58 to 65% range. RTEs excluding auxiliary consumption were 58 to 72%. For most runs, the SOC did not go below 50%, with one run approaching 32% and another 18% at the low end. Hence, only ~50% of the FBESS energy content was used up per discharge for five out of seven runs. The results indicate that the FBESS performs well when discharged to 18% SOC, with an RTE of 60%, and increasing to 70% when auxiliary consumption is excluded, thus providing greater opportunity for net benefits from this service. Results for the energy arbitrage tests are shown in Figure 3.19 and Table 3.6.

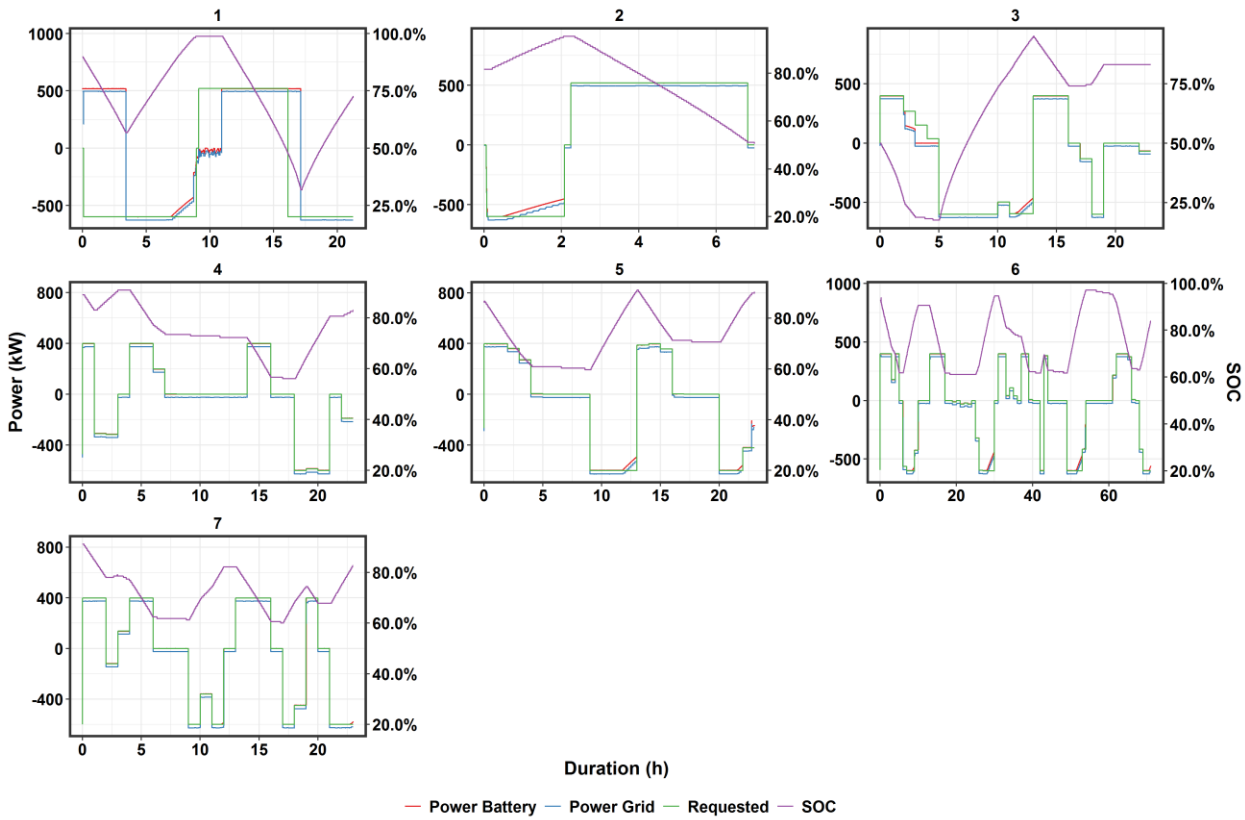

Figure 3.19. Energy Arbitrage Test Profiles

Table 3.6. Energy Arbitrage Test Results

Date	2016-01-18	2016-01-20	2016-01-20	2016-01-21	2016-01-22	2016-01-23	2016-01-26
Duration (h)	21	7	23	23	23	71	23
Rest Fraction	0.08	0.05	0.26	0.48	0.39	0.46	0.26
Strings Active	2	2	2	2	2	2	2
Average Charge Power (kW)	263	573	518	460	585	469	518
Average Discharge Power (kW)	354	494	242	288	233	280	344
SOC Range	32-99	50-96	18-95	56-91	60-91	61-97	60-91
Charge Energy (kWh)	7,317	3,463	5,857	3,534	4,317	11,702	4,986
Discharge Energy (kWh)	4,746	2,260	3,537	2,039	2,629	6,768	3,097

Date	2016-01-18	2016-01-20	2016-01-20	2016-01-21	2016-01-22	2016-01-23	2016-01-26
RTE	64.9	65.3	60.4	57.7	60.9	57.8	62.1
Charge Energy No Rest (kWh)	5,006	3,393	5,639	3,069	3,910	10,438	4,647
Discharge Energy No Rest (kWh)	4,746	2,260	3,537	2,039	2,629	6,768	3,097
RTE No Rest	NA[a]	65.40	61.10	61.90	62.50	61.00	64.10
Charge Energy No Auxiliary (kWh)	4,539	3,225	5,320	2,877	3,710	9,766	4,386
Discharge Energy No Auxiliary (kWh)	2,654	2,374	3,747	2,185	2,815	7,316	3,316
RTE No Auxiliary	NA[(a)]	72.2	69.6	71.4	72.3	70.6	72.6
Mean Charge Temperature (ºC)	39	35	36	33	31	30	30
Mean Discharge Temperature (ºC)	38	36	36	33	32	30	29
Mean Temperature (ºC)	38	36	36	33	32	30	30

(a) For this run, the requested power signal was opposite to FBESS at the start of the test, resulting in no rest period and also compromising the calculations for cases where there are no auxiliary losses.

3.6 Use Case 1: System Capacity

3.6.1 Duty Cycle Summary

To determine the hours when the energy storage would be needed to provide capacity services, hourly system-wide load data was obtained for 2011 through 2015. The capacity trigger was set at the peak load point for each year. Capacity is required over a three-day period that includes the day prior to, and the day following, the annual peak load day. The capacity must be available during the 18 peak hours over the course of the 3-day peak: 3 hours in the morning peak and 3 hours in the evening peak each day.

Based on data provided by Avista, PNNL defined an hourly duty cycle that provided six hours of capacity each day, discharging during the peak loads for the day. A unique schedule was formed for three consecutive days according to Avista's capacity requirements.

3.6.2 Test Results

The average charge power was in the 455 to 570 kW range, while the average discharge power was in the 670 to 770 kW range. The high power levels resulted in mean temperature in the 36 to 42°C range. There was no difference between average charge and average discharge temperature. This seems counter-intuitive, because charging is endothermic. However, the starting temperature for charge is the high temperature at the end of discharge, while the starting temperature for discharge is the lower temperature at the end of charge.

Test durations ranged from 9 hours to 110 hours. Most of the runs were done in the 45 to >98% SOC range, while one run extended to 24% SOC. As expected, the RTE for this run was at the low end of the 60 to 64% range. Because of low rest durations, the RTE without rest was ~1% higher. Excluding auxiliary consumption, the RTE was in the 67 to 71% range. The 6 to 7% increase in RTE when auxiliary consumption is excluded appears to indicate that active cooling did not occur during these tests.

The FBESS delivered the required power for all runs. This was possible because the model developed by PNNL to estimate the rate of change of SOC during operation at constant power allowed setting the duty cycle for which the FBESS provided constant power for required duration during discharge. Results are shown in Figure 3.20 and Table 3.7.

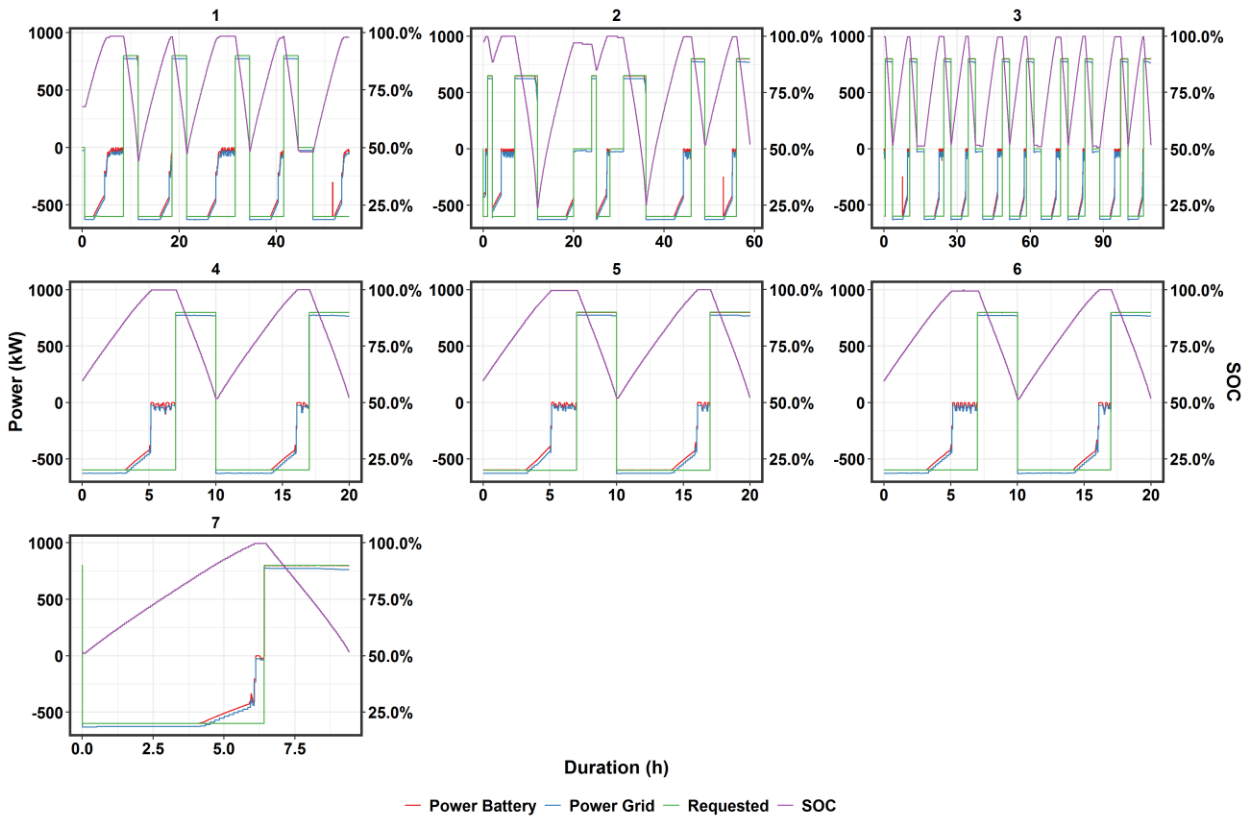

Figure 3.20. System Capacity Test Profiles

Table 3.7. System Capacity Test Results

Date	2016-01-27	2016-01-30	2016-02-01	2016-02-02	2016-02-03	2016-02-04	2016-02-05
Duration (h)	55	59	110	20	20	20	9
Rest Fraction	0.21	0.18	0.21	0.12	0.14	0.11	0.03
Strings Active	2	2	2	2	2	2	2
Average Charge Power (kW)	457	477	494	484	481	484	569
Average Discharge Power (kW)	772	669	772	772	772	772	771
SOC Range	44-98	24-100	51-100	52-100	52-100	51-100	51-100
Charge Energy (kWh)	18,157	19,905	37,284	7,280	7,168	7,267	3,657
Discharge Energy (kWh)	10,848	12,086	23,157	4,633	4,634	4,628	2,314
RTE	59.7	60.7	62.1	63.6	64.7	63.7	63.3
Charge Energy No Rest (kWh)	17,941	19,661	36,527	7,278	7,164	7,267	3,655
Discharge Energy No Rest (kWh)	10,848	12,086	23,157	4,633	4,634	4,628	2,314
RTE No Rest	60.0	61.2	62.6	63.6	64.6	63.7	63.3
Charge Energy No Auxiliary (kWh)	16,778	18,488	34,378	6,855	6,737	6,841	3,461
Discharge Energy No Auxiliary (kWh)	11,221	12,526	23,944	4,790	4,788	4,788	2,394
RTE No Aux	66.4	67.4	68.8	69.9	71.1	70.0	69.2
Mean Charge Temperature (ºC)	36	38	41	40	41	41	42
Mean Discharge Temperature (ºC)	35	37	40	40	41	41	42
Mean Temperature (ºC)	36	37	41	40	41	40	42

3.7 Use Case 2: Regulation

3.7.1 Duty Cycle Summary

The duty cycle for regulation testing is developed using an area control error (ACE) signal internally calculated by Avista. This signal closely matches an industry standard frequency regulation signal. The formal frequency regulation signal calculated by Avista has limited variation as Avista uses contracted hydropower and allows frequency variation to minimize frequency regulation costs.

To use the ACE signal for frequency regulation, a scaling factor (defined as a response factor with a unit of kW/MW) must be defined to bring the multi-megawatt ACE signal down into the sub-megawatt operating range for ESSs; this value is called the response factor and will be a negative value, indicating the output of the ESS will work against ACE to regulate it. The response factor must be defined in consideration of how long the ACE signal will stay at a given power level; the ESS can operate at power levels greater than steady-state for brief periods of time. The ESS output power is defined by the power limits and response factor and must be chosen carefully to maximize the amount of regulation the ESS is providing while minimizing the amount of time it is saturated at the chosen power limits. To define the response factor and accompanying power limits, a year of historical ACE data was analyzed to determine the most appropriate combination of values.

The test was conducted in two ways. First the FBESS was controlled using the duty cycle developed based on the approach described above. Multiple runs of this duty cycle were performed using three different response factors. After that, multiple 24-hours tests were conducted by engaging an appropriate automatic mode for providing regulation service in the ESS control system. Appendix A provides detailed methodology development for this use case.

3.7.2 Test Results

For most runs, the SOC was in the 50 to 60% range, with only Run 1 starting at 86% SOC. While the SOC decreased during testing for most runs, for Run 3 SOC increased because it was heavily biased in favor of charge. The average charge and discharge power levels ranged from 7 to 28% of rated power, resulting in an RTE of 37 to 61%. As expected, runs with lowest average power levels had low RTEs and an associated higher increase in RTE when auxiliary consumption was excluded. The RTE when auxiliary consumption was excluded ranged from 50 to 72%. Results are shown in Figure 3.21 and Table 3.8.

The normalized error was in the 4 to 17% range. Surprisingly, the higher error was observed at higher average power levels. The error increased when auxiliary power consumption was excluded, which also was not expected.

As seen from the error distribution plot in Figure 3.22, the deviation from signal for a high percentage of responses falls within -10 to +10 kW. Runs 2 to 7 have a long tails, with errors extending to ±100 kW. As mentioned earlier, this higher error may be due to a communication lag within the FBESS after the signal has reached the FBESS. It is instructive that the peak for the error with auxiliary load included occurs at approximately -25 kW, which is the auxiliary consumption for the FBESS. While tracking with 2% of rated power is high, the nRMSE is greater than 2% of rated power due to the high contribution of points with large deviation from the signal.

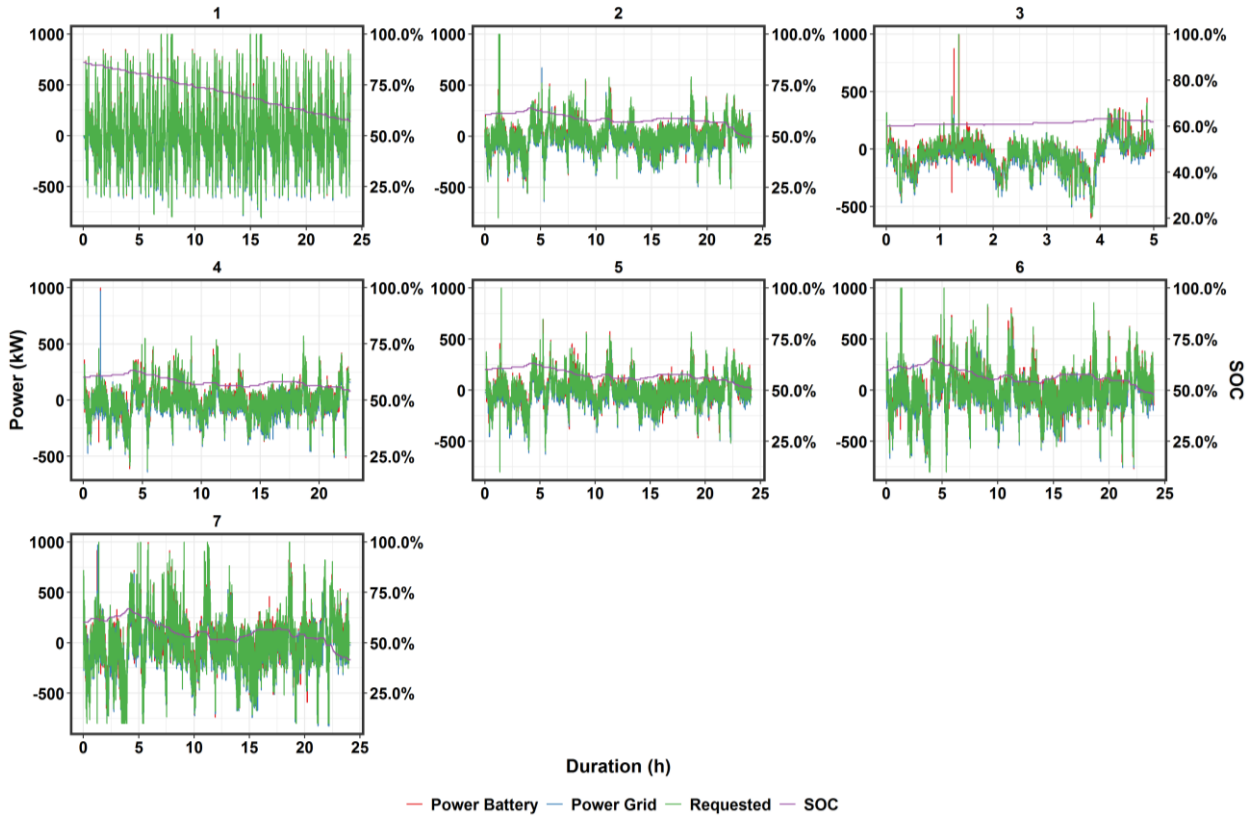

Figure 3.21. Frequency Regulation Test Profiles – Duty Cycle and Response

Table 3.8. Frequency Regulation Test Results

Date	2016-02-08	2016-02-10	2016-02-11	2016-02-16	2016-02-18	2016-02-19
Scale Factor (kW/MW)	10	10	10	10	15	20
Strings Active	2	1	1	1	1	1
Duration (h)	24	5	23	24	24	24
Rest Fraction	0.19	0.17	0.21	0.19	0.21	0.19
Start SOC (%)	60.6	60.0	60.1	60.1	59.8	60.1
End SOC (%)	48.6	61.8	53.9	50.8	47.8	41.5
Average Charge Power (kW)	123	157	128	124	172	219
Average Discharge Power (kW)	74	68	74	77	127	182
RTE (%)	37	43	41	38	51	51
RTE No Auxiliary (%)	50.4	69.3	61.3	57.7	62.4	56.9
Normalized RMSE (kW/rated kW)	0.064	0.113	0.119	0.102	0.164	0.172
Normalized RMSE No Auxiliary (kW/rated kW)	0.080	0.206	0.170	0.155	0.231	0.286
Normalized MAE (kW/rated kW)	0.046	0.086	0.089	0.081	0.104	0.111
Normalized MAE No Auxiliary (kW/rated kW)	0.046	0.122	0.110	0.106	0.151	0.183
Tracking 2%	0.88	0.84	0.87	0.88	0.85	0.85
Tracking 2% No Auxiliary	0.71	0.55	0.63	0.61	0.63	0.65
Signal Tracking 2%	0.64	0.53	0.62	0.62	0.64	0.62
Signal Tracking 2% No Auxiliary	0.72	0.64	0.67	0.70	0.68	0.70

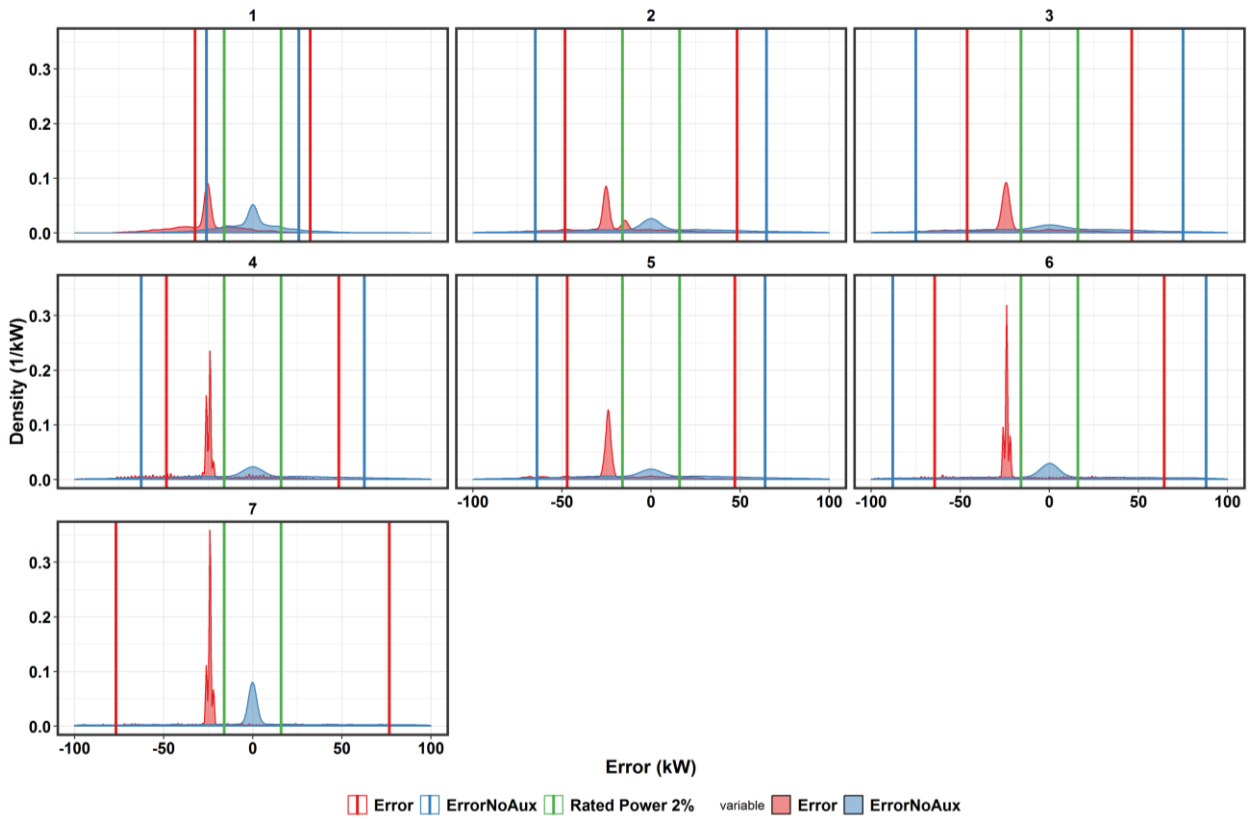

Figure 3.22. Frequency Regulation Test Error Distribution

3.8 Use Case 2: Frequency Regulation Auto

3.8.1 Duty Cycle Summary

In addition to signal generated in advance, frequency regulation was carried out in "Auto" mode, using a scale factor of 8 kW/MW. The "Auto" mode requires the FBESS to respond to real-time grid conditions.

3.8.2 Test Results

All these runs use a scale factor of 8 kW/MW, with the first three runs using only one string. The signal tracking within 2% of rated power was good. The normalized error was high, ranging from 9 to 39% of rated power. The RTE was low at 40 to 54%, due to average power levels of 4 to 24% of rated power. Test results for the Frequency Response Auto use cases are shown in Figure 3.23 and Table 3.9.

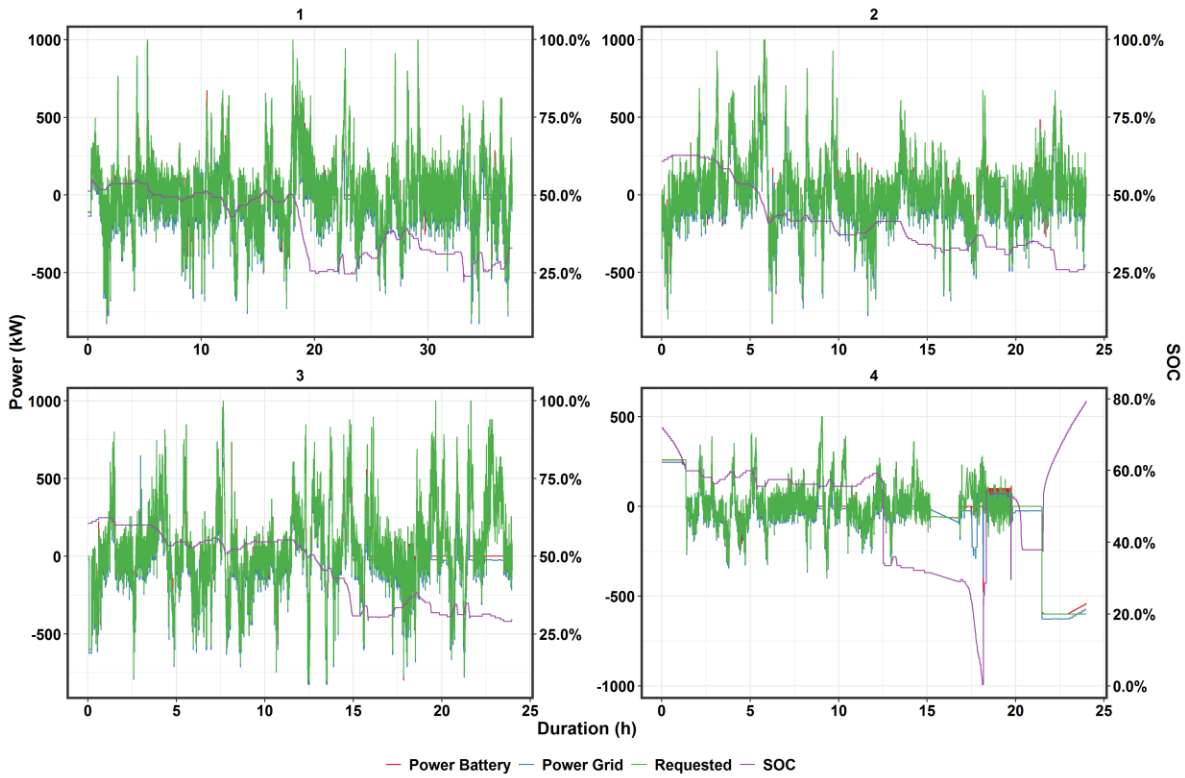

Figure 3.23. Frequency Regulation Auto Test Error Distribution

Table 3.9. Frequency Regulation Auto Test Results

Date	2016-02-23	2016-02-25	2016-03-01	2016-03-15
Scale Factor (kW/MW)	8	8	8	8
Strings Active	1	1	1	2
Duration (h)	37	24	24	24
Rest Fraction	0.13	0.14	0.12	0.11
Start SOC (%)	51.2	60.8	60.6	64.7
End SOC (%)	32.9	27.3	29.6	86.0
Average Charge Power (kW)	192	171	210	241
Average Discharge Power (kW)	122	137	121	42
RTE (%)	42	41	40	54
RTE No Auxiliary (%)	55.6	54.2	49.5	63.7
Normalized RMSE (kW/rated kW)	0.223	0.176	0.389	0.090
Normalized RMSE No Auxiliary (kW/rated kW)	0.253	0.193	0.386	0.093
Normalized MAE (kW/rated kW)	0.121	0.108	0.195	0.051
Normalized MAE No Auxiliary (kW/rated kW)	0.111	0.080	0.176	0.048
Tracking 2%	0.94	0.94	0.93	0.85
Tracking 2% No Auxiliary	0.86	0.88	0.87	0.78
Signal Tracking 2%	0.57	0.61	0.63	0.62
Signal Tracking 2% No Auxiliary	0.89	0.90	0.90	0.90

Figure 3.24 shows the error distribution. As seen earlier, the error distribution when auxiliary consumption is included peaks at -25 kW, the auxiliary consumption for the FBESS. Due to high contribution from responses with large deviation from the signal, the nRMSE is higher than 2% of rated power, even though signal tracking within 2% of rated power is high.

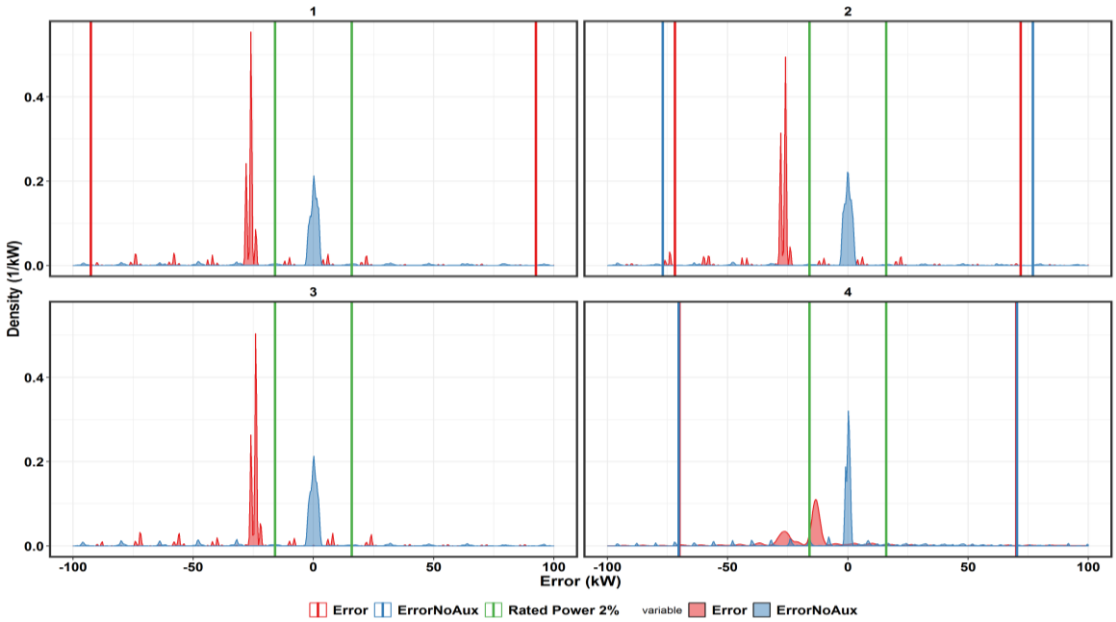

Figure 3.24. Frequency Regulation Auto Test Error Distribution

3.9 Load Following

3.9.1 Duty Cycle Summary

Because load following is not a distinct service to Avista, the same testing protocol used for frequency regulation was used here with one significant difference. As in the case of frequency regulation, the ACE signal was used as the raw input signal, and response factor was defined to allow the FBESS to provide the greatest amount of balancing without operating in a saturated state (at the lower or upper power limit) for extended periods of time. The signal sent to the FBESS, though, will be the average of the past five minutes of this scaled signal. This operation smoothed out the rapid changes in the ACE signal and showed the trends in system imbalance on the multi-minute scale.

3.9.2 Test Results

A scale factor of 8 to 20 kW/MW was applied. The average power ranged from 18 to 40% of rated power, resulting in low RTE of 35 to 48%. The normalized error was in the 8 to 18% range, which is high considering the signal tracking within 2% of rated power was high at 90 to 93%. Depending on the marketplace, the criteria for signal tracking could differ, making the FBESS excellent or good in this respect. The ΔSOC was in the 7 to 25% range for these runs, thus allowing the FBESS to be used for applications such as peak shaving for 2 to 4 hours by adjusting the starting SOC upward. As seen in Figure 3.25, the error distribution peaks at -25 kW when auxiliary consumption is included. Hence, it is important that this deviation is accounted for, especially when working with volatile signals or for mission critical services such as peak shaving. Results from load following tests are shown in Figure 3.26 and Table 3.10.

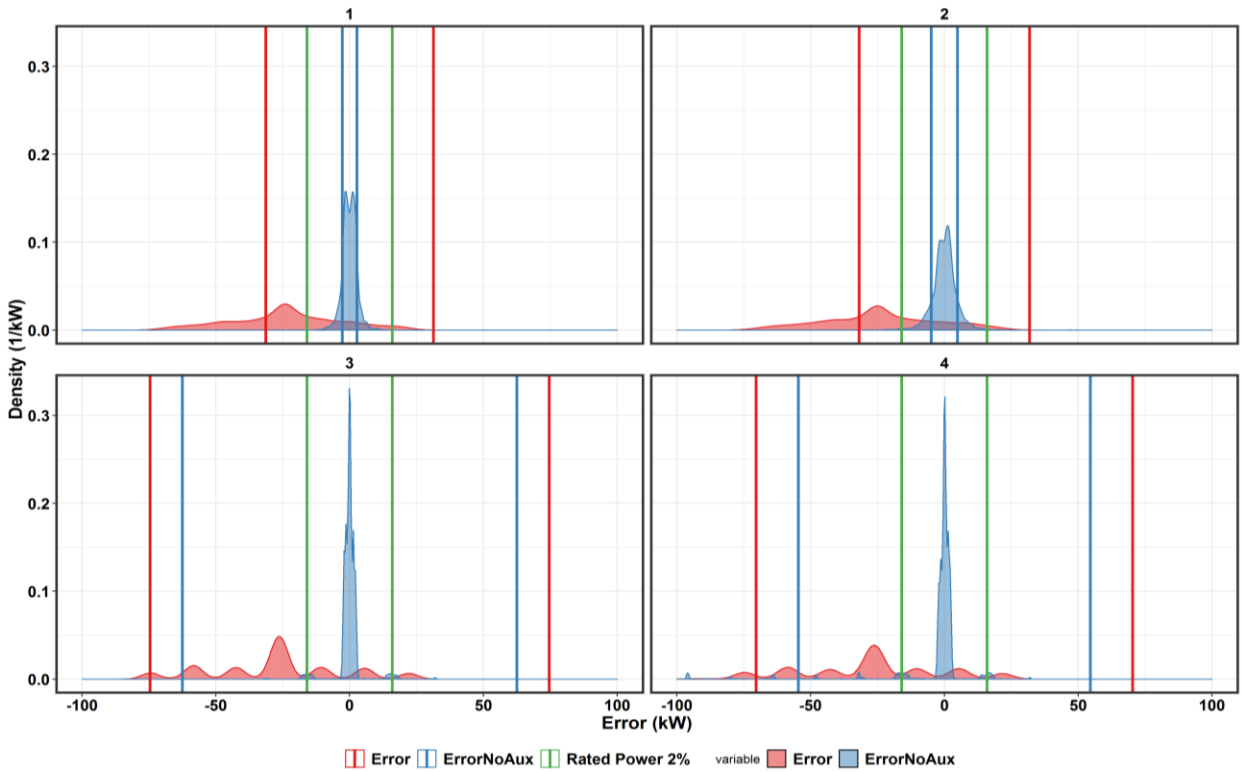

Figure 3.25. Load Following Test Error Distribution

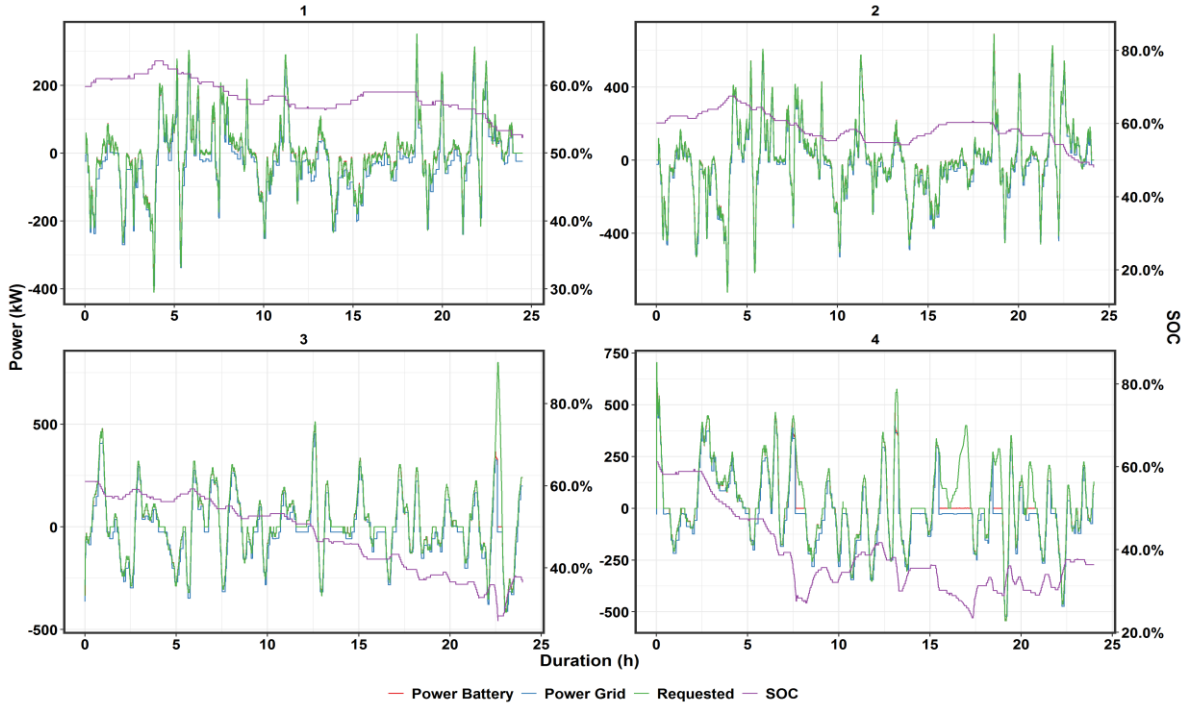

Figure 3.26. Load Following Test Profiles

Table 3.10. Load Following Test Results

Date	2016-02-20	2016-02-21	2016-02-27	2016-02-29
Scale Factor (kW/MW)	10	20	8	8
Strings Active	1	1	1	1
Duration (h)	24	24	24	24
Rest Fraction	0.05	0.02	0.21	0.19
Start SOC (%)	59.8	60.2	61.0	61.2
End SOC (%)	52.7	48.1	36.5	36.4
Average Charge Power (kW)	94	165	163	175
Average Discharge Power (kW)	43	112	122	135
RTE (%)	35	48	42	41
RTE No Auxiliary (%)	61.2	65.4	60.3	55.3
Normalized RMSE (kW/rated kW)	0.078	0.080	0.186	0.176
Normalized RMSE No Aux (kW/rated kW)	0.007	0.012	0.156	0.137
Normalized MAE (kW/rated kW)	0.066	0.067	0.094	0.113
Normalized MAE No Aux (kW/rated kW)	0.005	0.008	0.022	0.042
Tracking 2%	0.92	0.90	0.93	0.93
Tracking 2% No Auxiliary	0.99	0.96	0.97	0.97
Signal Tracking 2%	0.57	0.55	0.68	0.65
Signal Tracking 2% No Auxiliary	0.91	0.85	0.93	0.93

3.10 Use Case 3: Load Shaping dpdt

3.10.1 Duty Cycle Summary

This use case could be tested in a number of ways (e.g., limiting load within a certain threshold or limiting rate of change of load with time). For Avista, this test was conducted by limiting fast variations of feeder load. Using historical 10 second or faster feeder load data from 2011 through 2015, a low-pass filter was designed by PNNL and implemented by Avista (with the algorithm provided by PNNL). This filter is able to remove the signal components that vary faster than those on a 10-minute time scale (i.e., the cut-off frequency of the filter will be 10 minutes). The current feeder load was fed through this filter, and the difference in the filtered feeder load was used to define the current ramp rate of the feeder. The output of the FBESS was this ramp rate multiplied by a response factor to more thoroughly exercise the FBESS. This use case assumes there are no solar photovoltaic ramp rates to mitigate and the load ramp rate on the feeder is minimal. For pre-recorded signals, 1-secod solar data measured in Hawaii and provided by from National Renewable Energy Laboratory was used. This data was run through a validated model to estimate the amount of energy generated.

3.10.2 Test Results

The response factor was reduced by a factor of 2 to account for only one active string during testing. The rest times for these runs were 40 to 65% of test duration, resulting in a low RTE of 41 to 47%. Excluding auxiliary consumption, the RTEs ranged from 55 to 64%. The first two runs were “live” based on feeder load, while the last run was based on a pre-recorded signal.

Surprisingly, the highest RTE was found for the run with the lowest average power levels of 115 kW, where PCS efficiency would be expected to dominate. The average power levels for all runs were low, in

the 115 kW to 245 kW range, resulting in low RTEs even when auxiliary consumption was excluded. Signal tracking was high within 2% of rated power, while normalized RMSE was high at 10 to 15% of the signal when auxiliary power consumption was included. Excluding auxiliary consumption, this error remained high for two runs, at 12 to 13% of rated power. Note that Run 1 has a data hole. Runs 2 and 3 were "live" runs based on feeder load. There was no rest during testing. Results from load shaping tests are shown in Figure 3.27 and Table 3.11.

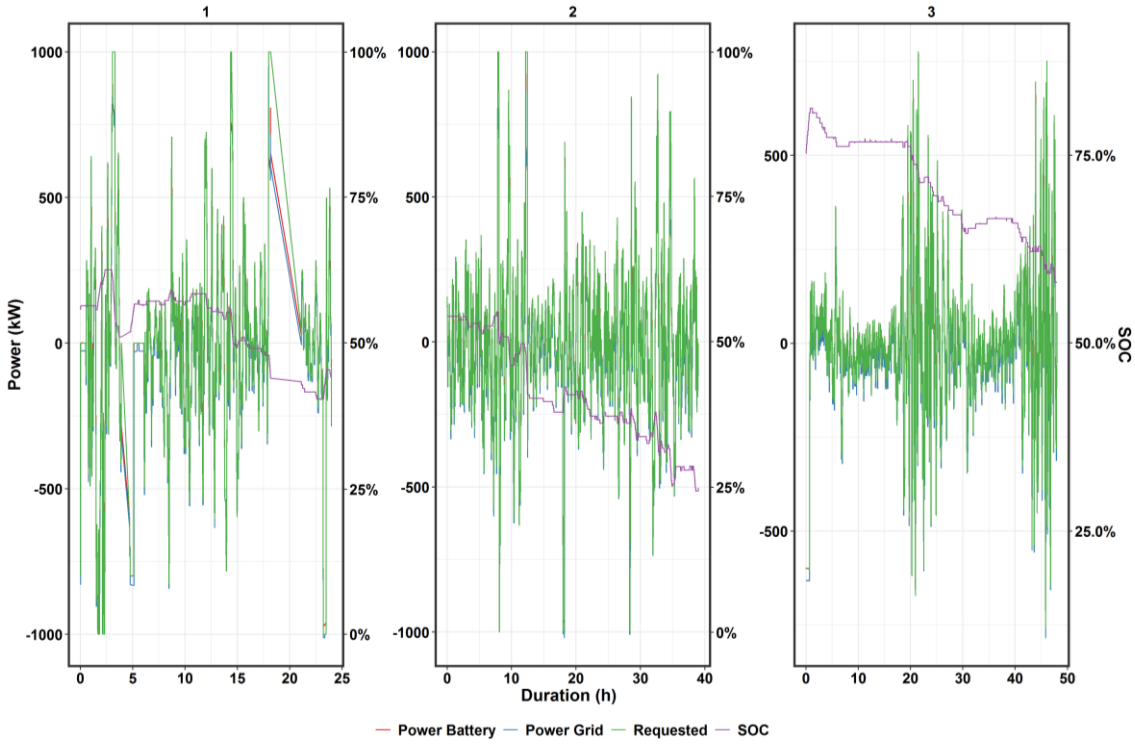

Figure 3.27. Load Shaping Test Profiles

Table 3.11. Load Shaping Test Results

Date	2016-04-14	2016-04-15	2016-04-18
Strings Active	1	1	1
Duration (h)	24	39	48
Start SOC (%)	55.8	54.4	75.3
End SOC (%)	44.2	24.3	58.1
Average Charge Power (kW)	291	207	137
Average Discharge Power (kW)	194	142	88
RTE (%)	42	47	41
RTE No Auxiliary (%)	55.3	63.0	63.7
Normalized RMSE (kW/rated kW)	0.157	0.152	0.093
Normalized RMSE No Auxiliary (kW/rated kW)	0.133	0.124	0.026
Normalized MAE (kW/rated kW)	0.098	0.093	0.077
Normalized MAE No Auxiliary (kW/rated kW)	0.052	0.040	0.015
Tracking 2%	0.92	0.94	0.91
Tracking 2% No Auxiliary	0.74	0.78	0.89
Signal Tracking 2%	0.61	0.55	0.54
Signal Tracking 2% No Auxiliary	0.67	0.65	0.67

As seen in Figure 3.28, when the auxiliary consumption is included, the error peaks at -25 kW. The RMSE is 2 to 3 times 2% of rated power, while tracking with 2% of rated power is high. This is due to a high contribution from responses that have large deviations from the signal.

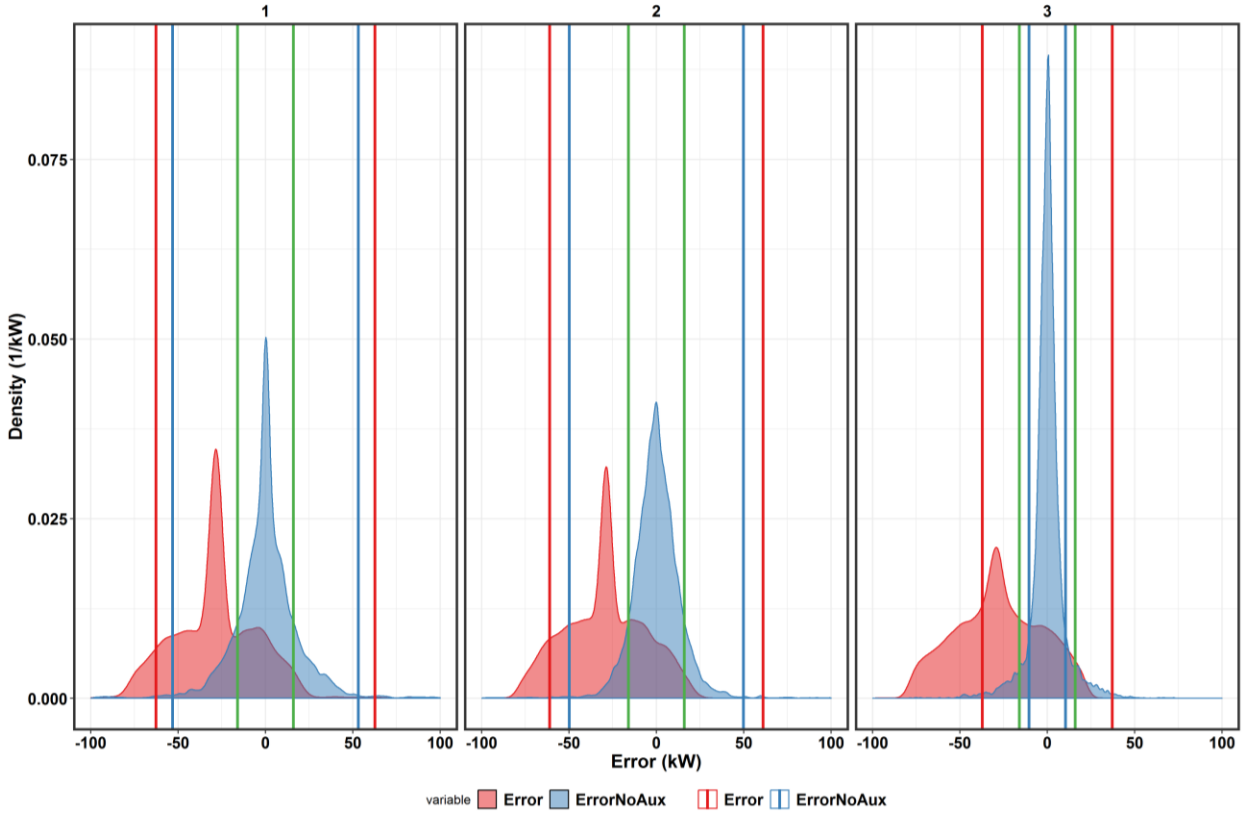

Figure 3.28. Load Shaping Test Error Distribution

3.11 Use Case 3: VAR Support – Power Factor Regulation

3.11.1 Duty Cycle Summary

This use case is tested by verifying the ability of the FBESS inverters to provide vars to achieve a certain objective. Achieving a PF of 1 at a certain location in the feeder was set as an objective in this case. Avista has instrumentation at their substation that measures the total reactive power load in the distribution feeder every five seconds. To determine the reactive power output of the ESS to meet the target, the difference between the current reactive demand of the feeder and the current ESS reactive power output is calculated every 10 seconds. This difference is added to the existing FBESS output to define the total reactive power output. Note that for these tests, the capacitor bank control (CBC) of the integrated volt/var controller (IVVC) for the feeder was disabled, while the FBESS provided vars to keep the feeder PF near 1. No attempt was made to lower the target feeder voltage.

3.11.2 Test Results

Note that power factor regulation (PFREG) does not have any configuration parameters, and simply requests the amount of reactive power needed. The PFREG test was done at a PF of 0.5, with the SOC

maintained in the 45 to 55% range. The FBESS was charged when SOC was <45%, and discharged for all other values. The intent was to open the capacitors depending on the vars in the feeder.

For Run 1 at 2016-03-22 11:25, we determined that there was an inductive spike in vars, accompanied by a real power spike due to the 0.5 PF requirement. The spike in requested vars was due to the Avista distribution-management system (DMS) algorithm compensating for some event. The event did not register on TUR117.CB.KVAR because the DMS updates the TUR117 values every five seconds and the performance interval is recorded only every 10 seconds. Synchronizing the algorithm signal recording frequency with the var measurement frequency in the Avista DMS would have helped identify the event. Both switched capacitors were still closed at that time so it was not due to a capacitor opening. Additionally, if a capacitor opened, a capacitive spike in requested and delivered vars would have occurred. Because inductive vars were requested, the event was probably due to an inductive load such as a motor dropping off.

The two switched caps on TUR 116 were opened at noon for Run 1, and the FBESS provided ~750 kvar while discharging at 425 kW. Testing continued for 4.5 hours after the capacitor banks were opened, with the FBESS performing as designed.

For the next PFREG scheduled for 2016-03-23, String 1 faulted three times while getting FBESS SOC to 50% using 600 kW discharge. The string was taken offline, and the FBESS discharged at 300 kW. Both capacitor banks were open for this test. For most of the test duration, the FBESS was able to provide the requested vars. During the first 10 minutes, while requested vars were 900 kvars, the FBESS could provide only 250 to 450 kvar because it was operating on one string at a PF of 0.5. The vars became limited at a PF of about 0.87 rather than 0.5. Avista was requesting 900 kvar and 520 kW to meet the 0.5 PF requirement, which a single string cannot provide. The inverter has two settings for dealing with this: a watt priority mode and a var priority mode. The Avista code always sets the inverter to watt priority when updating P and Q values. Performance would have improved if priority was given to vars. Within 10 minutes of this event, the capacitor bank was closed to reduce the vars needed and the PFREG recovered as the requested vars decreased to around 200 kvar. The program was subsequently changed to use var priority mode for PFREG. For the next run, only one capacitor bank was opened instead of two to keep the total kvars demand within the range of a single air circuit breaker.

Before Run 2, it was determined that the minimum 0.5 power factor constraint was a software-imposed limitation by UET, and the minimum PF for the inverters was 0.001. This constraint was removed because the minimum PF of the inverters was 0.001. Testing at Avista showed that the minimum PF was 0.01. The 0.5 hard-coded constraint was removed from the software, and the PF was assigned a user-configurable parameter that defaults to 0.01. A test run for 15 minutes with both capacitors in line showed that 400 to 450 kvars were needed to compensate for inductive load. This indicates that the reactive power demand was 1,050 kvar, counting the vars supplied by the two 300 kvar capacitor banks. Because the maximum kvars per-string was 450 kvar,[7] opening a switched capacitor was not an option.

Because of the low PF and associated low real power flow, the SOC decreased from 52 to 40% due to self-discharge over 40 hours. At low PFs, because the real power requested is negligible, starting the test at the high SOC would be essential to extend the test duration. The requested real power is always negative even though the software commands the FBESS to discharge when the SOC is >45%.

[7] Avista engineers assumed it was 600 kvar; however, per the UniEnergy FBESS Technical Specifications, only 450 kvars were available from each string.

Signal tracking within 2% of rated power was very high at 93 to 99%, and the normalized RMSE was 1 to 3%, except for Run 2, where the 900 kvar request could not be met. From the error distribution plots, the error was bound within ±20 kvars for most data points.

As seen in Figure 3.29, the error distribution is narrow and peaks at 0 kvar, and is within ±20 kvar. The RMSE is less than 2% of rated power for two runs. Results from var support PF regulation tests are shown in Figure 3.30 and Table 3.12.

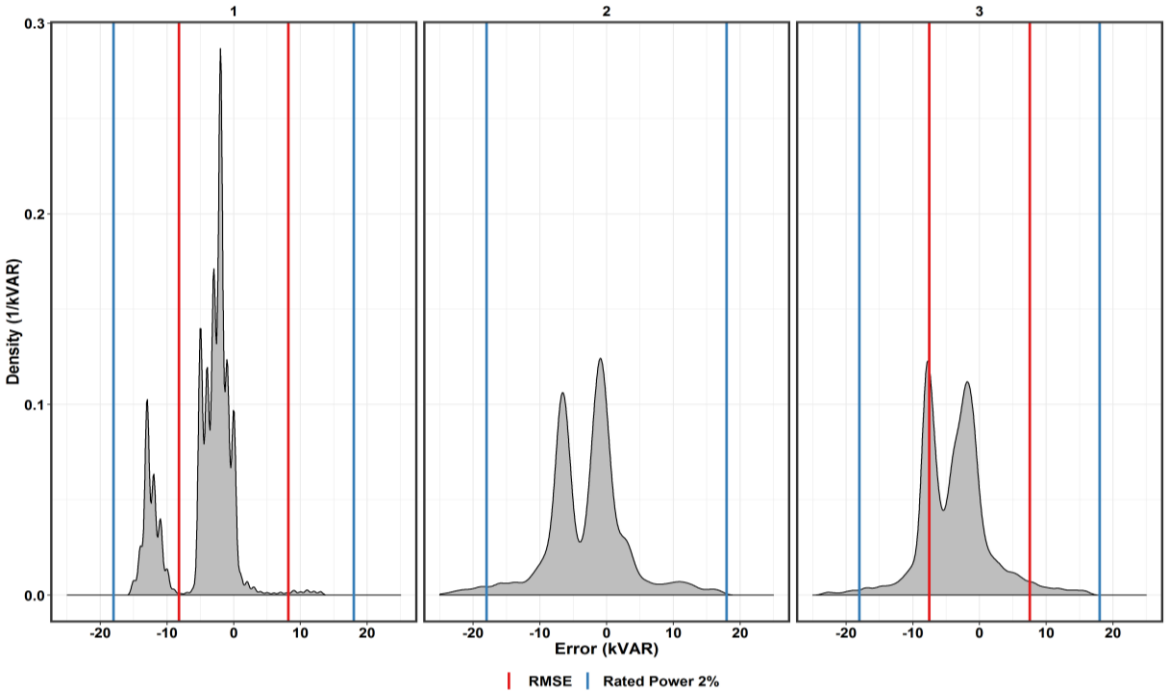

Figure 3.29. VAR Support Power Factor Regulation Test Error Distribution

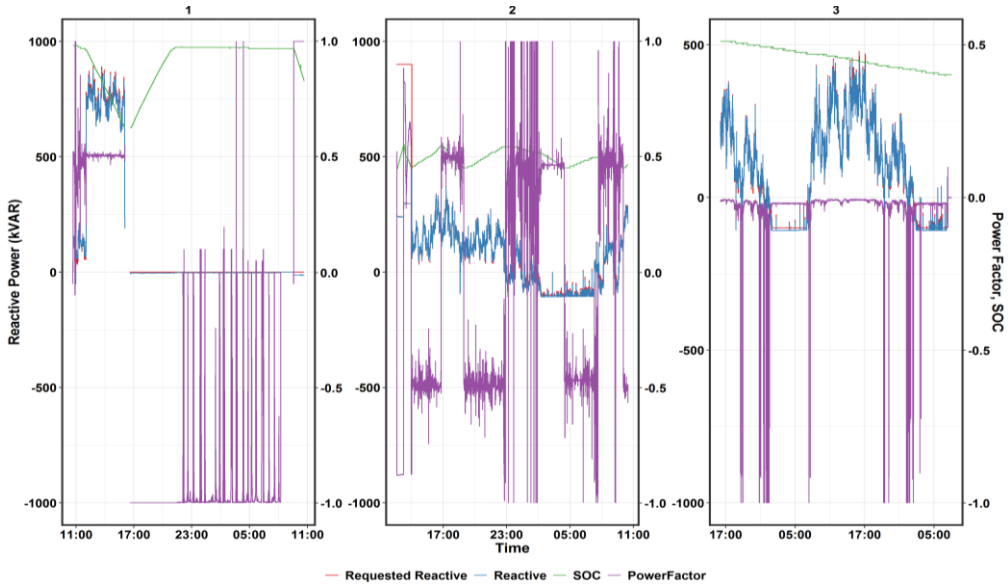

Figure 3.30. VAR Support Power Factor Regulation Test Profile

Table 3.12. VAR Support Power Factor Regulation Test Results

Date	2016-03-22[(a)]	2016-03-23	2016-03-30
Duration (h)	24	22	40
Rest Fraction	0.06	0.01	0.02
Number of Capacitors Switched In	2, 0	0	2
Strings Active	2	1	1
SOC Range	63-98	45-55	40-51
RMSE Reactive (kvar/rated kvar)	0.009	0.180	0.033
Reactive Tracking 2%	0.99	0.99	0.93
Reactive Signal Tracking 2%	1.00	0.60	0.02
Mean Temperature (ºC)	35	35	30

(a) Test started with both bank capacitors switched in, then both were opened at 12 noon.

3.12 Use Case 3: Deferment of Distribution Upgrade – Peak Shaving Dynamic

3.12.1 Duty Cycle Summary

The feeder in which the ESS is installed is currently not experiencing loads that are nearing the capacity of any equipment. To induce the FBESS to behave as if this was the situation, an artificial demand limit was defined in which the FBESS sought to enforce by reducing the total feeder load by discharging. Statistical analysis of recent feeder load data was used to estimate the expected peak load on the feeder during the testing period. Based on this value, the artificial load limit was defined as a specified fraction (85 to 95%). This will define when the FBESS will discharge; charging will take place when the feeder load is beneath a certain fraction of the load (70 to 80%) so as to ensure that the act of charging does not drive the feeder load back above the artificial load limit. Adjustment of these values may be necessary based on early test results. Because the periods of peak load on a feeder are relatively brief, it is not anticipated that the FBESS will need dedicated recharging periods outside of those provisioned by the above algorithm. This test was conducted with and without var.

3.12.2 Test Results

Set points for the feeder power levels to trigger FBESS discharge were selected based on:

1. Weekday or weekend.
2. To ensure FBESS discharges.
3. To ensure discharge duration is not too large, the FBESS SOC would be too low to sustain required power.
4. To ensure discharge duration is not too small. Cutting it so fine may result in the FBESS not being called upon to discharge.

The PF varied from 0.01 when no real power was requested to residing at less than -0.9 or greater than 0.9 when charge or discharge power was requested. The PF sign was assigned a negative sign when the requested vars was the same sign as requested watts and vice versa.

For some tests, the feeder load did not exceed the set point, resulting in the FBESS not being called upon to discharge. For other tests, the set point was too low, resulting in extended discharge periods that were too long for the FBESS to provide required power. While the FBESS performed these functions as intended, this use case shows the importance of:

1. A reliable model to predict peak feeder load and duration.
2. An intelligent algorithm to set the trigger point for FBESS discharge such that FBESS can meet the required power for the required duration.
3. The FBESS being readied for responding to discharge command by bringing it to the required SOC.

The RTE for some runs was <7% due to the extremely small durations for which the FBESS was called upon to discharge.

As seen in Figure 3.31, the error distribution peaks at -5 to 5 kvar. The RMSE is near 2% of the rated power for most runs. Results from dynamic peak shaving test are shown in Figure 3.32 and Table 3.13.

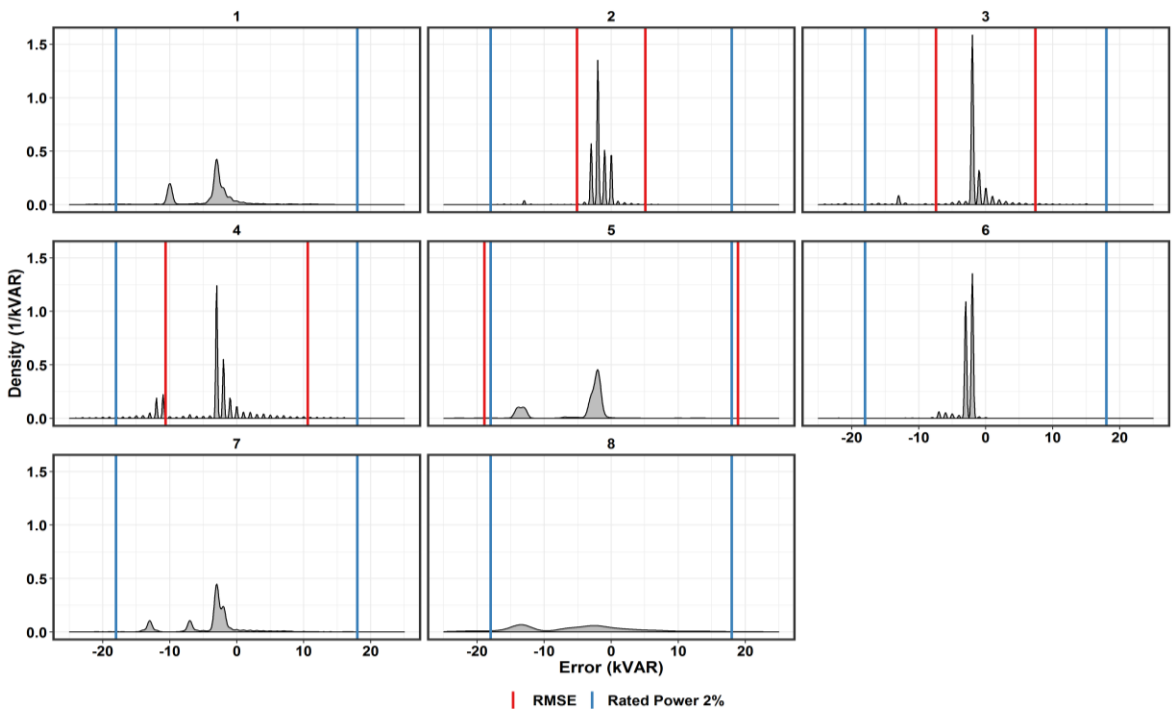

Figure 3.31. Dynamic Peak Shaving Error Distribution for Reactive Power

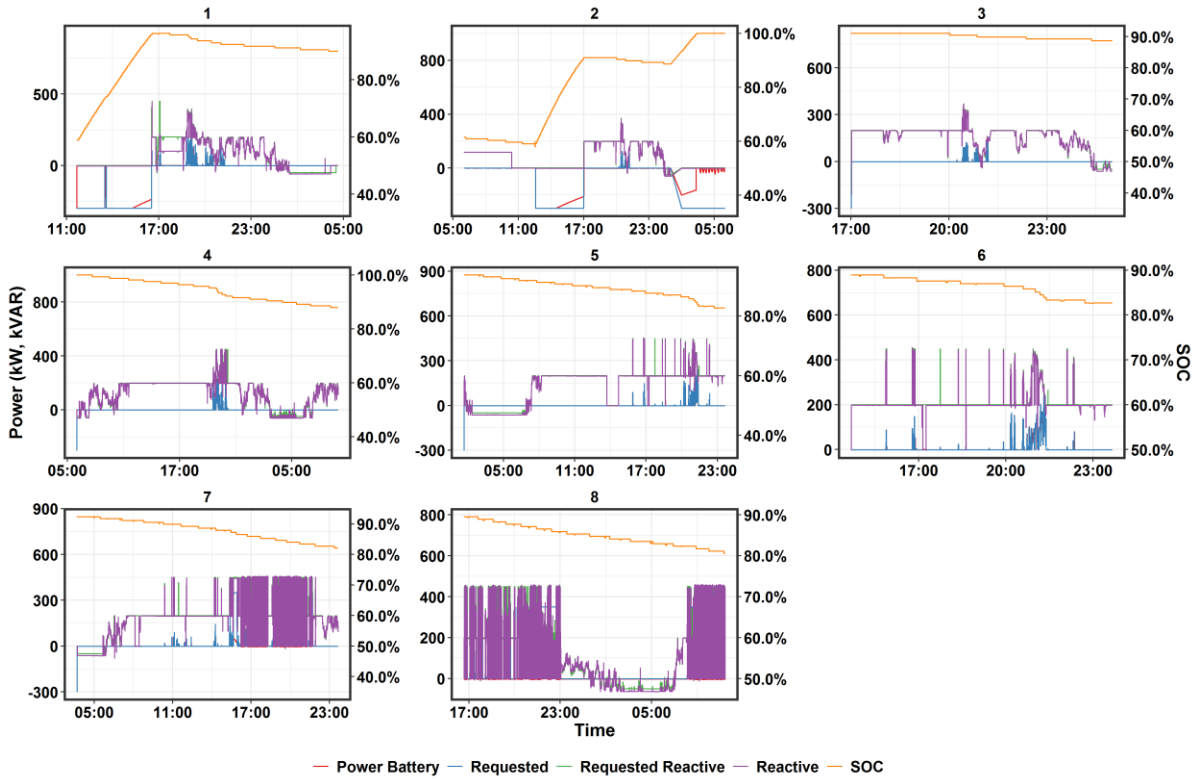

Figure 3.32. Dynamic Peak Shaving Test Profiles

Table 3.13. Dynamic Peak Shaving Test Results

Date	2016-04-22	2016-05-24	2016-05-25	2016-05-25	2016-06-03	2016-06-03	2016-06-04	2016-06-05
Starting Weekday	Fri	Tue	Wed	Wed	Fri	Fri	Sat	Sun
Discharge Start	2016-04-22 23:31	2016-05-25 03:26	2016-05-25 03:26	2016-05-26 03:36	2016-06-03 22:53	2016-06-03 22:53	2016-06-04 17:56	2016-06-05 23:47
Set Point (kW)	3,880	3,700	3,700	3,700	3,700	3,400	3,100	2,900
Peak Discharge (kW)	184	121	121	275	255	255	129	NA
Average Discharge (kW)	93	85	85	131	102	102	77	NA
Duration (h)	17	24	8	28	22	9	20	17
Rest Fraction	0	0	0	0	0	0	0	0
Discharge Fraction	0.07	0.01	0.03	0.03	0.04	0.10	0.27	0.36
Charge Fraction	0.92	0.89	0.97	0.97	0.91	0.90	0.73	0.64
Strings Active	1	1	1	1	1	1	1	1
SOC Range	59-96	58-100	89-91	88-100	83-94	83-89	82-92	80-90
Start SOC	59	61	91	100	94	89	92	90
End SOC	90	100	89	88	83	83	82	80
RTE	51.3	49.9	5.2	7.3	7.7	15.9	2.5	NA
RMSE Reactive (kvar/rated kvar)	0.177	0.027	0.039	0.056	0.095	0.131	0.547	0.568
Reactive Tracking 2%	0.92	0.98	0.95	0.92	0.98	0.99	0.94	0.87
Reactive Signal Tracking 2%	0.37	0.47	0.04	0.04	0.10	0.14	0.27	0.36
Mean Temperature (ºC)	35	28	28	32	24	25	26	27

3.13 Use Case 5: Enhanced Voltage Control

3.13.1 Duty Cycle Summary

The IVVC in the feeder was used to conduct this use case test by using the FBESS inverter var capability to source/sink var for implementing conservation voltage reduction (CVR) as a form of enhanced voltage control. For some tests, the switching capacitors on the feeder was disabled, and only the FBESS and voltage regulators were used to regulate voltage on the feeder.

There are potentially multiple means by which the ESS inverter can provide value when used for CVR. Given the installation location of the FBESS at the end of the distribution feeder, using the var output to improve the end-of-line voltage will help flatten the voltage profile and potentially allow the IVVC system to operate at a lower voltage, thereby increasing CVR benefits. Alternatively, it may be possible for the FBESS to adequately flatten the voltage profile of the existing feeder(s) without the assistance of other IVVC assets (voltage regulators and switched capacitors). If this is the case, the value of the FBESS is 1) avoided capital costs for replacement of the existing devices when they reach end-of-life and 2) any value provided by the general CVR benefits described above. As a secondary test, the FBESS was placed in PFREG mode (regulating the head of the feeder to unity power factor), and the IVVC system engaged with only the voltage regulator online (physical switched capacitors still disconnected). This test determined if the IVVC is able to appropriately regulate the voltage of the feeder with the FBESS acting in an independent manner. In both scenarios, smart meter data from the feeder were used to determine if the IVVC is able to achieve lower target voltages on the feeder without triggering low-voltage alarms from the smart meters. To most fully estimate the benefits of all of these use cases, testing had to be conducted over a variety of system conditions, most especially different circuit loads. The FBESS could be included and excluded from the IVVC on a periodic basis, with an interval defined by how long it takes the IVVC to re-equilibrate after such changes.

3.13.2 Test Results

During this service, real power alternating between 10 kW and -30 kW was requested, possibly to maintain the FBESS within desired SOC range. This may also be due to the minimum PF requirement of 0.01. Because real power exchange with the grid is not relevant for this use case, only reactive power was plotted.

Multiple runs were conducted for this use case, with the FBESS controlled by IVVC in various modes. For all the runs, only one string (String 2) was available. Run 1, lasting 48 hours (2016-04-04), was done using the FBESS as two virtual capacitors. This virtual capacitor mode had to be manually engaged as opposed to via the schedule file. One capacitor was set at 150 kvars, and the other at 300 kvars.

The Run 1 results were not as desired, the IVVC dispatched the battery as if it were two switched capacitor banks. However, the actual vars provided was incorrect due to a "race condition"[8] that could not be reproduced. The IVVC sometimes opens one of the virtual capacitors while closing the other. According to Avista, the commands arrive in the same millisecond. Because var adjustments were done asynchronously, this leads to vars requested being less or greater than required. This resulted in occasions when 900 and 1,500 kvars were requested, even though the requested vars should not exceed the string rating of 450 kvar. This resulted in high RMSE and poor signal tracking for Run 1.

[8] "Race condition" is the term used by Avista to describe the situation.

The virtual capacitor mode generated commands several minutes or even hours apart. Hence, to keep the connector closed, the FBESS was sent PFREG commands every 15 seconds, thus keeping the connector closed. After changing modes, there was a system fault, which may or may not be related to the mode change. There were delays in getting the SEL meter voltage data available to the Avista PI system; it was important to get this information to ensure the SEL facility was not adversely impacted before the IVVC set point voltage could be lowered at the pre-selected location in the feeder.

Planning for alternate ways to implement the IVVC/CVR algorithm occurred in May, June, and July of 2016. The voltage control mode for regulator tap control was enabled on TUE 117, and the CBC was disabled. The FBESS was set to var-following using the PFREG command to control the PF at the desired feeder location near 1 to get the best feeder PF. The voltage controlling portion of the IVVC was used to reduce feeder voltage. This was implemented using a PFREG command in a schedule file and changing the voltage control set point in the Avista DMS. One run was completed successfully from 2016-10-20 to 2016-10-21. According to Avista, this run was able to keep the feeder voltage at low levels with the voltage at the desired location controlled at 118 V. The PF in the feeder was optimally controlled, while the voltage at SEL remained at desired levels. For this run (Run 2), the FBESS was run in PFREG mode. The RMSE was 0.025 kW/rated kW, which is good tracking performance. The reference signal tracking was only 51% within 2% of rated power.

Consideration was given to command the FBESS to provide real power to further control feeder voltage. However, it was not found to be very effective even when feeder load was not very large.

The error distribution plot (Figure 3.33) shows that for Run 1, the RMSE is expectedly very large (and is not seen within the scale of the plot). For Run 2, the RMSE is within the 2% rated power dead band.

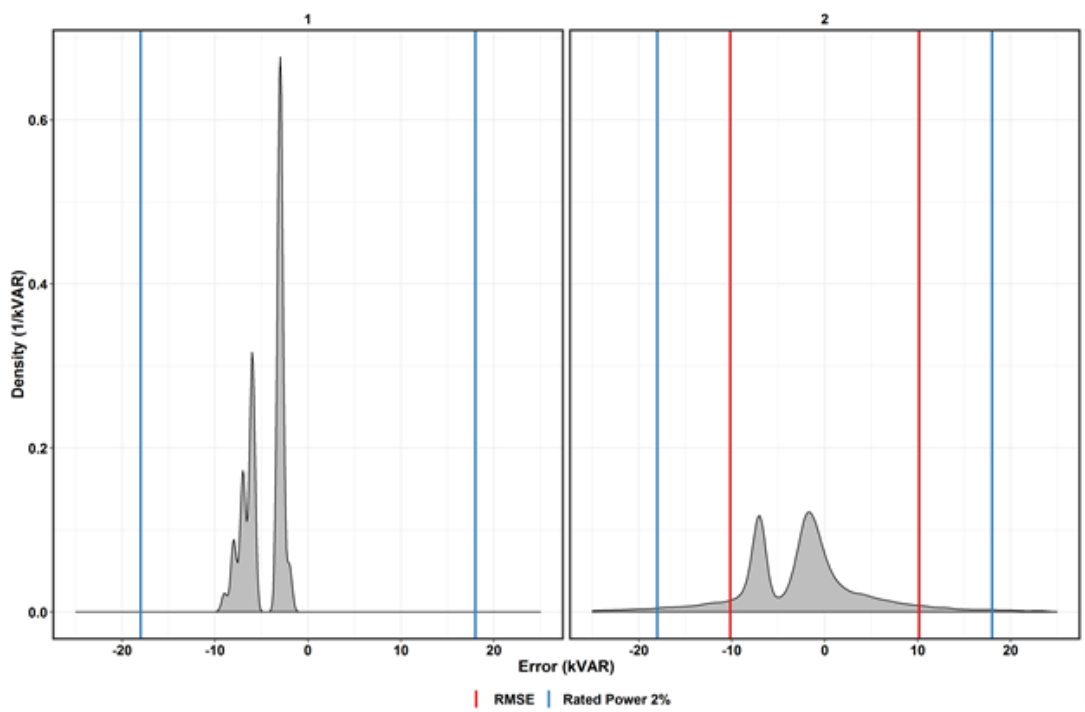

Figure 3.33. Error Distribution for IVVC

Results from CVR-IVVC tests are shown in Figure 3.34 and Table 3.14.

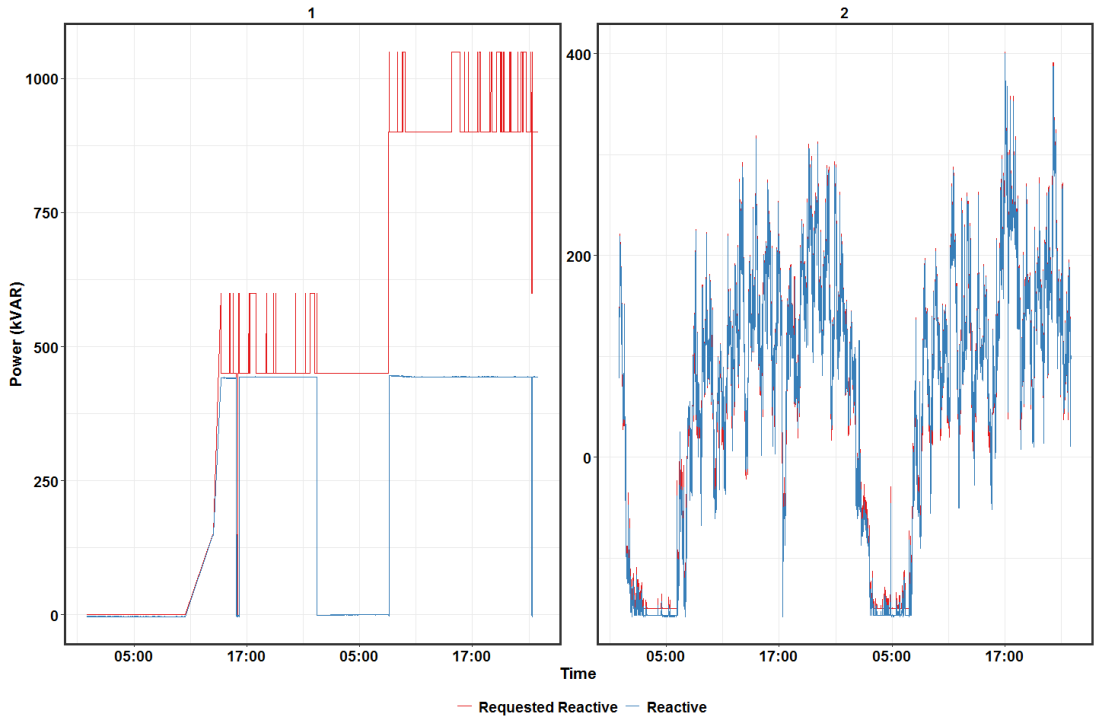

Figure 3.34. CVR/IVVC Grid Service. FBESS as two virtual capacitors with IVVC in CBC mode (left) and IVVC in voltage control mode with FBESS in PFREG mode (right).

Table 3.14. CVR-IVVC Test Results

Date	2016-04-04	2016-10-20
Duration (h)	48	48
Rest Fraction	0	0
Strings Active	1	1
SOC Range	42-75	30-41
RMSE Reactive (kvar/rated kvar)	0.875	0.025
Reactive Tracking 2%	0.24	0.51
Reactive Signal Tracking 2%	0.56	0.56
Mean Temperature (ºC)	31	26

3.14 Use Case 6: Microgrid Operations

3.14.1 Duty Cycle Summary

Avista has developed its own test plan to verify the capabilities of the FBESS to perform the operations needed during islanded microgrid operation. That test, however, did not fulfill all of the project needs associated with evaluating performance of the battery during islanding operations. Therefore, PNNL produced a separate test plan and duty cycles for this use case following the approach of the DOE Protocol, with relevant modifications to incorporate the Avista FBESS parameters (Viswanathan et al. 2014). The approach used for developing the duty cycles is briefly described below.

The key to developing the duty cycle was to determine the output that would be able to serve microgrid load in conjunction with intermittent generation resources (e.g., solar and wind) while ensuring operational limits (e.g., charging/discharging power, minimum and maximum SOC) are not violated. Three use cases were considered: 1) a microgrid with a mix of power from renewable resources (solar and wind generation), 2) a microgrid with power from renewable resources but no frequency regulation, and 3) a microgrid with no power from renewable resources and no frequency regulation. All of the use cases include var support, power quality, frequency response, and black start.

To develop a generic duty cycle, the DOE microgrid test working group chose published data for load and solar- and wind-generated power. The frequency regulation signal was obtained from the Pennsylvania New Jersey Maryland (PJM) market. The balancing signal was generated power minus load. Frequency response consisted of primary, secondary, and tertiary response. Primary frequency response involved charging or discharging the ESS for 30 seconds. Secondary response was simply a response to the frequency regulation signal. Tertiary frequency response corresponded to tertiary frequency control provided by generators in standby mode and therefore are not relevant to the ESS.

For the purpose of determining the duty cycle for an ESS in an islanded mode, parameters were set so the peak charge and discharge power would not exceed the ESS rated power, and the energy used would not exceed the ESS rated energy. During the duty cycle, the ESS charges or discharges based on the difference between load and generation.

3.14.2 Test Results

The AEG inverter did not have islanding capabilities. Hence, the AEG inverter was replaced by the NPS inverter, and a Turner Energy Storage System Site Recommissioning Test Plan developed. A copy of this plan is placed in Appendix A. Islanding tests were completed successfully during the first two weeks of April. A test report has not been provided to PNNL.

Duty cycles using multiple cases for microgrids from the DOE-OE protocol were provided to Avista using feeder specific parameters. These were not executed due to FBESS unavailability.

3.15 Use Case 7: Optimal Utilization of Energy Storage

At the end of the Use Cases 1-6, the FBESS was to have been deployed to optimize benefits by responding to all use cases addressed; due to multiple delays, testing was stopped, and this use case was not done.

4.0 Lessons Learned

This section provides an at-a-glance view of important lessons learned on the technical aspects of the Avista Turner FBESS based on the experience gained during the testing process and the results obtained. Remarks on the overall testing effort and the importance of the test results are provided in Chapter 6, Conclusions.

4.1 Lessons Learned from Test Results

1. The FBESS discharge power was constant down to various SOC levels, with the discharge power affecting the SOC at which power starts tapering, with this SOC being higher for higher discharge powers. The charge power did not affect the discharge energy, which is as expected. Discharge energy increased with decreasing discharge power levels in the 400 to 1,000 kW range.
2. The RTE peaked at 520 kW discharge, 600 kW charge. As expected, excluding auxiliary consumption led to higher RTE at low discharge power levels.
3. The discharge energy ranged from 2,040 to 3,395 kWh. When auxiliary consumption is excluded, the range was 2,050 to 3,635 kWh.
4. When the auxiliary consumption was excluded throughout the test, the RTE increased by 8 to 10%, with larger increases at lower charge and discharge rates.
5. The cumulative AC-AC RTE calculated for the individual strings was 63% for both strings at the end of testing, while the DC-DC RTE was 73%.
6. The cumulative coulombic efficiency decreased from 98% at the start to 95% at the end of testing, indicating electrolyte cross-over did not appear to be a big issue, and was suitably addressed by periodic maintenance.
7. At the Electric Power Research Institute Energy Storage Integration Council meeting held in November 16, 2017, the following key gaps were identified as meriting further study:
   a. SOC calibration procedure;
   b. Seasonal testing for auxiliary load;
   c. SOC loss rate due to reactive power injection; and,
   d. State of health definition and tests.

   All these gaps were addressed in this project.
8. BMS-related issues include:
   a. The presence of the variable speed drive suggests the BMS adjusts flow rate based on power level and SOC; and
   b. Power tapered during charge and discharge when various SOC thresholds were reached.
9. The internal resistance was lowest at 60 to 90% SOC for charge and discharge. Charge and discharge resistance were highest at 30% SOC.
10. Maximum discharge power of 1,000 kW could not be attained at ≤ 30% SOC, while maximum charge power of 800 kW could not be attained at >60% SOC. The maximum power operating envelope as a

function of operating mode and SOC needs to be considered for applications such as frequency regulation and peak shaving, where a certain power is bid by the battery owner.

11. The maximum charge rate was set by UET to be 200 kW/sec, and decreased with increasing SOC to 50 kW/s at 90 to 100% SOC. The maximum discharge ramp rate was ~10% higher than the maximum set rate of 300 kW/s.
12. The requested power commands were met by the PCS without accounting for auxiliary consumption. Hence, power exchange with the grid differed from requested power by the auxiliary consumption, in addition to any tracking error for power at the PCS. Because the grid operator cares only about the power that is exchanged between the FBESS and the grid, it is prudent to have the BMS adjust the PCS input or output such that the requested power is exchanged with the grid. Otherwise, there would be significant tracking errors for volatile signals. For use cases such as peak shaving, if auxiliary consumption is too high, the power delivered to the grid during peak periods may not be sufficient to meet the demand.
13. There was no difference between average charge and average discharge temperature. This seems counter-intuitive because charging involves an endothermic reaction. However, the starting temperature for charge is the high temperature at the end of discharge, while the starting temperature for discharge is the lower temperature at the end of charge.
14. Auxiliary consumption at fixed power for charge is higher compared to discharge. Charge may require a greater flow rate per kW to prevent gas evolution by facilitating faster mass transport and lowering over-potential. Charge resistance is lower than discharge resistance across the SOC range, thus lending support to this hypothesis.

4.2 Lessons Learned in Design of Data Transfer

The data transfer setup was quite smooth. Data was transferred from the Avista SCADA to the server of the PNNL contractor and parsed into a MySQL database. Using a MySQL connector, this data was downloaded onto a PNNL computer and a PNNL shared drive, where all data resides. Options for transferring all the data to a PNNL storage site are being explored. Some data tags were only available every 10 seconds, while other tags were available every second.

4.3 Lessons Learned in Design of Test Setup

1. Detailed line diagrams were provided by Avista.
2. Auxiliary power consumption was not monitored because this tag was not part of the MESA tag list for the FBESS (Miller 2017).
3. For each string, one meter measured power exchange with the grid, while another measured power flow in and out of the PCS. The auxiliary consumption was calculated from the difference of these power flows.
4. UET defined a “Connection Point,” which was a virtual meter that added the power flow through each PCS. The location where the PF was being controlled was not shared with the team. The minimum PF for the AEG inverter was assumed to be higher than its actual minimum PF. This resulted in having to flow more real power during VAR support than needed.
5. Each string can be placed in local mode and balanced by UET.

6. There is no active heating. Thermal management becomes operational at only at temperatures >35ºC. The difference between maximum and minimum temperature was less than 5ºC, indicating the thermal management system was effective.

4.4 Lessons Learned from Site Related Issues

1. Because strings dropped out during testing, the requested power was adjusted to reflect the active strings.
2. It would have been useful to have tags that show the number of active strings, and the strings that are active.
3. The FBESS provided the requested vars for the relevant use case. However, the effectiveness of the Avista algorithm to keep the PF at 1 or the feeder voltage at 118 VAC at the specific location in the feeder was verifiable only by the Avista engineer, since this data was not available to PNNL.
4. The communication lag between the time the signal was sent from Avista headquarters and the time it was received by the FBESS was estimated to be 10 seconds.
5. When a string dropped out, UET placed it in local mode and did the necessary maintenance/repairs. The ongoing test was completed before UET brought the string online.

5.0 Novel Findings

5.1 State-of-Charge Model

A nonlinear state of charge model was developed during experimentation to be used in economic modeling and to aid in developing schedules for the testing.

The rate of change of state of charge, dSOC/dt, could be modeled by Equation 1, as seen in Figure 5.1.

$$\frac{dSOC}{dt} = a(SOC - b)^c \tag{1}$$

Where a, b, and c were functions of power and temperature. In Equation 1, b represents the SOC at which power begins to taper, also referred to as the taper SOC. Since c is negative, as SOC approaches b, $(SOC - b)^c$ and hence dSOC/dt blows up, in line with observed data – therefore this function naturally puts a lower bound on the SOC range for discharge at a fixed power and temperature.

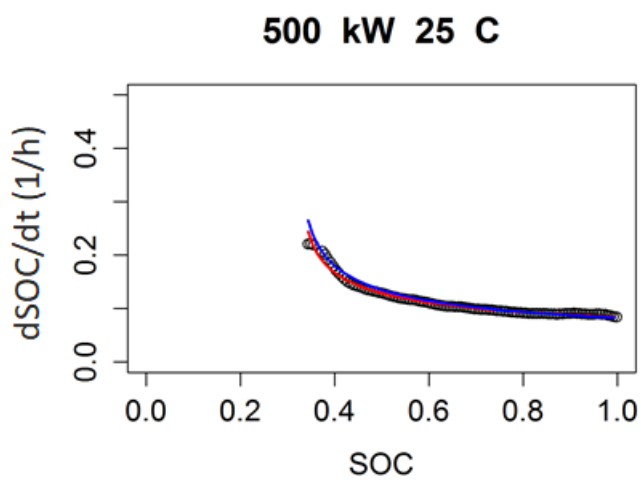

Figure 5.1. Example of dSOC/dt vs SOC for an Example Half-Cycle

The model was developed using all charge or discharge half-cycles within which the power was constant over an SOC range of at least 30%, corresponding to 66 charge and 67 discharge half-cycles. The dSOC/dt was calculated from the data by locally estimated scatterplot smoothing (LOESS) the SOC with respect to time and then taking the numerical derivative. The smoothing step is important because the SOC is only recorded after a 0.6% change in SOC, meaning the SOC vs. time looks like a staircase when zoomed in; additionally, the act of taking the derivative amplifies noise. For each half-cycle, the coefficients a, b, and c were regressed, giving us a database of half-cycles, with each half-cycle having its own a, b, and c coefficients. These coefficients were regressed vs. the average power at the grid and average temperature during the half-cycle using Equations 2-4. This regression is done separately for charge and discharge.

$$a = P\left(K + K_p P + K_T T\right) \tag{2}$$

$$b = P\left(K + K_p P + K_T T\right) \tag{3}$$

$$c = \left(K + K_p P + K_T T\right) \tag{4}$$

These coefficients are given in Table 5.1.

Table 5.1. Regression Constants for Non-Linear Model

Parameter	Mode	K	K_P	K_T
a	Discharge	1.17E-04 $kW^{-1}h^{-1}$	5.87E-08 $kW^{-2}h^{-1}$	-2.61E-08 $kW^{-1}h^{-1}C^{-1}$
b	Discharge	8.10E-04 kW^{-1}	1.26E-07 kW^{-2}	-9.85E-06 C^{-1}
c	Discharge	-6.53E-01 kW^{-1}	6.02E-04 kW^{-2}	-1.05E-03 C^{-1}
a	Charge	7.351E-05 $kW^{-1}h^{-1}$	2.061-08 $kW^{-2}h^{-1}$	-5.545E-07 $kW^{-1}h^{-1}C^{-1}$
b	Charge	0	0	0
c	Charge	-1.353 kW^{-1}	3.895E-04 kW^{-2}	-1.357E-02 C^{-1}

Using this model, the SOC change in 1 hour at various charge and discharge rates in the 100 kW to 1,000 kW range was provided to Avista. Avista used these charts to develop an algorithm to optimally deploy the FBESS to charge and discharge as needed based on grid conditions and market prices. An example of the validation of this model during peak shaving can be observed in Figure 5.2 below, with the dotted black line representing the predictive model and the solid gold line representing the measured SOC.

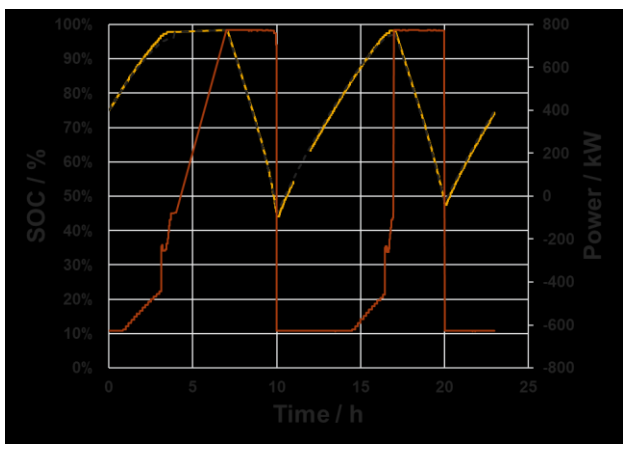

Figure 5.2. Example of Applying Non-Linear Model

Subsequent modeling work moved away from this method of SOC prediction, as it has some flaws that were fixed and improved upon. The main flaws are that the model predicts dSOC/dt, while the objective is to predict SOC as a function of time. Hence the error in regressing SOC as a function of time should be minimized, not dSOC/dt. Moreover, the smoothing required to calculate dSOC/dt removes some signal along with the noise. Calculating a, b, and c is a regression of a regression, leading to accumulated error. Finally, this method locks us into the function form of Equation 1, which isn't very flexible and doesn't allow us to investigate all possible relationships between dSOC/dt and power, SOC, and temperature. All these issues have been fixed in our next iteration of the model, which has not yet been applied to Avista, but will be in future work.

5.2 Temperature Change Analysis

The FBESS temperature increased during discharge and decreased during charge, with no charge during rest as seen in Figure 5.3. The rate of change of temperature was regressed vs. power and difference

between FBESS and ambient temperature, as shown in Table 5.2, with an adjusted R^2 of 0.96. The positive coefficient for power shows an endothermic effect for negative power (or charge). The ohmic heating effect is represented by the coefficient of the P^2 term. The entropic term dominates for this high energy to power battery, consistent with the findings of Viswanathan et al. (2010). Note that at 1,600 kW, the E/P is 8,800 kWh/1,600 kW, or 5.5 hours, while at 500 kW, the E/P is 17.6 hours.

When the ΔT between FBESS and ambient is increased, temperature increase is lower, either because of heat loss to ambient or active cooling being initiated.

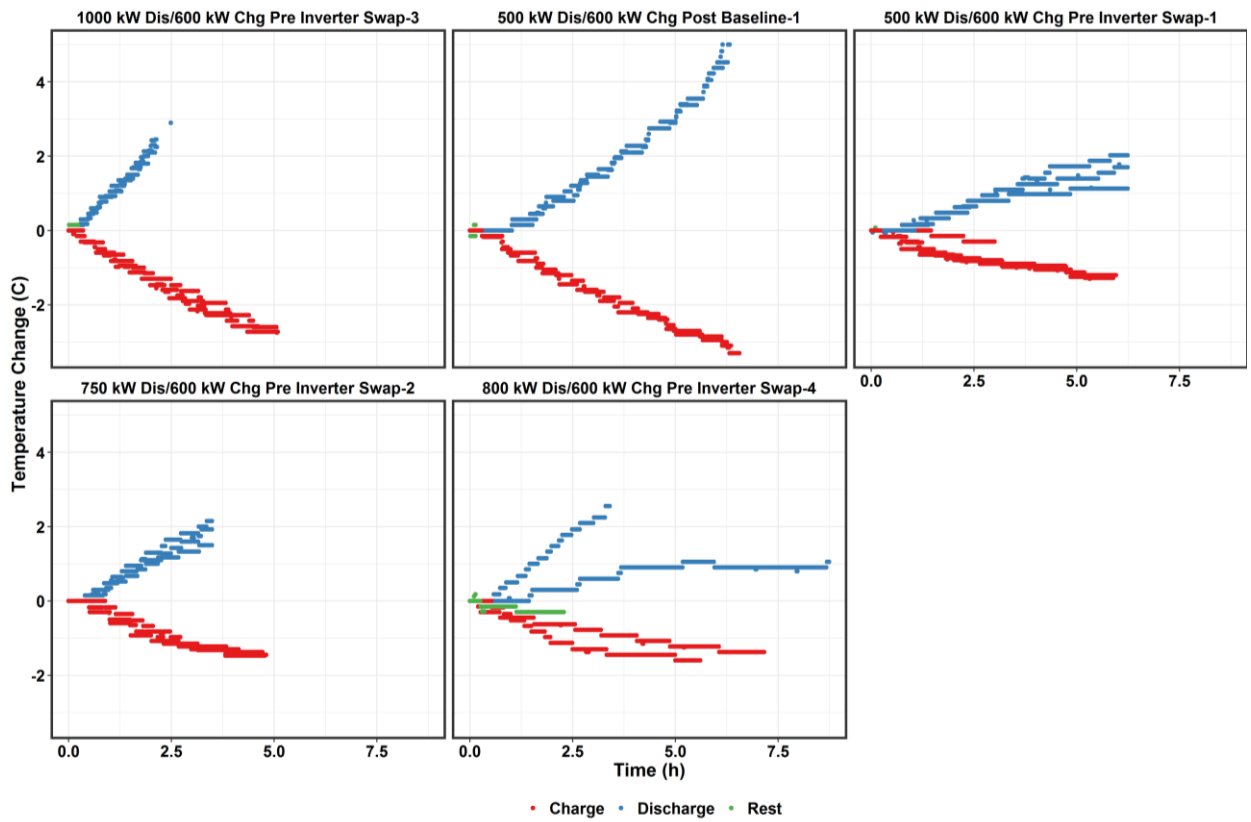

Figure 5.3. Temperature Change for the Various Baseline Capacity Tests for Charge, Rest, and Discharge. The endothermic effect of charge is shown.

Table 5.2. Regression Results for Rate of Temperature Change as Function of Power, Power Squared, and Difference between FBESS and Ambient Temperature

Parameter	Coefficient	Standard Error	Units
Power (kW)	0.0011	2.97e-06	C/kWh
Power Squared (kW^2)	1.87e-07	6.88e-09	C/(kW^2-h)

6.0 Conclusions

Avista has deployed a 1 MW/3.2 MWh UET vanadium FBESS. As part of Washington CEF 1, a $3.2 million grid modernization grant was awarded to Avista, and Avista matched that amount by $3.8 million. The FBESS is located on the Avista 12-kV distribution system between the Turner Substation and the SEL manufacturing facility in Pullman, Washington. The CEF grant supported exploration of energy storage applications and associated benefits for the following use cases that were identified as applicable for Avista, and were defined based on the following utility- and site-specific characteristics:

- Energy Shifting,
- Grid Flexibility,
- Improved Distribution Systems Efficiency, and
- Enhanced Voltage Control.

The analyses of FBESS's tested performance confirm that the technical characteristics (e.g., capacities) and performance (e.g., response rate) of the Avista FBESS are sufficient to meet the demands of the use cases evaluated in this project. Because individual battery strings failed during testing, the delivered power and energy during testing were less than scheduled. On several occasions, testing had to be done with less than two strings.

The findings documented in this report will help Avista understand the performance of the FBESS in its current state and to apply these results in designing appropriate operational strategies. In addition, the results and lessons presented herein will be beneficial in general for any task or effort that involves technical assessment on similar types of FBESSs based on field deployment results.

Some specific conclusions are:

- The range of discharge energy capacity for all tested cycles and C-rates ranged from 2,020 to 3,600 kWh. The energy delivered at a rated power of 1,000 kW was approximately two-thirds the rated energy of 3,200 kWh, which was obtained at 520 kW discharge.
- The range of RTEs for all RPTs performed was 57 to 75%, depending on which losses were included. When auxiliary losses were included, RTEs ranged from 57 to 65%, increasing to 63 to 75% when auxiliary consumption was excluded.
- RTE peaked at 520 kW discharge when auxiliary consumption was included, while it increased with decreasing power level when auxiliary consumption was excluded. Low power levels at which a peak is expected to occur for the latter were not investigated. In the power range investigated, the RTE without auxiliary consumption showed the same trend as DC-DC RTE, both increasing with decreasing power levels.
- The FBESS provided energy at constant power across various SOC ranges, with this SOC range depending on power level and electrolyte temperature. Its performance was reliably modeled, thus enabling deployment for various energy use cases with accurate quantification of net benefits.
- The increase in RTE when excluding auxiliary consumption was highest for low power levels and high rest periods, as expected. It is anticipated that at less than 15 to 25% of rated power, RTE would decrease because of low PCS efficiency.
- The response time of the FBESS ranged from 3 to 10 seconds for the range of test cycles performed. For charge, the response time increased from 4 to 10 seconds as SOC increased from 20 to 60%, reaching a maximum power of 800 kW. At >60% SOC, the maximum power attained decreased linearly to 400 kW at 100% SOC. Hence, while the response time was lower (to attain this lower

maximum power), the ramp rate decreased from a maximum of 200 kW/s at 30% SOC to 50 kW/s at 90 to 100% SOC. The results are consistent with UET limiting charge ramp rates to 200 kW/s.

- The response time for discharge was 3 seconds. The ramp rate ranged from 340 kW/s at 90% SOC, with a slight decrease to 315 kW/s at 30% SOC, with maximum attained power at ~1,000 kW in the 90 to 40% range, dropping slightly to 950 kW at 30% SOC. The results are consistent with UET limiting discharge ramp rates to 300 kW/s.
- The FBESS charge and discharge resistance, corrected for two strings, was in a tight range for discharge, decreasing from 0.100 ohms to 0.110 ohms as SOC decreased from 90 to 40%. There was a spike in internal resistance at 30% SOC to 0.125 ohms. On a four-string normalized basis, the resistance is 0.05 to 0.055 ohms, in line with MESA 2 findings.
- The internal resistance during charge was slightly lower than discharge pulse resistance across the SOC range investigated. It decreased from 0.11 ohms at 20% SOC to 0.095 ohms at 100% SOC. This is consistent with auxiliary power consumption being higher for charge compared to discharge at same power, possibly because of higher flow rates to avoid potential gassing during charge.
- The tracking error trend for volatile signals was constant at ~1 to 2% of rated power across the FBESS power range, and increased as expected with auxiliary consumption across the FBESS power range. The RTE peaked at 40% of rated power, while excluding auxiliary consumption resulted in RTE increasing with decreasing power levels.
- For some use cases, such as arbitrage and system capacity, pre-assigned signals were sent to the FBESS. For other use cases such as frequency regulation, load following, and load shaping, both pre-assigned duty cycles and live runs were conducted, with the Avista DMS sending the signal request to the FBESS based on grid conditions. Var-following, which essentially regulated power at a specific location, CVR with IVVC control and dynamic peak shaving consisted of live runs with the Avista DMS sending the commands to the FBESS based on grid conditions. For all of these use cases, the FBESS performed as designed and expected.
- In the case of volatile signals, the FBESS performed the DOE Protocol at 1,200 kW discharge and 1,000 kW charge, with peak discharge power levels 20% higher than rated power, and peak charge levels 25% higher than maximum continuous charge power of 800 kW and 11% higher than peak charge power of 900 kW per the UET technical specifications.
- The FBESS was used effectively to time shift energy based on signals received from a wind farm in Avista's service area. Using appropriate scaling factors to account for asymmetric maximum continuous charge and discharge power, signals from the wind farm were followed effectively by the FBESS, with RTEs in the 65 to 75% range.
- Dynamic peak shaving was successfully demonstrated, with some runs also providing vars to additionally support the grid PF. Because the FBESS was called on to discharge for very brief durations, the RTE was in the <8% range for several runs. For this use case, the availability and reliability of the FBESS to shave peaks is more important than RTE.
- For dynamic peak shaving, it is important to ensure that the set point of the feeder load at which the FBESS is triggered is selected such that the FBESS discharge can be sustained for the entire duration that the feeder load exceeds the set point. When feeder peak load is much lower than the value at which distribution pipes are saturated, a set point must be selected as a percentage of the peak such that FBESS is commanded to discharge for 2 to 4 hours. When the feeder peak is significantly higher than the value at which distribution pipelines are stressed, a set point must be selected as a percentage of feeder peak load that sends commands to FBESS to discharge for 2 to 4 hours. This shows the importance of having an algorithm that can accurately predict peak feeder load and duration. Suitably engaging the FBESS with other use cases will help ensure the RTE and performance of the FBESS across all use cases is sufficiently high to provide net benefits.

- To improve distribution system efficiency, var support and load balancing was done. Four-quadrant operation of the PCS was demonstrated successfully, with PFs ranging from 0.01 to 0.99. The FBESS performed var support very well, with excellent signal tracking on a normalized RMSE basis. Except for an occasion when a sudden increase in load occurred, the capacitive vars requested was much higher at 1,500 kvar than a single string could handle. Most of the time, the FBESS could supply the requested vars. During the same test, for a 900 kvar request, the actual vars delivered corresponded to a PF of 0.85, even though the minimum PF was set at 0.5. The reason for this was the FBESS was operating in watts-limiting mode. Once the actual lower limit of 0.01 for FBESS PF FBESS was identified, runs were done by setting the FBESS PF to 0.01. This allowed the FBESS to provide more vars as needed.
- Load balancing to improve distribution system efficiency was done using pre-assigned signals based on historic load data and using live runs, with suitable scaling factor to account for the ratio of feeder peak load to FBESS rated power. The FBESS performed well, tracking the signal well because its ramp rates of 100 to 200 kW/s during charge and 300 kW/s during discharge was sufficient to meet the signal ramp rates.
- Two approaches were used for CVR with IVVC control:
  - The one-string FBESS set up as two discrete virtual capacitors at 300 kvar and 150 kvar. These capacitors were manually engaged and subsequently controlled by IVVC using CBC. Because of the asynchronous nature of signal transmission, commands to open one capacitor while closing the other reached the FBESS with a few milliseconds lag, resulting in over- or under-deployment of vars.
  - The CBC control described above sent signals once every hour or less. To keep the contactors closed, the FBESS was controlled using a PFREG command, where signals were sent every few seconds, thus enabling the contactor to remain closed. The voltage regulation function of IVVC was used to control the feeder voltage at a specified setting of 118 V AC, while the PFREG commands helped maintain the PF near a value of 1.
- The aggregate availability of the FBESS over the test period was 56%. The total test duration was 365 days, out of which 162 days, or 44%, were lost for various reasons. Fifty-eight days, or 16%, of the test duration were lost to stack-related issues, which included stack SOC mismatches and an electrolyte leak from the stack. Forty days, or 11%, were lost to PCS-related issues. Some of these issues were related to prolonged exercise of the PCS during charge at high SOC, and some were related to corrosion of electronic components due to the leaked electrolyte. Issues related to the PCS software contributed to another nine lost days or 2% of the test duration. Pump-related issues contributed to nine lost days or 2% of test duration, while a pump tub housing leak contributed to eight lost days. Thermal management failure contributed to seven lost days, while AC breaker trips that could not be reset remotely contributed to seven lost days. Human errors and weather contributed to six and seven lost days, respectively. Maintenance, communication failure and miscellaneous contributed to a total of 11 missed days. The FBESS was ultimately taken off-line for extended maintenance, and the full test program could not be completed.
- Auxiliary consumption at fixed power for charge is higher compared to discharge. Charge may require greater flow rate per kilowatt to prevent gas evolution by facilitating faster mass transport and lowering over-potential. Charge resistance is lower than discharge resistance across the SOC range, thus lending support to this hypothesis.
- The cumulative charge and discharge ampere hours and the coulombic efficiencies for String 2 is shown in Figure 2.5. The coulombic efficiency was near 100% initially and decreased with time, ending up at 95%, which is indicative of electrolyte crossover.

7.0 References

Miller A (Ed.). Undated. SunSpec Energy Storage Models. Document 12032, Draft Version 4. Available at http://mesastandards.org/wp-content/uploads/2017/09/SunSpec-Alliance-Specification-Energy-Storage-ModelsD4rev0.25.pdf.

Modular Energy Storage Architecture (MESA). 2016. *MESA Open Standards for Energy Storage – Draft*. Available at http://mesastandards.org/wp-content/uploads/2016/11/MESA-ESS-Specification-November-2016-Draft-2.pdf.

Ridley D. 2019, Conversation between Dave Ridley of Uni Energy Technologies and V.V. Viswanathan of PNNL on February 5, 2019

Siemens. Undated. "SIMATIC WinCC Open Architecture." Available at https://w3.siemens.com/mcms/topics/en/stationary-energy-storage-devices/scada-system/Pages/default.aspx.

Schenkman BL and DR Borneo. 2015. "Sandia Third-Party Witness Test of UniEnergy Technologies 1 MW/3.2 MWh Uni.System™. SAND2016-6187R, Sandia National Laboratories, Albuquerque, New Mexico. Available at https://www.sandia.gov/ess-ssl/publications/SAND2015-6187R.pdf

Sun C. 2015. Information provided by Chauncey Sun of Uni Energy Technologies by email or by telephone conversation with VV Viswanathan of PNNL in late 2015, captured in a word document "UET and Avista system notes.docx" prepared by Viswanathan, last edited 07/19/2017

DPS Telecon. Tutorial On DNP3: Intro, Communication, And Objects - Part 1. (n.d.). Retrieved from https://www.dpstele.com/dnp3/tutorials.php

UniEnergy Technologies (UET). Undated. "Uni.System:™ Grid-Scale Energy Storage Solution." Available at http://uetechnologies.com/images/product/UET_UniSystem_Product_Sheet_reduced.pdf.

UniEnergy Technologies (UET). 2015. "Uni.System Overview". May 5, 2015

Viswanathan VV, D Choi, D Wang, S Towne, RE Williford, J-G Zhang, J Liu, and Z Yang. 2010. "Effect of entropy of lithium intercalation in cathodes and anodes on Li-ion battery thermal management." Journal of Power Sources 195(11)3720-3729. Available at https://www.sciencedirect.com/science/article/pii/S0378775309021119.

Viswanathan VV, DR Conover, AJ Crawford, S Ferreira, and D Schoenwald. 2014. *Protocol for Uniformly Measuring and Expressing the Performance of Energy Storage Systems*. PNNL-22010 Rev. 1, Pacific Northwest National Laboratory, Richland, Washington. Available at https://www.sandia.gov/ess-ssl/docs/ESS_Protocol_Rev1_with_microgrids.pdf\.

Viswanathan VV, PJ Balducci, ME Alam, AJ Crawford, TD Hardy, and D Wu. 2017. *Washington Clean Energy Fund: Energy Storage System Performance Test Plans and Data Requirements*. PNNL-26492, Pacific Northwest National Laboratory, Richland, Washington.

Appendix A

Supplemental Information

Appendix A

Supplemental Information

A.1 Baseline Results No Taper

Table A.1. Baseline Results with All Taper Removed, Constant Charge, and Discharge Only

Index2	Test	Cycle	Date	Duration (h)	Rest Time (min)	Strings Active	Req Discharge Power (kW)	Req Charge Power (kW)	SOC Range	Charge Energy (kWh)	Discharge Energy (kWh)	RTE	Charge Energy No Rest (kWh)	RTE No Rest	Charge Energy No Aux (kWh)	Discharge Energy No Aux (kWh)	RTE No Aux	DC RTE	Coul Eff.	Mean Temp (C)
Baseline	1	1	2015-09-08	16.00	10	2	520	600	21-100	5,249	3,183	60.60	5,235	60.80	4,814	3,306	68.70	NA	NA	NA
Baseline	2	1	2015-09-09	16.00	10	2	520	600	22-100	5,272	3,171	60.10	5,255	60.30	4,853	3,363	69.30	NA	NA	NA
Baseline	2	2	2015-09-10	17.00	16	2	520	600	27-100	4,940	2,990	60.50	4,863	61.50	4,546	3,422	75.30	NA	NA	NA
Baseline	2	Cumulative	NA	33.00	26	2	NA	NA	NA	10,212	6,161	60.30	10,118	60.90	9,399	6,785	72.20	NA	NA	NA
Baseline	2	Mean	NA	16.50	13	2	520	600	25-100	5,106	3,080	60.30	5,059	60.90	4,700	3,392	72.30	NA	NA	NA
Baseline	3	1	2015-09-15	18.00	10	2	400	600	38-100	4,732	2,962	62.60	4,728	62.60	4,285	3,152	73.60	NA	NA	NA
Baseline	4	1	2015-09-26	20.00	10	2	400	600	1-100	5,722	3,481	60.80	5,717	60.90	5,295	3,635	68.60	NA	NA	NA
Baseline	4	2	2015-09-26	20.00	10	2	400	600	7-100	5,673	3,571	62.90	5,671	63.00	5,269	3,767	71.50	NA	NA	NA
Baseline	4	3	2015-09-27	20.00	10	2	400	600	7-100	5,693	3,606	63.30	5,663	63.70	5,283	3,812	72.20	NA	NA	NA
Baseline	4	Cumulative	NA	60.00	30	2	NA	NA	NA	17,088	10,658	62.40	17,051	62.50	15,847	11,214	70.80	NA	NA	NA
Baseline	4	Mean	NA	20.00	10	2	400	600	5-100	5,696	3,553	62.30	5,684	62.50	5,282	3,738	70.80	NA	NA	NA
Baseline	5	1	2015-10-02	11.00	5	2	800	600	43-100	4,256	2,532	59.50	4,254	59.50	3,941	2,601	66.00	NA	NA	NA
Baseline	6	1	2015-10-10	11.00	10	2	800	600	40-100	4,502	2,548	56.60	4,497	56.70	4,172	2,612	62.60	NA	NA	NA
Baseline	6	2	2015-10-10	11.00	10	2	800	600	45-100	4,231	2,573	60.80	4,171	61.70	3,874	2,662	68.70	NA	NA	NA
Baseline	6	3	2015-10-11	11.00	10	2	800	600	46-100	4,201	2,583	61.50	4,191	61.60	3,794	2,663	70.20	NA	NA	NA
Baseline	6	Cumulative	NA	33.00	30	2	NA	NA	NA	12,934	7,704	59.60	12,859	59.90	11,840	7,937	67.00	NA	NA	NA
Baseline	6	Mean	NA	11.00	10	2	800	600	43-100	4,311	2,568	59.60	4,286	60.00	3,947	2,646	67.20	NA	NA	NA
Post-Baseline	1	1	2016-01-13	16.00	3	2	520	600	18-99	5,109	3,200	62.60	5,104	62.70	4,846	3,365	69.40	74.10	94.30	31.70
Post-Baseline	1	2	2016-01-13	16.00	2	2	520	600	18-99	5,121	3,254	63.50	5,119	63.60	4,865	3,416	70.20	75.00	94.50	34.20
Post-Baseline	1	Cumulative	NA	32.00	5	2	NA	NA	NA	10,230	6,454	63.10	10,223	63.10	9,711	6,781	69.80	NA	NA	NA
Post-Baseline	1	Mean	NA	16.00	3	2	520	600	18-99	5,115	3,227	63.00	5,112	63.20	4,856	3,390	69.80	74.50	94.40	32.90
Pre-Inverter Swap	1	1	2016-11-08	15.00	3	1	520	600	29-99	4,770	3,061	64.20	4,774	64.10	4,509	3,235	71.70	75.60	93.30	36.30
Pre-Inverter Swap	1	2	2016-11-09	15.00	3	1	520	600	31-99	4,716	3,057	64.80	4,708	64.90	4,441	3,244	73.00	77.10	94.90	36.90
Pre-Inverter Swap	1	3	2016-11-10	14.00	2	1	520	600	31-99	4,671	3,056	65.40	4,669	65.50	4,412	3,243	73.50	78.10	96.00	36.60
Pre-Inverter Swap	1	Cumulative	NA	44.00	8	1	NA	NA	NA	14,157	9,174	64.80	14,151	64.80	13,362	9,722	72.80	NA	NA	NA
Pre-Inverter Swap	1	Mean	NA	14.70	3	1	520	600	30-99	4,719	3,058	64.80	4,717	64.80	4,454	3,241	72.70	76.90	94.70	36.60
Pre-Inverter Swap	2	1	2016-11-10	10.00	2	1	750	600	43-99	4,025	2,500	62.10	4,023	62.10	3,786	2,607	68.90	72.60	94.70	37.10
Pre-Inverter Swap	2	2	2016-11-11	10.00	3	1	750	600	44-99	3,930	2,497	63.50	3,929	63.60	3,702	2,607	70.40	73.80	96.00	37.20
Pre-Inverter Swap	2	3	2016-11-11	11.00	1	1	750	600	43-99	4,001	2,491	62.30	3,999	62.30	3,756	2,607	69.40	72.80	94.40	37.70

Index2	Test	Cycle	Date	Duration (h)	Rest Time (min)	Strings Active	Req Discharge Power (kW)	Req Charge Power (kW)	SOC Range	Charge Energy (kWh)	Discharge Energy (kWh)	RTE	Charge Energy No Rest (kWh)	RTE No Rest	Charge Energy No Aux (kWh)	Discharge Energy No Aux (kWh)	RTE No Aux	DC RTE	Coul Eff.	Mean Temp (C)
Pre-Inverter Swap	2	Cumulative	NA	31.00	6	1	NA	NA	NA	11,956	7,488	62.60	11,951	62.70	11,244	7,821	69.60	219.20	NA	NA
Pre-Inverter Swap	2	Mean	NA	10.30	2	1	750	600	43-99	3,985	2,496	62.60	3,984	62.70	3,748	2,607	69.60	73.10	95.00	37.30
Pre-Inverter Swap	3	1	2016-11-12	10.00	3	1	1,000	600	38-99	4,206	2,353	55.90	4,198	56.10	3,930	2,428	61.80	64.80	95.10	38.60
Pre-Inverter Swap	3	2	2016-11-12	10.00	3	1	1,000	600	39-99	4,170	2,362	56.60	4,168	56.70	3,902	2,440	62.50	65.50	95.50	39.10
Pre-Inverter Swap	3	3	2016-11-13	10.00	3	1	1,000	600	38-99	4,185	2,362	56.40	4,180	56.50	3,924	2,440	62.20	65.40	95.40	38.60
Pre-Inverter Swap	3	Cumulative	NA	30.00	9	1	NA	NA	NA	12,561	7,077	56.30	12,546	56.40	11,756	7,308	62.20	195.70	NA	NA
Pre-Inverter Swap	3	Mean	NA	10.00	3	1	1,000	600	38-99	4,187	2,359	56.30	4,182	56.40	3,919	2,436	62.20	65.20	95.30	38.80
Pre-Inverter Swap	4	1	2016-11-13	33.00	28	1	420	600	7-99	5,985	3,547	59.30	5,611	63.20	5,295	3,795	71.70	80.00	99.00	36.20

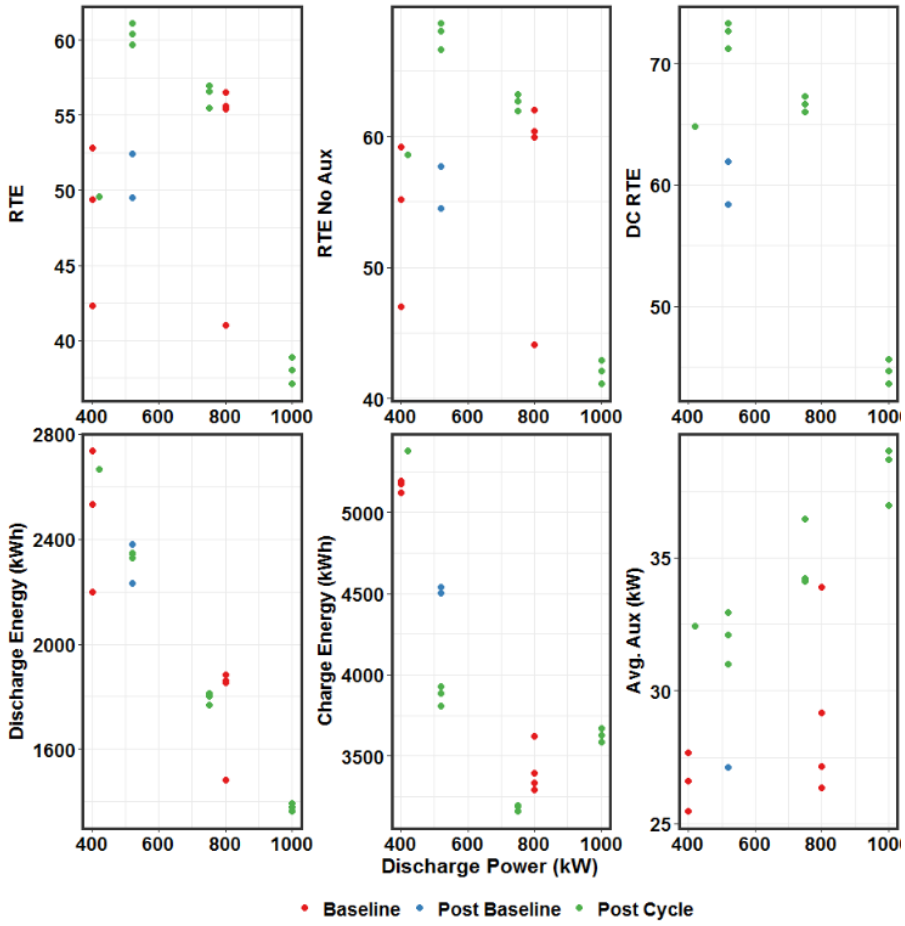

Figure A.1. Baseline Results for Constant Power Charge and Discharge

A.2 Baseline Results All Taper

Table A.2. Baseline Results including All Taper Regions

Index2	Test	Cycle	Date	Duration (h)	Rest Time (min)	Strings Active	Req Discharge Power (kW)	Req Charge Power (kW)	SOC Range	Charge Energy (kWh)	Discharge Energy (kWh)	RTE	Charge Energy No Rest (kWh)	RTE No Rest	Charge Energy No Aux (kWh)	Discharge Energy No Aux (kWh)	RTE No Aux	DC RTE	Coul Eff.	Mean Temp (C)
Baseline	1	1	2015-09-08	16.0	10	2	520	600	21-100	5,280	3,183	60.3	5,266	60.4	4,844	3,306	68.2	NA	NA	NA
Baseline	2	1	2015-09-09	16.0	10	2	520	600	22-100	5,304	3,171	59.8	5,287	60.0	4,883	3,363	68.9	NA	NA	NA
Baseline	2	2	2015-09-10	17.0	16	2	520	600	16-100	4,870	2,990	61.4	4,926	60.7	4,606	3,422	74.3	NA	NA	NA
Baseline	2	Cumulative	NA	33.0	26	2	NA	NA	NA	10,174	6,161	60.6	10,213	60.3	9,489	6,785	71.5	NA	NA	NA
Baseline	2	Mean	NA	16.5	13	2	520	600	31-100	5,087	3,080	60.6	5,106	60.4	4,744	3,392	71.6	NA	NA	NA
Baseline	3	1	2015-09-15	18.0	10	2	400	600	38-100	4,713	2,962	62.8	4,728	62.6	4,285	3,152	73.6	NA	NA	NA
Baseline	4	1	2015-09-26	20.0	10	2	400	600	1-100	5,742	3,483	60.7	5,738	60.7	5,315	3,637	68.4	NA	NA	NA
Baseline	4	2	2015-09-26	20.0	10	2	400	600	7-100	5,691	3,571	62.7	5,692	62.7	5,289	3,767	71.2	NA	NA	NA
Baseline	4	3	2015-09-27	20.0	10	2	400	600	7-100	5,703	3,606	63.2	5,673	63.6	5,293	3,812	72.0	NA	NA	NA
Baseline	4	Cumulative	NA	60.0	30	2	NA	NA	NA	17,136	10,660	62.2	17,103	62.3	15,897	11,216	70.6	NA	NA	NA
Baseline	4	Mean	NA	20.0	10	2	400	600	27-100	5,712	3,553	62.2	5,701	62.3	5,299	3,739	70.5	NA	NA	NA
Baseline	5	1	2015-10-02	11.0	5	2	800	600	43-100	4,321	2,532	58.6	4,317	58.7	4,001	2,601	65.0	NA	NA	NA
Baseline	6	1	2015-10-10	11.0	10	2	800	600	40-100	4,579	2,548	55.6	4,570	55.8	4,242	2,612	61.6	NA	NA	NA
Baseline	6	2	2015-10-10	11.0	10	2	800	600	45-100	4,308	2,573	59.7	4,244	60.6	3,944	2,662	67.5	NA	NA	NA
Baseline	6	3	2015-10-11	11.0	10	2	800	600	46-100	4,268	2,583	60.5	4,254	60.7	3,854	2,663	69.1	NA	NA	NA
Baseline	6	Cumulative	NA	33.0	30	2	NA	NA	NA	13,155	7,704	58.6	13,068	59.0	12,040	7,937	65.9	NA	NA	NA
Baseline	6	Mean	NA	11.0	10	2	800	600	48-100	4,385	2,568	58.6	4,356	59.0	4,013	2,646	66.1	NA	NA	NA
Post-Baseline	1	1	2016-01-13	16.0	3	2	520	600	18-99	5,145	3,200	62.2	5,135	62.3	4,876	3,365	69.0	74.1	94.3	31.7
Post-Baseline	1	2	2016-01-13	16.0	2	2	520	600	18-99	5,155	3,254	63.1	5,151	63.2	4,895	3,416	69.8	75.0	94.5	34.2
Post-Baseline	1	Cumulative	NA	32.0	5	2	NA	NA	NA	10,300	6,454	62.7	10,286	62.7	9,771	6,781	69.4	NA	NA	NA
Post-Baseline	1	Mean	NA	16.0	3	2	520	600	30-99	5,150	3,227	62.7	5,143	62.8	4,886	3,390	69.4	74.5	94.4	32.9
Pre-Inverter Swap	1	1	2016-11-08	15.0	3	1	520	600	29-99	4,833	3,061	63.3	4,828	63.4	4,559	3,235	71.0	75.6	93.3	36.3
Pre-Inverter Swap	1	2	2016-11-09	15.0	3	1	520	600	31-99	4,774	3,057	64.0	4,762	64.2	4,491	3,244	72.2	77.1	94.9	36.9
Pre-Inverter Swap	1	3	2016-11-10	14.0	2	1	520	600	31-99	4,720	3,056	64.7	4,711	64.9	4,452	3,243	72.8	78.1	96.0	36.6
Pre-Inverter Swap	1	Cumulative	NA	44.0	8	1	NA	NA	NA	14,327	9,174	64.0	14,301	64.1	13,502	9,722	72.0	NA	NA	NA
Pre-Inverter Swap	1	Mean	NA	14.7	3	1	520	600	32-99	4,776	3,058	64.0	4,767	64.2	4,501	3,241	72.0	76.9	94.7	36.6
Pre-Inverter Swap	2	1	2016-11-10	10.0	2	1	750	600	43-99	4,083	2,500	61.2	4,076	61.3	3,836	2,607	68.0	72.6	94.7	37.1
Pre-Inverter Swap	2	2	2016-11-11	10.0	3	1	750	600	44-99	4,016	2,497	62.2	4,004	62.4	3,772	2,607	69.1	73.8	96.0	37.2
Pre-Inverter Swap	2	3	2016-11-11	11.0	1	1	750	600	43-99	4,113	2,491	60.6	4,105	60.7	3,856	2,607	67.6	72.8	94.4	37.7
Pre-Inverter Swap	2	Cumulative	NA	31.0	6	1	NA	NA	NA	12,212	7,488	61.3	12,185	61.5	11,464	7,821	68.2	NA	NA	NA
Pre-Inverter Swap	2	Mean	NA	10.3	2	1	750	600	44-99	4,071	2,496	61.3	4,062	61.5	3,821	2,607	68.2	73.1	95.0	37.3
Pre-Inverter Swap	3	1	2016-11-12	10.0	3	1	1,000	600	38-99	4,279	2,353	55.0	4,262	55.2	3,990	2,428	60.9	64.8	95.1	38.6
Pre-Inverter Swap	3	2	2016-11-12	10.0	3	1	1,000	600	39-99	4,242	2,362	55.7	4,232	55.8	3,962	2,440	61.6	65.5	95.5	39.1
Pre-Inverter Swap	3	3	2016-11-13	10.0	3	1	1,000	600	38-99	4,246	2,362	55.6	4,234	55.8	3,964	2,440	61.6	65.4	95.4	38.6
Pre-Inverter Swap	3	Cumulative	NA	30.0	9	1	NA	NA	NA	12,767	7,077	55.4	12,728	55.6	11,916	7,308	61.3	NA	NA	NA
Pre-Inverter Swap	3	Mean	NA	10.0	3	1	1,000	600	50-99	4,256	2,359	55.4	4,243	55.6	3,972	2,436	61.4	65.2	95.3	38.8
Pre-Inverter Swap	4	1	2016-11-13	33.0	28	1	420	600	7-99	6,025	3,538	58.7	5,642	62.7	5,325	3,795	71.3	80.0	99.0	36.2

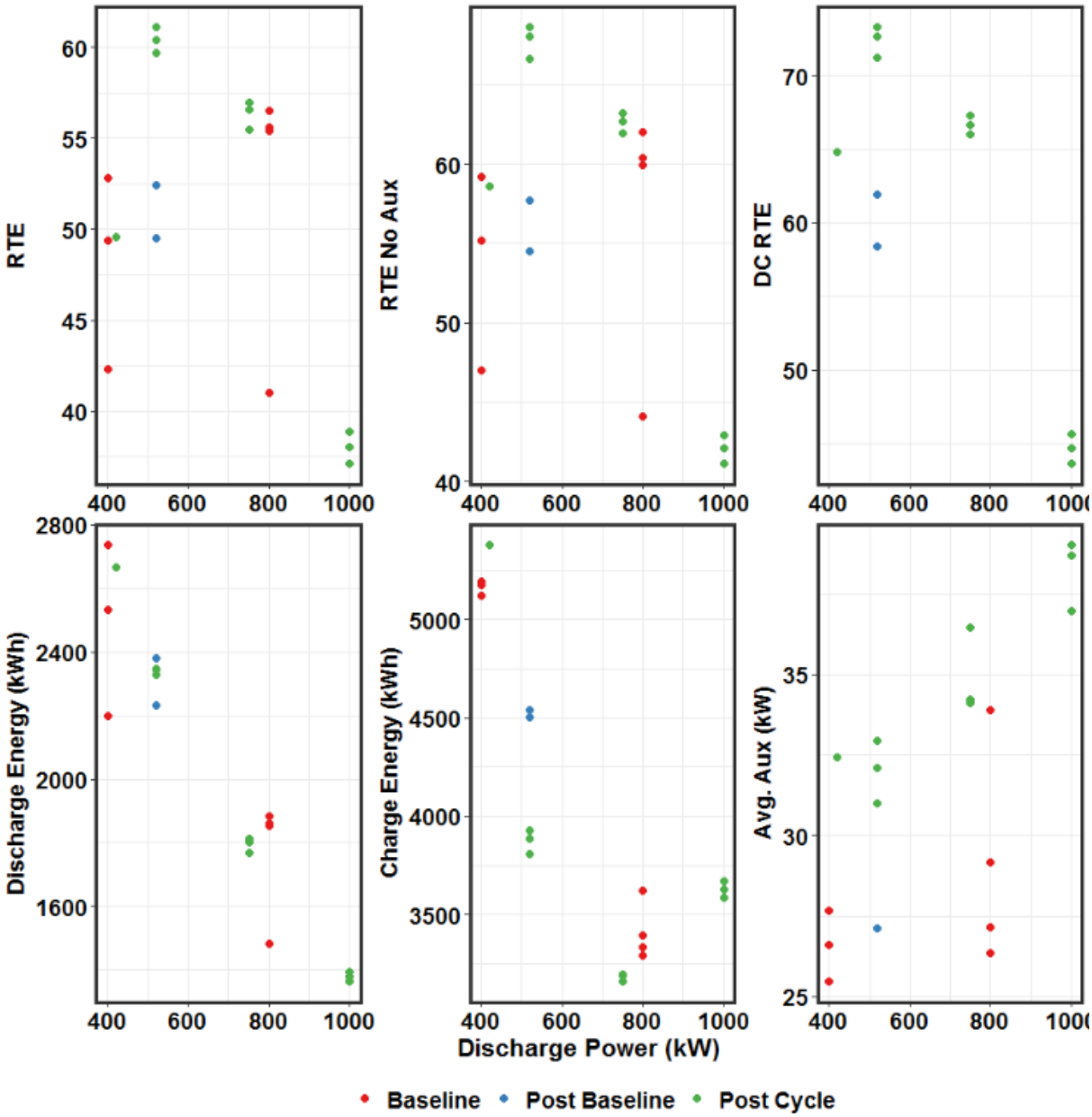

Figure A.2. Baseline Results including All Taper Regions

A.3 FBESS Technical Specifications

Table A.3. Technical Specifications

UNLIMITED CYCLES

NO CAPACITY FADE

NO THERMAL RUNAWAY

100% USE OF CHARGE

FACTORY INTEGRATION

MODULAR ASSEMBLY

BUILT-IN SECONDARY CONTAINMENT

FACTORY TESTING

RAPID PERMITTING

PLUG & PLAY

RATED TO TRANSPORT AND SEISMIC CODES

ZERO-COST DISPOSAL

100% RECYCLABLE

© 2016, UniEnergy Technologies, LLC

UNI.SYSTEM™ (AC) PERFORMANCE DATA			
Peak Power	600 kW_{AC}		
Maximum Energy	2.2 MWh_{AC}		
Discharge time	2h	4h	8h
Power	600 kW_{AC}	500 kW_{AC}	275 kW_{AC}
AC (Roundtrip) Efficiency	≈70%		
Voltage	12.47kV +/- 10%		
Current THD (IEEE 519)	<5%THD		
Response Time	<100ms		
Reactive Power	+/- 450kVAR		
Humidity	95%RH noncondensing		
Footprint	820 ft^2 ($76m^2$)		
Envelope	41'[W] x 20'[D] x 9.5'[H] (12.5m[W]x6.1m[D]x2.9m[H])		
Total Weight	375,000 lbs (170,000 kg)		
Cycle and Design Life	Unlimited cycles over the 20 year life		
Ambient Temp.	-40°F to 122°F (-40°C to 50°C)		
Self Discharge	Max 2% of stored enegy		

A.4 Site Layout

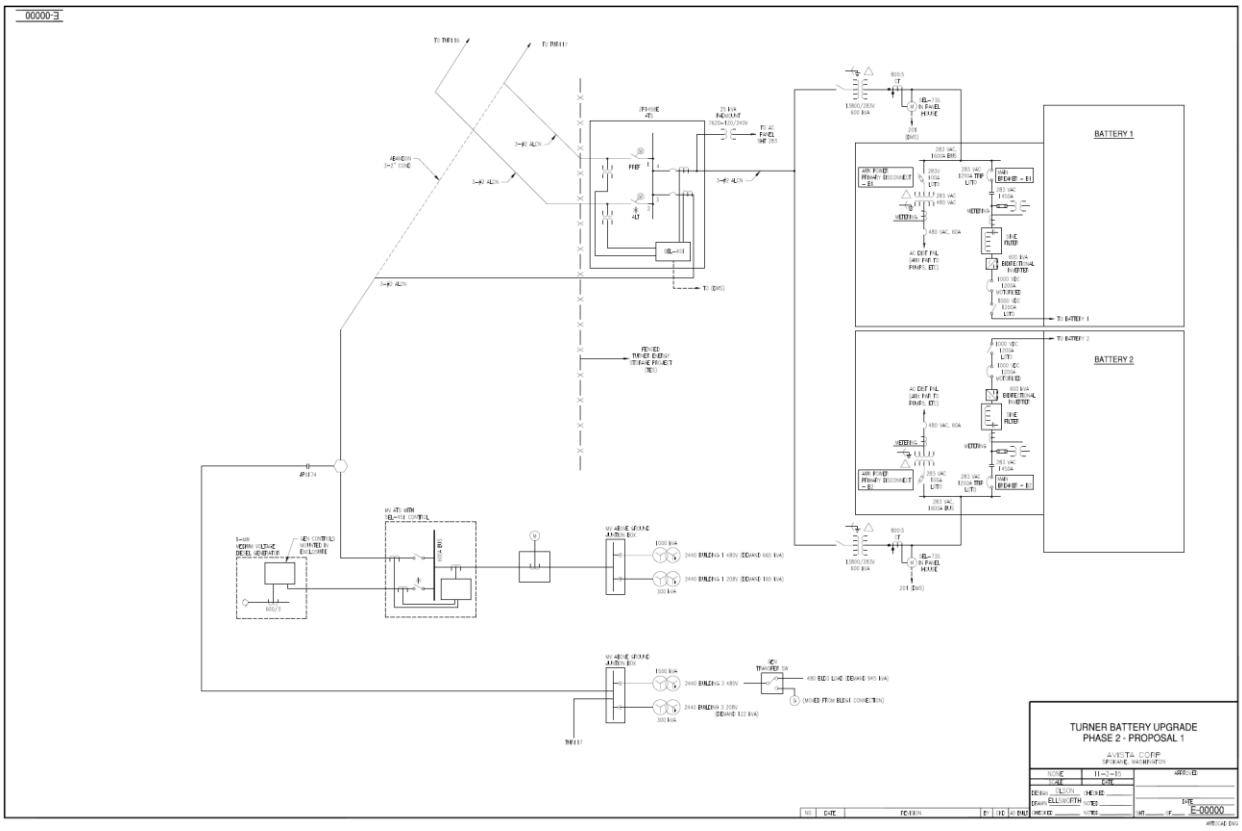

Figure A.3. Site Drawing

Figure A.4. Avista Utilities Facility

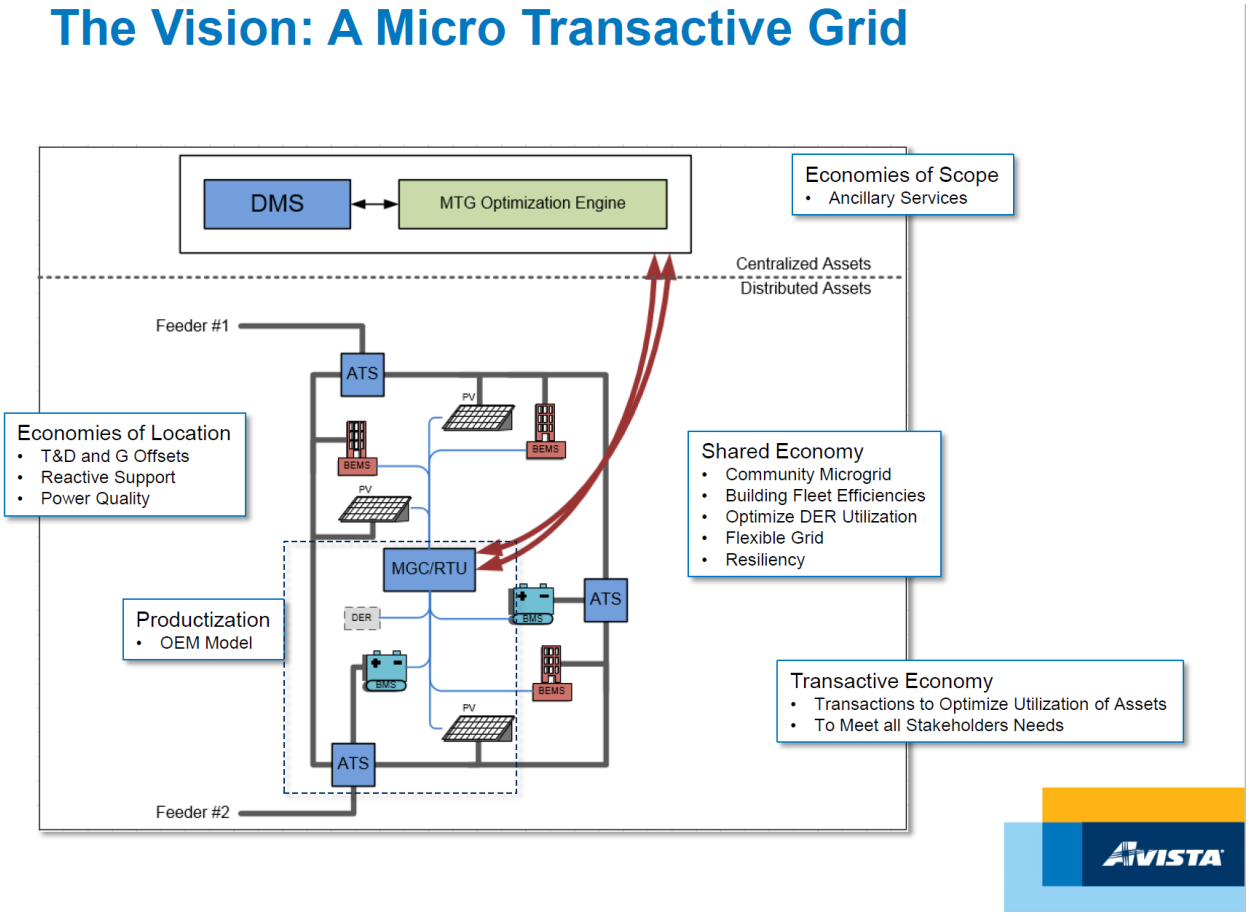

Figure A.5. Avista Vision for Micro Transactive Grid

A.5 ACE and Load Following Duty Cycle Development Methodology

There is no logic local to the FBESS to deal with "balancing and frequency control" (as the North American Electric Reliability Corporation document calls it). Any changes in FBESS input or output will have to be done via Avista's program at Avista headquarters. That could be with a schedule based on historical data or "real-time" algorithms.

For "real-time" or historical signals, every input Avista's automatic generation control (AGC) system uses available via the Avista PI system is available. That includes frequency, ACE values, AGC set points, etc.

For scheduled response based on historical data, Avista provided historical frequency data.

For "real-time" runs, which are preferred, preference, commands were implemented through the scheduler.

The following responses were considered in developing the final algorithm:

- *Governor response* – Governor-style frequency response with a dead band and kW/Hz response. The dead band and slope are defined in a configuration file and are read only when the schedule processor

begins providing an ancillary service. Frequency is read from an Avista distribution feeder using a Global Positioning System clock and input in to the schedule processor from PI.

- *ACE response with dynamic limit* – kW per ACE MW (computed by Avista's AGC system and read from a PI tag) response with dead band limits defined by a PI tag, currently plus or minus the L10 limit.
- *ACE Response with static limit* – Like ACE response with dynamic limit but with configuration file defined static dead band limits.
- *AGC Response* – Responds to the AGC megawatt set point value Avista is currently sending to their generating unit that is under AGC control. The intention is to make the battery look as if it is being dispatched by the AGC system without requiring integration in to that system. The response is kilowatts = k0 + k1*(set point^k2). (Thus, if k2 is 1, the response is linear. Having the ability for a non-linear response came out of discussions about trying to scale the response of our 1MW system to something noticeable when the AGC set point could be many megawatts.) The k0, k1, and k2 constants are defined in a configuration file and are read only when the schedule processor begins providing an ancillary service.

A.6 Methodology Development for dp/dt

A.6.1 Approach for Historical Load and Solar Data

Avista uses historical signals to developing their forecasts. This was shared with PNNL. Solar data from the National Renewable Energy Laboratory measured in Hawaii were used. While this is not a good proxy for Spokane, it was decided to use that data for testing purposes. The solar parameters from these measurements were available. They were run through a validated model to estimate the amount of electrical energy generated. This was done every 10 seconds, which is the same data rate as the feeder load data Avista provided.

A.6.2 Approach for Live Data

This would be live load data. There is no meaningful solar generation installed on the feeder in Pullman. An algorithm was developed with appropriate scaling factor for the FBESS to generate commands for the FBESS to follow.

A.7 Maintenance and Refurbishment of FBESS Prior to Islanding Test

The following maintenance visit by UniEnergy Technologies (UET) during the week on May 7, 2018, addresses multiple issues including pump/tub assembly, faulty factory weld, SOC balancing, remote inverter validation, and overall system validation. The UET field team accomplished the following tasks:

1. Replaced the catholyte pump/tub assembly of String 1 Battery 4
2. Repaired a faulty factory weld in the anolyte pump tub of String 2 Battery 2
3. Matched SOCs of all batteries
4. Supported remote Northern Power Systems (NPS) validation
5. Completed operational validation of the system over the weekend
6. Proposed plans for a routine maintenance schedule after the long down time since November 2016.

A.8 Turner Energy Storage System Site Recommissioning Test Plan

Turner Energy Storage System
Site Recommissioning Test Plan

Avista 1MW/3.2MWh Uni. System™

Revision: Draft v 2.3

A.9 Pullman Test Plan

Scope: Test the basic operation of each string as well as the combined operation of the dual strings. Testing also includes the basic operation of the ATS. Testing will be split into three parts:

1. Part 1: Test ATS transfer from the Preferred Source to the Alternate Source
2. Part 2: Test individual operation of each string (test degraded mode operation)
3. Part 3: Test combined operation of each string (test normal operation).

It is envisioned that the "Izer" will form the foundation of command/control with the installed system, and simple scheduling via the Spirae Prototype system will be used to test various modes.

The following table shows the assets and corresponding test with respect to the Pullman site.

Table A.4. Assets and Testing Use Case Function

Use Case Function	String 1	String 2	Combined
Grid to Island and Return Idling, Low Load	Optional; Required on Combined Failure	Optional; Required on Combined Failure	√
Grid to Island and Return Idling, Full Load	Optional; Required on Combined Failure	Optional; Required on Combined Failure	√
Grid to Island and Return, Full-Power Discharge	Optional; Required on Combined Failure	Optional; Required on Combined Failure	√
Grid to Island and Return, Full Power Charge	Optional; Required on Combined Failure	Optional; Required on Combined Failure	√
Time to Derate (Discharging)	Optional; Required on Combined Failure	Optional; Required on Combined Failure	√
Time to Derate (Charging)	Optional; Required on Combined Failure	Optional; Required on Combined Failure	√

A.10 Test Coverage

The tests must "cover" the anticipated functions that the Turner Energy Storage System (TESS) will perform. The following table shows the Izer modes on the left as well as the various use cases that will be expected to perform.

Table A.5. Spirae Use Case Coverage and Required Izer/TESS Functionality

Izer Function	UC0 Recharge	UC1 Arbitrage	UC2 Freq Response	UC4 Peak Load Management	UC3 Generation Following	UC5 Volt/VAR Support	UC6 Reliability
Dispatch		√	√	√	√	√	√
Charge	√	√	√		√	√	
GOV			√		√	√	

Additionally, there is an additional requirement to characterize charging limits as a function of battery SOC.

Table A.6. Tests and Possible Sequencing

Test Number	Section Number	Brief Description	Initial SOC 80 - 100	Initial SOC 60 - 80	Initial SOC 40 - 60	Initial SOC 20 - 40
1	3.1	String Grid to Island and Return – IDLE, Low Load	>85%			
2	3.1	String Grid to Island and Return – IDLE, Full Load	>85%			
3	3.2	String Grid to Island and Return -- Discharge	>85%			
4	3.3	String Grid to Island and Return – Charging		~60%		
5	3.5	Discharge Time to Derate	>85%			
6	3.6	Recharge Time to Derate			~50%	

A.11 Site Configuration for Testing

To ensure SEL load is safely bypassed from the TES site and properly served from the alternate route of TUR 117, the following Test Site Configuration must be implemented and verified prior to each test. See one-line diagram in Figure A.6 following switching order below for clarification. Switching order for configuration follows. Note: This verification process is repeated in all following switching orders for all tests.

- CLOSE elbows going EAST in JP0174
- OPEN elbows going WEST in JP0174
- Verify ATS Way 1 is CLOSED (preferred source, TUR 117)
- Verify ATS Way 2 is OPEN (alternate source, TUR 116)
- Verify ATS Way 3 is CLOSED and connected to Crestchic Test Load (CTL)
- Verify ATS Way 4 is CLOSED (TES)
- Verify TES main breakers B1 and B2 are OPEN
- Verify TES string 1 and string 2 in IDLE
- Push manual/auto PB to make ATS Auto
- Push local/remote PB to make ATS Remote
- Push Way 1/Way 2 PB to make Way 1 Preferred Source
- Verify with DSO DMS is operating normally
- Verify TUR 116 Voltage Control is Disabled
- Verify TUR 117 Voltage Control is Disabled

A.12 System Configuration Verification Order

Order Name: PAL 18-3

SWITCHING DATE/TIME: mm-dd-yyyy (DAY), hh:mm AM/PM

FEEDER/LOCATION: TUR 116 and TUR 117, TES Battery Site in Pullman, WA

PERSON IN CHARGE: Bo Morgan (07) **SWITCHMAN:** Tim Wacker (520),

Bo Morgan (07)

Alex Weenink – UET (206 599 9347)

DESCRIPTION: Preliminary Verification of system configuration prior to testing sequence

PREPARED BY: Caitlin Greeney, 1-15-2018

VERIFIED BY: _____ **DATE:** _____

DSO Engineer

COMPLETED BY: _____ **DATE:** _____

Distribution Dispatcher

TIME	STEP	WHO	ACTION
	1	DD	VERIFY TUR 116 VOLTAGE CONTROL IS DISABLED
	2	DD	VERIFY TUR 117 VOLTAGE CONTROL IS DISABLED
	3	07	CHECK CLOSED ELBOWS GOING EAST IN JP0174
	4	07	CHECK OPEN ELBOWS GOING WEST IN JP0174
	5	07	CHECK CLOSED ZP1458E-1 (PREFERRED SOURCE - TUR 117)
	6	07	CHECK OPEN ZP1458E-2 (ALTERNATE SOURCE - TUR 116)
	7	07	CHECK CLOSED ZP1458E-3 IS CLOSED AND CONNECTED TO TEST LOAD SET TO 0 KVA
	8	07	CHECK CLOSED ZP1458E-4 (TOWARD TES)
	9	UET	CHECK OPEN TES MAIN BREAKERS B1 AND B2
	10	07	CHECK ZP1458E IS IN “AUTO”
	11	07	CHECK ZP1458E IS IN “REMOTE”
	12	07	CHECK ZP1458E “PREFERRED SOURCE” IS SOURCE 1 (TUR 117)
	13	ENG	NOTIFY THE ENGINEER VERIFICATION IS COMPLETE.

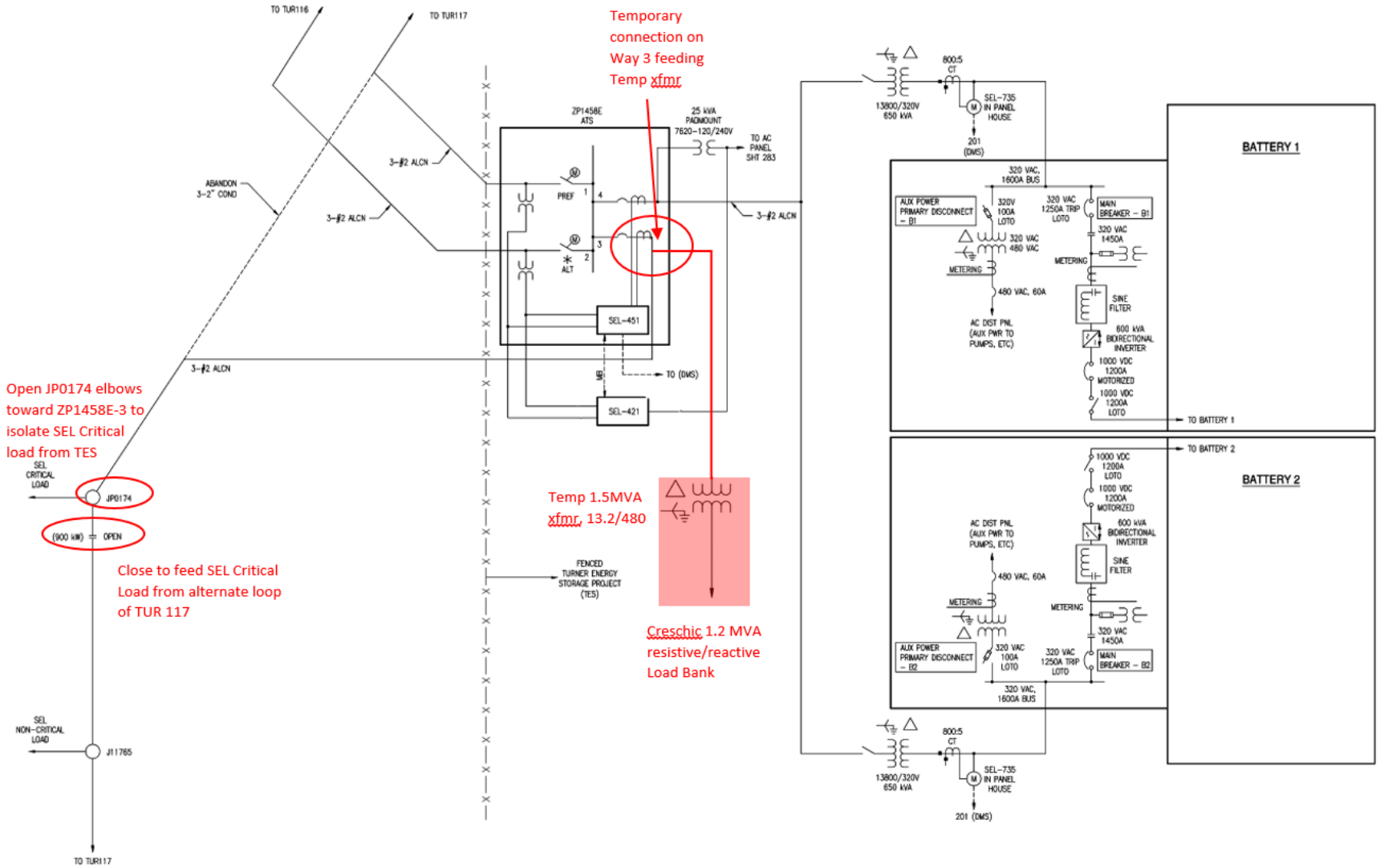

Figure A.6. Online Diagram of Testing Configuration of TUR 116, TUR 117, and TES

A.13 Performance Tests

A.13.1 Grid to Island and Return – TES Idling, Low Load

A.13.1.1 Purpose

The purpose of this test is to transfer (verbage here because technically not "transferring" in traditional sense) to islanded mode and to support the load without interruption (less than 10 cycles,), and then re-sync the battery to preferred feeder. This test directly supports Use Case 6A (Loss of Preferred Source) and Use Case 6C (Loss of Preferred and Alternate Source). The load reactance is configured inductively and the battery is idling (neither charging nor discharging).

A.13.1.2 Initial Conditions

Verify TES site is in Test Configuration:

1. Verify elbows going east in JP0174 are CLOSED
2. Verify elbows going west in JP0174 are OPEN
3. Verify ATS Way 1 is CLOSED (preferred source)
4. Verify ATS Way 2 is OPEN (alternate source)
5. Verify ATS Way 3 is CLOSED and connected to Crestchic CTL (CTL)
6. Verify ATS Way 4 is CLOSED (TES)
7. Verify Main Breakers B1 and B2 in TES are CLOSED
8. Verify TES string 1 and string 2 in IDLE
9. Verify ATS is in Auto mode
10. Verify ATS is in Remote mode
11. Verify Way 1 (TUR 117) is the Preferred Source
12. Verify TUR 116 Voltage Control is Disabled
13. Verify TUR 117 Voltage Control is Disabled
14. The battery has a SOC greater than 85%.
15. Adjust CTL to 100 KVA at .95 power factor.
16. Verify main breakers B1 and B2 in TES are closed and TES is connected to the grid.
17. Confirm battery is in idle mode, call DSO engineer (Jill Hamm) to confirm.
18. Verify Hinoki data logger is connected and functioning
19. OPEN and STAND OFF elbows in J14779 (on 116) to ZP1458E-2

A.13.1.3 Test Sequence Description

1. Open and standoff A phase elbow in JP0012 (on 117) to ZP1458E-1. Verify transfer to islanded mode after 10 cycles.
2. Record duration of transfer to island. Download event recorder to verify transfer time is less than 10 cycles.
3. Record the waveform number from the Hinoki data logger and the SEL 421.
4. After ~60 seconds, record the time to derate (ToD) _____ and system state of charge (SOC) _____
5. Capture voltage and current waveforms on the Hinoki data logger to verify that the battery is supporting the CTL through the switch to island mode

A.13.1.4 Anticipated Results

1. The system disconnects from grid power and supports the load without interruption
2. The data logger captures the grid-to-island waveforms for voltage and current during the transfer. Waveform shall be stored for reporting /documentation purposes.
3. The Time to Derate (TTD) value indicates a stable and decreasing value as battery capacity is reduced.

A.13.1.5 Return to Grid-Connected State

1. Make A phase elbow JP0012 (on 117) to ZP1458E-1
2. Verify that UET system has received good voltage, frequency from ZP1458E-1, and that UET sees frequency.
3. Observe 2 minutes delay and verify ZP1458E-1 (Way 1) syncs back in to the battery and automatically closes. Record voltage _____ and frequency _____
4. If fails (no sync after 5 minutes) we need to back out of syncing and start troubleshooting why. Reduce CTL to idle, open main breakers B1 and B2, and put ZP1458E in Manual mode to being troubleshooting process.
5. If system syncs, record transfer duration time. Download event recorder to verify duration is less than 10 cycles. Be sure to clear event recorder.
6. Reduce CTL to idle mode (0kva)

A.13.1.6 Success Criteria

1. The test shall be successful when the unit accepts transfer of the full load without interruption of service.
2. The test shall be successful when the unit performs the transfer without significant overvoltage/overcurrent, as measured across the load and captured by the data logger, during the transfer. Review voltage and current waves to check for satisfaction.

If all success criteria pass, continue to next test. Check if charging is needed.

TEST ENDS

A.13.1.7 Switching Order

Order Name: PAL 18-7

SWITCHING DATE/TIME: mm-dd-yyyy (DAY), hh:mm AM/PM

FEEDER/LOCATION: TUR 116 and TUR 117, TES Battery Site in Pullman, WA

PERSON IN CHARGE: Bo Morgan (07) SWITCHMAN: Tim Wacker (520)

Bo Morgan (07)

Alex Weenink – UET (206 599 9347)

DESCRIPTION: TES ISLANDING TEST AT LOW LOAD, RETURN TO GRID IN IDLE

PREPARED BY: Caitlin Greeney, 1-15-2018

VERIFIED BY: _____ DATE: _____

DSO Engineer

COMPLETED BY: _____ DATE: _____

Distribution Dispatcher

TIME	STEP	WHO	ACTION
	1	DD	NOTIFY THE S.O. TO CHECK THE TRANSMISSION SYSTEM AND THAT LOAD WILL BE TRANSFERRED BETWEEN TUR117 and TES.
	2	DD	CONFIRM THAT OTHER CREWS DO NOT HAVE A HLH AND NO ASNBF HAVE BEEN ISSUED ON TUR116 AND TUR117.
	3	DD	VERIFY TUR 116 VOLTAGE CONTROL IS DISABLED.
	4	DD	VERIFY TUR 117 VOLTAGE CONTROL IS DISABLED.
	5	07	CHECK CLOSED ELBOWS GOING EAST IN JP0174.
	6	520	CHECK CLOSED ZP1458E-1 (PREFERRED SOURCE – TUR 117).
	7	520	CHECK OPEN ZP1458E-2 (ALTERNATE SOURCE – TUR 116).
	8	520	CHECK CLOSED ZP1458E-3 AND CONNECTED TO TEST LOAD, SET TO 0 KVA.
	8	520	CHECK CLOSED ZP1458E-4 (TOWARD TES).
	9	UET	CHECK CLOSED TES MAIN BREAKERS B1 AND B2.
	10	520	CHECK ZP1458E IS IN “AUTO”.
	11	520	CHECK ZP1458E IS IN “REMOTE”.
	12	520	CHECK ZP1458E “PREFERRED SOURCE” IS SOURCE 1 (TUR 117).
	14	ENG	VERIFY TES SOC IS GREATER THAN 85%.
	15	UET	SET TEST LOAD TO 100 KVA AT .95 PF.

	15	07	CHECK OPEN ELBOWS IN J14779 TO ZP1458E-2 (ON TUR 116, TO PREVENT TRANSFER TO ALTERNATE SOURCE).
	15	07	OPEN PHASE AN ELBOW IN JP0012 FEEDING SOUTH TO ZP1458E-1 (SIMULATING THE LOSS OF TUR 117 FROM ZP1458E-1).
	16	520	VERIFY TES TRANSFERS TO ISLANDED MODE.
	17	520	RECORD TRANSFER DURATION TIME. DOWNLOAD EVENT RECORDER TO VERIFY TRANSFER DURATION. CLEAR EVENT RECORDER.
	18	UET	VERIFY HINOKI DATA LOGGER CAPTURES THE WAY1-TO-WAY2 (ZP1458E-1 TO ZP1458E-2) SOURCE WAVEFORMS FOR VOLTAGE AND CURRENT DURING THE TRANSFER. STORE THE WAVEFORMS FOR REPORT.
	19	ENG	OBSERVE 60 SECOND DELAY. RECORD TIME TO DERATE (TTD) AND SYSTEM SOC.
	20	07	CLOSE A PHASE ELBOW IN JP0012 FEEDING SOUTH TO ZP1458E-1 (ON TUR 117).
	21	520	OBSERVE A 2 MINUTE DELAY AS THE ZP1458E LOOKS FOR GOOD VOLTAGE ON ZP1458E-1 (WAY 1, TUR 117) PRIOR TO CONNECTION.
	22	520	RECORD TIME OF TRANSFER DURATION. DOWNLOAD EVENT RECORDER TO VERIFY TRANSFER TIME. CLEAR EVENT RECORDER.
	23	UET	REDUCE TEST LOAD TO IDLE MODE (0 KVA).
	24	DD	VERIFY ZP1458E-1 IS CLOSED IN DMS.
	25	DD	VERIFY ZP1458E-2 IS OPEN IN DMS.
	26	DD	VERIFY ZP1458E-1 VOLTAGE IS BETWEEN 7.62KV and 8KV IN DMS.
	27	DD	NOTIFY THE SO SWITCHING IS COMPLETE.

A.13.2 Grid to Island and Return – TES Idling, Full Load, same edits as above sequence

A.13.2.1 Purpose

The purpose of this test is to transfer to islanded mode and to support the load without interruption (less than 10 cycles), and then re-sync the battery to preferred feeder. This test directly supports Use Case 6A (Loss of Preferred Source) and Use Case 6C (Loss of Preferred and Alternate Source). The load reactance is configured inductively and the battery is idling (neither charging nor discharging).

A.13.2.2 Initial Conditions

Verify TES site is in Test Configuration:

1. Verify elbows going west in JP0174 are OPEN
2. Verify elbows going east in JP0174 are CLOSED
3. Verify ATS Way 1 is CLOSED (preferred source)
4. Verify ATS Way 2 is OPEN (alternate source)
5. Verify ATS Way 3 is CLOSED and connected to Crestchic Load Bank (CTL)
6. Verify ATS Way 4 is CLOSED (TES)
7. Verify Main Breakers B1 and B2 in TES are CLOSED

8. Verify TES string 1 and string 2 in IDLE
9. Verify ATS is in Auto mode
10. Verify ATS is in Remote mode
11. Verify Way 1 (TUR 117) is the Preferred Source
12. Verify TUR 116 Voltage Control is Disabled
13. Verify TUR 117 Voltage Control is Disabled
14. The battery has a SOC greater than 85%.
15. Adjust CTL to 1064 kVA at .95 power factor.
16. Verify main breakers B1 and B2 in TES are closed and TES is connected to the grid.
17. Confirm battery is in idle mode, call DSO engineer (Jill Hamm) to confirm.
18. Verify Hinoki data logger is connected and functioning
19. Verify elbows in J14779 (on 116) to ZP1458E-2 are open and stood off

A.13.2.3 Test Sequence

1. Open and standoff A phase elbow in JP0012 (on 117) to ZP1458E-1. Verify transfer to islanded mode after 10 cycles.
2. Record duration of transfer to island. Download event recorder to verify transfer time is less than 10 cycles.
3. Record the waveform number from the power quality meter and the SEL 421.
4. After ~60 seconds, record the TTD) _____ and system state of charge (SOC) _____ (see relay tech).
5. Capture voltage and current waveforms on the Hinoki data logger to verify that the battery is supporting the CTL through the switch to island mode

A.13.2.4 Anticipated Results

1. The system disconnects from grid power and supports the load without interruption
2. The data logger captures the grid-to-island waveforms for voltage and current during the transfer. Waveform shall be stored for reporting /documentation purposes.
3. The TTD value indicates a stable and decreasing value as battery capacity is reduced.

A.13.2.5 Return to Grid-Connected state

1. Make A phase elbows JP0012 (on 117) to ZP1458E-1
2. Verify that UET system has received good voltage, frequency from ZP1458E-1, and that UET sees frequency.
3. Observe 2 minutes delay and verify ZP1458E-1 (Way 1) syncs back in to the battery and automatically closes. Record voltage _____ and frequency _____

4. If fails (no sync after 5 minutes) we need to back out of syncing and start troubleshooting why. Reduce CTL to idle, open main breakers B1 and B2, and put ATS in Manual mode to being troubleshooting process.
5. If system syncs, record transfer duration time. Download event recorder to verify duration. Be sure to clear event recorder.
6. Reduce CTL to idle mode (0kva)

A.13.2.6 Success Criteria

1. The test shall be successful when the unit accepts transfer of the full load without interruption of service.
2. The test shall be successful when the unit performs the transfer without significant overvoltage/overcurrent, as measured across the load and captured by the data logger, during the transfer. Review voltage and current waves to check for satisfaction.

If all success criteria pass, continue to next test. Check if charging is needed.

TEST ENDS

A.13.2.7 Switching Order

Order Name: PAL 18-8

SWITCHING DATE/TIME: mm-dd-yyyy (DAY), hh:mm AM/PM

FEEDER/LOCATION: TUR 116 and TUR 117, TES Battery Site in Pullman, WA

PERSON IN CHARGE: Bo Morgan (07) **SWITCHMAN:** Tim Wacker (520)

Bo Morgan (07)

Alex Weenink – UET (206 599 9347)

DESCRIPTION: TES ISLANDING TEST AT FULL LOAD, RETURN TO GRID IN IDLE

PREPARED BY: Caitlin Greeney, 1-15-2018

VERIFIED BY: _____ **DATE:** _____

DSO Engineer

COMPLETED BY: _____ **DATE:** _____

Distribution Dispatcher

TIME	STEP	WHO	ACTION
	1	DD	NOTIFY THE S.O. TO CHECK THE TRANSMISSION SYSTEM AND THAT LOAD WILL BE TRANSFERRED BETWEEN TUR117 and TES.
	2	DD	CONFIRM THAT OTHER CREWS DO NOT HAVE A HLH AND NO ASNBF HAVE BEEN ISSUED ON TUR116 AND TUR117**.**
	3	DD	VERIFY TUR 116 VOLTAGE CONTROL IS DISABLED.
	4	DD	VERIFY TUR 117 VOLTAGE CONTROL IS DISABLED.
	5	07	CHECK CLOSED ELBOWS GOING EAST IN JP0174.
	6	520	CHECK CLOSED ZP1458E-1 (PREFERRED SOURCE – TUR 117).
	7	520	CHECK OPEN ZP1458E-2 (ALTERNATE SOURCE – TUR 116).
	8	520	CHECK CLOSED ZP1458E-3 AND CONNECTED TO TEST LOAD, SET TO 0 KVA.
	8	520	CHECK CLOSED ZP1458E-4 (TOWARD TES).
	9	UET	CHECK CLOSED TES MAIN BREAKERS B1 AND B2.
	10	520	CHECK ZP1458E IS IN “AUTO”.
	11	520	CHECK ZP1458E IS IN “REMOTE”.
	12	520	CHECK ZP1458E “PREFERRED SOURCE” IS SOURCE 1 (TUR 117).
	13	ENG	VERIFY TES SOC IS GREATER THAN 85%.
	14	UET	SET TEST LOAD TO 1064 KVA AT .95 PF.
	15	07	CHECK OPEN ELBOWS IN J14779 TO ZP1458E-2 (ON TUR 116, TO PREVENT TRANSFER TO ALTERNATE SOURCE).
	16	07	OPEN PHASE AN ELBOW IN JP0012 FEEDING SOUTH TO ZP1458E-1 (SIMULATING THE LOSS OF TUR 117 FROM ZP1458E-1).
	17	520	VERIFY TES TRANSFERS TO ISLANDED MODE.
	18	520	RECORD TRANSFER DURATION TIME. DOWNLOAD EVENT RECORDER TO VERIFY TRANSFER TIME DURATION. CLEAR EVENT RECORDER.
	19	UET	VERIFY HINOKI DATA LOGGER CAPTURES THE WAY1-TO-WAY2 (ZP1458E-1 TO ZP1458E-2) SOURCE WAVEFORMS FOR VOLTAGE AND CURRENT DURING THE TRANSFER. STORE THE WAVEFORMS FOR REPORT.
	20	ENG	OBSERVE 60 SECOND DELAY. RECORD TTD AND SYSTEM SOC.
	21	07	CLOSE A PHASE ELBOW IN JP0012 FEEDING SOUTH TO ZP1458E-1 (ON TUR 117).
	22	520	OBSERVE A 2 MINUTE DELAY AS THE ZP1458E LOOKS FOR GOOD VOLTAGE ON ZP1458E-1 (WAY 1, TUR 117) PRIOR TO CONNECTION.
	23	520	RECORD TIME OF TRANSFER DURATION. DOWNLOAD EVENT RECORDER TO VERIFY TRANSFER DURATION. CLEAR EVENT RECORDER.
	24	UET	REDUCE TEST LOAD TO IDLE MODE (0 KVA).
	25	DD	VERIFY ZP1458E-1 IS CLOSED IN DMS.
	26	DD	VERIFY ZP1458E-2 IS OPEN IN DMS.
	27	DD	VERIFY ZP1458E-1 VOLTAGE IS BETWEEN 7.62KV and 8KV IN DMS.
	28	DD	NOTIFY THE SO SWITCHING IS COMPLETE.

A.13.3 Grid to Island and Return – Discharge

A.13.3.1 Purpose

The purpose of this test is to swing the operating point of the charger/inverter from grid-connected full-power discharging to islanded full-load-support operations. The system is in full power dispatch (~1064 KVA at 0.95 PF inductive) at the time of transfer.

An additional purpose of this test is to transfer to islanded mode and to support the load without interruption. This test directly supports Use Case 6A (Loss of Preferred Source) and Use Case 6C (Loss of Preferred and Alternate Source). The load reactance is configured inductively.

A.13.3.2 Initial Conditions

Verify TES site is in Test Configuration:

1. Verify elbows going east in JP0174 are CLOSED
2. Verify elbows going west in JP0174 are OPEN
3. Verify ATS Way 1 is CLOSED (preferred source)
4. Verify ATS Way 2 is OPEN (alternate source)
5. Verify ATS Way 3 is CLOSED and connected to Crestchic Load Bank (CTL)
6. Verify ATS Way 4 is CLOSED (TES)
7. Verify Main Breakers B1 and B2 in TES are CLOSED
8. Verify TES string 1 and string 2 in IDLE
9. Verify ATS is in Auto mode
10. Verify ATS is in Remote mode
11. Verify Way 1 (TUR 117) is the Preferred Source
12. Verify TUR 116 Voltage Control is Disabled
13. Verify TUR 117 Voltage Control is Disabled
14. The battery has a SOC greater than 85%.
15. Adjust CTL to 1064 kVA at .95 power factor.
16. Verify main breakers B1 and B2 in TES are closed and TES is connected to the grid.
17. Confirm battery is in idle mode, call DSO engineer (Jill Hamm) to confirm.
18. Verify Hinoki data logger is connected and functioning
19. Verify elbows in J14779 (on 116) to ZP1458E-2 are open and stood off

A.13.3.3 Test Sequence

1. Command TES to discharge at 1064 kVA at .95 power factor. Record actual value.

2. Open and standoff A phase elbow in JP0012 (on 117) to ZP1458E-1. Verify transfer to islanded mode.
3. Record duration time of transfer to islanded mode. Download event recorder to verify transfer duration
4. Record the waveform number from the Hinoki data logger and the SEL 421.
5. After ~60 seconds, record the TTD _____ and system state of charge (SOC) _____
6. Capture voltage and current waveforms on the Hinoki data logger to verify that the battery is supporting the CTL through the switch to island mode

A.13.3.4 Anticipated Results

1. The system disconnects from grid power and supports the load without interruption
2. The data logger captures the grid-to-island waveforms for voltage and current during the transfer. Waveform shall be stored for reporting /documentation purposes.
3. The time to derate (TTD) value indicates a stable and decreasing value as battery capacity is reduced.

A.13.3.5 Return to Grid-Connected State

1. Make Phase A elbow JP0012 (on 117) to ZP1458E-1
2. Verify that UET system has received good voltage, frequency from ZP1458E-1, and that UET sees frequency. 2 minutes later, ZP1458E and TES should automatically sync.
3. If fails (no sync after 5 minutes) we need to back out of syncing and start troubleshooting why. Reduce CTL to idle, open main breakers B1 and B2 to being troubleshooting process.
4. If system syncs, record transfer time. Download event recorder. Be sure to clear event recorder
5. Reduce CTL to IDLE mode (0 kVA)
6. Command TES to idle mode (0 kVA)

A.13.3.6 Success Criteria

1. The test shall be successful when the unit accepts transfer of the full load without interruption of service.
2. The test shall be successful when the unit performs the transfer without significant overvoltage/overcurrent, as measured across the load and captured by the Hinoki data logger, during the transfer. Review voltage and current waves to check for satisfaction

If all success criteria pass, continue to next test. Check if charging is needed.

TEST ENDS

A.13.3.7 Switching Order

Order Name: PAL 18-9

SWITCHING DATE/TIME: mm-dd-yyyy (DAY), hh:mm AM/PM

FEEDER/LOCATION: TUR 116 and TUR 117, TES Battery Site in Pullman, WA

PERSON IN CHARGE: Bo Morgan (07) **SWITCHMAN:** Tim Wacker (520),

Bo Morgan (07)

Alex Weenink – UET (206 599 9347)

DESCRIPTION: TES ISLANDING TEST AT FULL LOAD, TES IS DISCHARGING PRIOR TO ISLANDING

PREPARED BY: Caitlin Greeney**,** 1-15-2018

VERIFIED BY: _____ **DATE:** _____

DSO Engineer

COMPLETED BY: _____ **DATE:** _____

Distribution Dispatcher

TIME	STEP	WHO	ACTION
	1	07/DD	NOTIFY THE S.O. TO CHECK THE TRANSMISSION SYSTEM AND THAT LOAD WILL BE TRANSFERRED BETWEEN TUR116 and TUR117.
	2	DD	CONFIRM THAT OTHER CREWS DO NOT HAVE A HLH AND NO ASNBF HAVE BEEN ISSUED ON TUR116 AND TUR117**.**
	3	DD	VERIFY TUR 116 VOLTAGE CONTROL IS DISABLED.
	4	DD	VERIFY TUR 117 VOLTAGE CONTROL IS DISABLED.
	5	07	CHECK CLOSED ELBOWS GOING EAST IN JP0174.
	6	520	CHECK CLOSED ZP1458E-1 (PREFERRED SOURCE – TUR 117).
	7	520	CHECK OPEN ZP1458E-2 (ALTERNATE SOURCE – TUR 116).
	8	520	CHECK CLOSED ZP1458E-3 AND CONNECTED TO TEST LOAD, SET TO 0 KVA.
	8	520	CHECK CLOSED ZP1458E-4 (TOWARD TES).
	9	UET	CHECK OPEN TES MAIN BREAKERS B1 AND B2.
	10	520	CHECK ZP1458E IS IN “AUTO”.
	11	520	CHECK ZP1458E IS IN “REMOTE”.
	12	07	CHECK OPEN ELBOWS IN J14779 TO ZP1458E-2 (ON TUR 116, TO PREVENT TRANSFER TO ALTERNATE SOURCE).
	13	ENG	VERIFY TES SOC IS GREATER THAN 85%.
	14	UET	SET TEST LOAD TO 1064 KVA AT .95 PF.
	15	ENG	COMMAND TES TO DISCHARGE AT 1064 KVA AT .95 POWER FACTOR. RECORD ACTUAL VALUE.
	16	07	OPEN PHASE AN ELBOW IN JP0012 FEEDING SOUTH TO ZP1458E-1 (SIMULATING THE LOSS OF TUR 117 FROM ZP1458E-1).

	17	520	VERIFY TES TRANSFERS TO ISLANDED MODE.
	18	520	RECORD TRANSFER DURATION TIME. DOWNLOAD EVENT RECORDER TO VERIFY. CLEAR EVENT RECORDER.
	19	UET	VERIFY HINOKI DATA LOGGER CAPTURES THE WAY1-TO-WAY4 (ZP1458E-1 TO ZP1458E-4) SOURCE WAVEFORMS FOR VOLTAGE AND CURRENT DURING THE TRANSFER. STORE THE WAVEFORMS FOR REPORT.
	20	ENG	OBSERVE 60 SECOND DELAY. RECORD TIME TO DERATE (TTD) AND SYSTEM STATE OF CHARGE (SOC).
	21	07	CLOSE A PHASE ELBOW IN JP0012 FEEDING SOUTH TO ZP1458E-1 (ON TUR 117).
	22	520	OBSERVE A 2 MINUTE DELAY AS THE ZP1458E LOOKS FOR GOOD VOLTAGE ON ZP1458E-1 (WAY 1, TUR 117) PRIOR TO CONNECTION.
	23	520	RECORD TIME OF TRANSFER DURATION. DOWNLOAD EVENT RECORDER TO VERIFY TRANSFER TIME DURATION. CLEAR EVENT RECORDER.
	24	UET	REDUCE CTL TO IDLE MODE (0 KVA).
	25	UET	COMMAND TES TO IDLE MODE (0 KVA).
	26	DD	VERIFY ZP1458E-1 IS CLOSED IN DMS.
	27	DD	VERIFY ZP1458E-2 IS OPEN IN DMS.
	28	DD	VERIFY ZP1458E-1 VOLTAGE IS BETWEEN 7.62KV and 8KV IN DMS.
	29	DD	NOTIFY THE SO SWITCHING IS COMPLETE.

A.13.4 Grid to Island and Return – Charging

A.13.4.1 Purpose

The purpose of this test is to swing the operating point of the charger/inverter from grid-connected full-power charging to islanded load-support operations. The load is roughly maximized to the amount of power available at 60% state of charge prior to transfer, and the system is full-power charging (-800 kW) at the time of transfer.

An additional purpose of this test is to transfer to islanded mode and to support the load without interruption. This test directly supports Use Case 6A (Loss of Preferred Source) and Use Case 6C (Loss of Preferred and Alternate Source). The load reactance is configured inductively.

A.13.4.2 Initial Conditions

Verify TES site is in Test Configuration:

1. Verify elbows going east in JP0174 are CLOSED
2. Verify elbows going west in JP0174 are OPEN
3. Verify ATS Way 1 is CLOSED (preferred source)
4. Verify ATS Way 2 is OPEN (alternate source)
5. Verify ATS Way 3 is CLOSED and connected to Crestchic CTL (CTL)
6. Verify ATS Way 4 is CLOSED (TES)

7. Verify Main Breakers B1 and B2 in TES are CLOSED
8. Verify TES string 1 and string 2 in IDLE
9. Verify ATS is in Auto mode
10. Verify ATS is in Remote mode
11. Verify Way 1 (TUR 117) is the Preferred Source
12. Verify TUR 116 Voltage Control is Disabled
13. Verify TUR 117 Voltage Control is Disabled
14. The battery has a SOC of approximately 65%. Record actual _____.
15. Adjust CTL to 1064 kVA at .95 power factor. Record actual: _____
16. Verify main breakers B1 and B2 in TES are closed and TES is connected to the grid.
17. Confirm battery is in idle mode, call DSO engineer (Jill Hamm) to confirm.
18. Verify load on TUR 116 toward JP0174 and J11765 (SEL manufacturing load) with DSO (Jill Hamm) to confirm that battery charging load will not overload lines.
19. Verify Hinoki data logger is connected and functioning
20. Verify elbows in J14779 (on 116) to ZP1458E-2 are open and stood off

A.13.4.3 Test Sequence

1. Command TES to charge at -800 kW. Record actual value.
2. Open and standoff A phase elbow in JP0012 (on 117) to ZP1458E-1. Verify transfer to islanded mode.
3. Record duration time of transfer to islanded mode. Download event recorder to verify transfer time duration
4. Record the waveform number from the Hinoki data logger and the SEL 421.
5. After ~60 seconds, record the TTD and system SOC
6. Capture voltage and current waveforms on the Hinoki data logger to verify that the battery is supporting the CTL through the switch to island mode

A.13.4.4 Anticipated Results

1. The system disconnects from grid power and supports the load without interruption
2. The data logger captures the grid-to-island waveforms for voltage and current during the transfer. Waveform shall be stored for reporting /documentation purposes.
3. The Time to Derate (TTD) value indicates a stable and decreasing value as battery capacity is reduced.

A.13.4.5 Return to Grid-Connected State

1. Make Phase A elbow JP0012 (on 117) to ZP1458E-1

2. Verify that UET system has received good voltage, frequency from ZP1458E-1, and that UET sees frequency. 2 minutes later, ZP1458E and battery should automatically sync. Record sent voltage _____ and frequency _____
3. If fails (no sync after 5 minutes) we need to back out of syncing and start troubleshooting why. Reduce CTL to idle, open main breakers B1 and B2 to being troubleshooting process.
4. If system syncs, record transfer time. Download event recorder _____. Be sure to clear event recorder
5. Reduce CTL to IDLE mode (0 kVA)
6. Command TES to idle mode (0 kVA)

A.13.4.6 Success Criteria

1. The test shall be successful when the unit accepts transfer of the full load without interruption of service.
2. The test shall be successful when the unit performs the transfer without significant overvoltage/overcurrent, as measured across the load and captured by the Hinoki data logger, during the transfer. Review voltage and current waves to check for satisfaction

If all success criteria pass, continue to next test. Check if charging is needed.

TEST ENDS

A.13.4.7 Switching Order

Order Name: PAL 18-10

SWITCHING DATE/TIME: mm-dd-yyyy (DAY), hh:mm AM/PM

FEEDER/LOCATION: TUR 116 and TUR 117, TES Battery Site in Pullman, WA

PERSON IN CHARGE: Bo Morgan (07) **SWITCHMAN:** Tim Wacker (520)

Bo Morgan (07)

Alex Weenink – UET (206 599 9347)

DESCRIPTION: TES ISLANDING TEST AT FULL LOAD, TES IS CHARGING PRIOR TO ISLANDING

PREPARED BY: Caitlin Greeney, mm-dd-yyyy

VERIFIED BY: _____ **DATE:** _____

DSO Engineer

COMPLETED BY: _____ **DATE:** _____

Distribution Dispatcher

TIME	STEP	WHO	ACTION
	1	07/DD	NOTIFY THE S.O. TO CHECK THE TRANSMISSION SYSTEM AND THAT LOAD WILL BE TRANSFERRED BETWEEN TUR116 and TUR117
	2	DD	CONFIRM THAT OTHER CREWS DO NOT HAVE A HLH AND NO ASNBF HAVE BEEN ISSUED ON TUR116 AND TUR117
	3	DD	VERIFY TUR 116 VOLTAGE CONTROL IS DISABLED
	4	DD	VERIFY TUR 117 VOLTAGE CONTROL IS DISABLED
	5	07	CHECK CLOSED ELBOWS GOING EAST IN JP0174
	6	520	CHECK CLOSED ZP1458E-1 (PREFERRED SOURCE – TUR 117)
	7	520	CHECK OPEN ZP1458E-2 (ALTERNATE SOURCE – TUR 116)
	8	520	CHECK CLOSED ZP1458E-3 AND CONNECTED TO TEST LOAD, SET TO 0 KVA
	8	520	CHECK CLOSED ZP1458E-4 (TOWARD TES)
	9	UET	CHECK OPEN TES MAIN BREAKERS B1 AND B2
	10	520	CHECK ZP1458E IS IN “AUTO”
	11	520	CHECK ZP1458E IS IN “REMOTE”
	12	07	CHECK OPEN ELBOWS IN J14779 TO ZP1458E-2 (ON TUR 116, TO PREVENT TRANSFER TO ALTERNATE SOURCE)
	13	ENG	VERIFY TES SOC IS APPROXIMATELY 65%
	14	UET	SET TEST LOAD TO 1064 KVA AT .95 PF
	15	ENG	COMMAND TES TO CHARGE AT -800 KW
	16	07	OPEN PHASE A ELBOW IN JP0012 FEEDING SOUTH TO ZP1458E-1 (SIMULATING THE LOSS OF TUR 117 FROM ZP1458E-1)
	17	520	VERIFY TES TRANSFERS TO ISLANDED MODE
	18	520	RECORD TRANSFER DURATION TIME. DOWNLOAD EVENT RECORDER TO VERIFY. CLEAR EVENT RECORDER
	19	UET	VERIFY HINOKI DATA LOGGER CAPTURES THE WAY1-TO-WAY4 (ZP1458E-1 TO ZP1458E-4) SOURCE WAVEFORMS FOR VOLTAGE AND CURRENT DURING THE TRANSFER. STORE THE WAVEFORMS FOR REPORT
	20	ENG	OBSERVE 60 SECOND DELAY. RECORD TIME TO DERATE (TTD) AND SYSTEM STATE OF CHARGE (SOC)
	21	07	CLOSE A PHASE ELBOW IN JP0012 FEEDING SOUTH TO ZP1458E-1 (ON TUR 117)
	22	520	OBSERVE A 2 MINUTE DELAY AS THE ZP1458E LOOKS FOR GOOD VOLTAGE ON ZP1458E-1 (WAY 1, TUR 117) PRIOR TO CONNECTION
	23	520	RECORD TIME OF TRANSFER DURATION. DOWNLOAD EVENT RECORDER TO VERIFY TRANSFER TIME DURATION. CLEAR EVENT RECORDER
	24	UET	REDUCE CTL TO IDLE MODE (0 KVA)
	25	UET	COMMAND TES TO IDLE MODE (0 KVA)
	26	DD	VERIFY ZP1458E-1 IS CLOSED IN DMS
	27	DD	VERIFY ZP1458E-2 IS OPEN IN DMS
	28	DD	VERIFY ZP1458E-1 VOLTAGE IS BETWEEN 7.62KV and 8KV IN DMS
	29	DD	NOTIFY THE SO SWITCHING IS COMPLETE

A.13.5 Discharge Time-to-Derate Test

A.13.5.1 Purpose

The purpose of this test is to verify the Time to Derate while under extreme load. This test will verify the operation of the system under islanded conditions and full loading as the battery is discharged to the point of derate.

A.13.5.2 Initial Conditions

Verify TES site is in Test Configuration:

1. Verify elbows going west in JP0174 are OPEN
2. Verify elbows going east in JP0174 are CLOSED
3. Verify ATS Way 1 is CLOSED (preferred source)
4. Verify ATS Way 2 is OPEN (alternate source)
5. Verify ATS Way 3 is CLOSED and connected to Crestchic CTL (CTL)
6. Verify ATS Way 4 is CLOSED (TES)
7. Verify Main Breakers B1 and B2 in TES are CLOSED
8. Verify TES string 1 and string 2 in IDLE
9. Verify ATS is in Auto mode
10. Verify ATS is in Remote mode
11. Verify Way 1 (TUR 117) is the Preferred Source
12. Verify TUR 116 Voltage Control is Disabled
13. Verify TUR 117 Voltage Control is Disabled
14. Verify battery has a 100% SOC. Record actual: _____
15. Verify main breakers B1 and B2 in TES are closed and TES is connected to the grid.
16. Confirm battery is in idle mode, call DSO engineer (Jill Hamm) to confirm.
17. Verify Hinoki data logger is connected and functioning
18. Verify elbows in J14779 (on 116) to ZP1458E-2 are open and stood off

A.13.5.3 Test Sequence

1. Command the TES to discharge at 1064 kVA at .95 power factor. Record actuals_____. Record start time _____
2. After ~60 seconds, record the TTD _____, system SOC _____, and real time _____
3. Verify with UET and NPS that battery is still supporting above CTL. Record CTL levels _____

4. After 2 minutes, record real time_____, SOC_____, and Time-to-Derate_____, kW_____, and kvar _____readings
5. Repeat previous step (chart provided as appendix) as the TTD decreases until TES power output collapses due to inability to dispatch at the commanded level

A.13.5.4 Success Criteria

1. A successful test is attained when:
   a. The TTD does not move outside of the expected tolerance (+/-20% predicted TTD) for the entire test;
   b. The TES output collapses on or after the TTD indicator hits zero plus error tolerance.

If all success criteria pass, continue to next test. Check if charging is needed.

A.13.5.5 Switching Order

Order Name: PAL 18-11

SWITCHING DATE/TIME: mm-dd-yyyy (DAY), hh:mm AM/PM

FEEDER/LOCATION: TUR 116 and TUR 117, TES Battery Site in Pullman, WA

PERSON IN CHARGE: Bo Morgan (07) **SWITCHMAN:** Tim Wacker (520)

Bo Morgan (07)

Alex Weenink – UET (206 599 9347)

DESCRIPTION: TTD DISCHARGE TEST

PREPARED BY: Caitlin Greeney, mm-dd-yyyy

VERIFIED BY: _____ **DATE:** _____

DSO Engineer

COMPLETED BY: _____ **DATE:** _____

Distribution Dispatcher

TIME	STEP	WHO	ACTION
	1	DD	VERIFY TUR 116 VOLTAGE CONTROL IS DISABLED.
	2	DD	VERIFY TUR 117 VOLTAGE CONTROL IS DISABLED.
	3	07	CHECK CLOSED ELBOWS GOING EAST IN JP0174.
	4	520	CHECK CLOSED ZP1458E-1 (PREFERRED SOURCE – TUR 117).
	5	520	CHECK OPEN ZP1458E-2 (ALTERNATE SOURCE – TUR 116).
	6	520	CHECK CLOSED ZP1458E-3 AND CONNECTED TO TEST LOAD, SET TO 0 KVA.
	7	520	CHECK CLOSED ZP1458E-4 (TOWARD TES).

TIME	STEP	WHO	ACTION
	8	UET	CHECK CLOSED TES MAIN BREAKERS B1 AND B2.
	9	520	CHECK ZP1458E IS IN “AUTO”.
	10	520	CHECK ZP1458E IS IN “REMOTE”.
	11	ENG	VERIFY TES SOC IS APPROXIMATELY 100%.
	12	ENG	COMMAND TES TO DISCHARGE AT 1064 KVA AT .95
	13	ENG	OBSERVE 60 SECOND DELAY. RECORD TIME TO DERATE (TTD) AND SYSTEM STATE OF CHARGE (SOC). REPEAT UNTIL POWER OUTPUT COLLAPSES.
	14	UET	REDUCE CTL TO IDLE MODE (0 KVA).
	15	UET	COMMAND TES TO IDLE MODE (0 KVA).
	16	DD	VERIFY ZP1458E-1 IS CLOSED IN DMS.
	17	DD	VERIFY ZP1458E-2 IS OPEN IN DMS.
	18	DD	VERIFY ZP1458E-1 VOLTAGE IS BETWEEN 7.62KV and 8KV IN DMS.
	19	DD	NOTIFY THE SO SWITCHING IS COMPLETE.

A.13.6 Recharge Time to Derate

A.13.6.1 Purpose

The purpose of this test is to verify the Time to Derate for charging upon re-establishing grid connection. This test will verify the operation of the system under return from islanded conditions and full loading as the battery is recharged. A secondary objective of this test is to characterize, for Spirae, the recharge behavior of the system so that dual-string system modeling can be updated.

A.13.6.2 Initial Conditions

Verify TES site is in Test Configuration:

1. Verify elbows going west in JP0174 are OPEN
2. Verify elbows going east in JP0174 are CLOSED
3. Verify ATS Way 1 is CLOSED (preferred source)
4. Verify ATS Way 2 is OPEN (alternate source)
5. Verify ATS Way 3 is CLOSED and connected to CTL
6. Verify ATS Way 4 is CLOSED (TES)
7. Verify Main Breakers B1 and B2 in TES are CLOSED
8. Verify TES string 1 and string 2 in IDLE
9. Verify ATS is in Auto mode

10. Verify ATS is in Remote mode
11. Verify Way 1 (TUR 117) is the Preferred Source Verify TUR 116 Voltage Control is Disabled
12. Verify TUR 117 Voltage Control is Disabled
13. The battery has a SOC at 60%. Record actual: _____
14. Verify main breakers B1 and B2 in TES are closed and TES is connected to the grid.
15. Confirm battery is in idle mode, call DSO engineer (Jill Hamm) to confirm.
16. Verify load on TUR 116 toward JP0174 and J11765 (SEL manufacturing load) with DSO (Jill Hamm) to confirm that battery charging load will not overload lines.
17. Verify Hinoki data logger is connected and functioning
18. Verify elbows in J14779 (on 116) to ZP1458E-2 are open and stood off

A.13.6.3 Test Sequence

1. Set CTL to 1064 kVA at .95 power factor. Record actual: _____
2. Command the TESS to charge -800 kW. Record actual: _____ Record real time: _____
3. After ~60 seconds, record the TTD _____and system SOC_____.
4. Verify with UET and NPS that battery is still supporting above CTL. Record CTL levels _____
5. After 2 minutes, record real time_____, SoC_____, and Time-to-Derate_____, kW_____, and kvar _____readings
6. Repeat previous step (chart provided as appendix) as the TTD decreases until TES is sufficiently charged.

A.13.6.4 Success Criteria

1. A successful test is attained when:
   a. The TTD does not move outside of the expected tolerance (+/-20% predicted TTD) for the entire test.
   b. The TESS output recharge level throttles as SOC increases above the TTD point.

If all success criteria pass, continue to next test. Check if charging is needed.

TEST ENDS

A.13.6.5 Switching Order

Order Name: PAL 18-12

SWITCHING DATE/TIME: mm-dd-yyyy (DAY), hh:mm AM/PM

FEEDER/LOCATION: TUR 116 and TUR 117, TES Battery Site in Pullman, WA

PERSON IN CHARGE: Bo Morgan (07) **SWITCHMAN:** Tim Wacker (520)

Bo Morgan (07)

Alex Weenink – UET (206 599 9347)

DESCRIPTION: TTD CHARGING TEST

PREPARED BY: Caitlin Greeney, mm-dd-yyyy

VERIFIED BY: _____ **DATE:** _____

DSO Engineer

COMPLETED BY: _____ **DATE:** _____

Distribution Dispatcher

TIME	STEP	WHO	ACTION
	1	DD	VERIFY TUR 116 VOLTAGE CONTROL IS DISABLED.
	2	DD	VERIFY TUR 117 VOLTAGE CONTROL IS DISABLED.
	3	07	CHECK CLOSED ELBOWS GOING EAST IN JP0174.
	4	520	CHECK CLOSED ZP1458E-1 (PREFERRED SOURCE – TUR 117).
	5	520	CHECK OPEN ZP1458E-2 (ALTERNATE SOURCE – TUR 116).
	6	520	CHECK CLOSED ZP1458E-3 AND CONNECTED TO TEST LOAD, SET TO 0 KVA.
	7	520	CHECK CLOSED ZP1458E-4 (TOWARD TES).
	8	UET	CHECK CLOSED TES MAIN BREAKERS B1 AND B2.
	9	520	CHECK ZP1458E IS IN “AUTO”.
	10	520	CHECK ZP1458E IS IN “REMOTE”.
	11	ENG	VERIFY TES SOC IS APPROXIMATELY 65%.
	12	ENG	COMMAND TES TO CHARGE AT -800 KW.
	13	ENG	OBSERVE 60 SECOND DELAY. RECORD TIME TO DERATE (TTD) AND SYSTEM STATE OF CHARGE (SOC). REPEAT UNTIL BATTERY REACHES FULL CHARGE.
	14	UET	REDUCE CTL TO IDLE MODE (0 KVA)
	15	UET	COMMAND TES TO IDLE MODE (0 KVA)
	16	DD	VERIFY ZP1458E-1 IS CLOSED IN DMS
	17	DD	VERIFY ZP1458E-2 IS OPEN IN DMS
	18	DD	VERIFY ZP1458E-1 VOLTAGE IS BETWEEN 7.62KV and 8KV IN DMS
	19	DD	NOTIFY THE SO SWITCHING IS COMPLETE

Pacific Northwest
NATIONAL LABORATORY

www.pnnl.gov

902 Battelle Boulevard
P.O. Box 999
Richland, WA 99352
1-888-375-PNNL (7665)

U.S. DEPARTMENT OF
ENERGY